





**Mathematical modelling of a reactor for the desulfurization of the  
effluent gases from electrolysis cells**

**By**

**Arash Fassadi Chimeh**

**Under supervision of prof. Duygu Kocaefe, and co-supervision of prof. Yasar Kocaefe**

**Dissertation presented to the University of Quebec at Chicoutimi with a view to  
obtaining the degree of master of applied sciences (M. Sc. A.) in Engineering**

**Jury members:**

**Professor Derek Harvey**, Department of Applied science at UQAC

**Dr. Mounir Baitech**, XPS – Expert Process Solutions, Falconbridge, ON, external member of examiners

**Professor Duygu Kocaefe**, Department of Applied science at UQAC, internal member of examiners

**Professor Yasar Kocaefe**, Department of Applied science at UQAC, internal member of examiners

Québec, Canada

© Arash Fassadi Chimeh, 2023

## RÉSUMÉ

La désulfuration semi-sèche est un moyen efficace d'élimination du  $\text{SO}_2$  des gaz effluents des cellules d'électrolyse dans les alumineries. Cette méthode ne nécessite aucun équipement supplémentaire pour le post-traitement, ce qui la rend une méthode économique. Le dioxyde de soufre ( $\text{SO}_2$ ) est efficacement éliminé des gaz effluents des alumineries par désulfuration semi-sèche. Contrairement aux centrales thermiques, ces gaz sont à basse température et contiennent une faible concentration de  $\text{SO}_2$ . En l'absence et en présence d'humidité, un sorbant alcalin en poudre – chaux hydratée – est injecté dans le gaz contenant du  $\text{SO}_2$  (phase gazeuse). La réaction est contrôlée par l'adsorption de  $\text{SO}_2$  sur la chaux. Au cours de ce mémoire, un épurateur à l'échelle du laboratoire a été modélisé mathématiquement à l'aide de deux approches de modélisation différentes : eulérienne - eulérienne et eulérienne - lagrangienne.

Dans la première partie de ce mémoire, la modélisation eulérienne-eulérienne est considérée incluant un filtre défini comme un milieu poreux. Dans cette section, la chaux est considérée comme un fluide hautement visqueux (mais Newtonien) à travers une réaction dans un écoulement multiphasique (gaz-liquide), isotherme et turbulent, où la vitesse de réaction cinétique est définie à l'aide du langage C de la fonction définie par l'utilisateur (UDF) en utilisant le logiciel commercial Ansys-Fluent. Une étude paramétrique a été réalisée pour étudier les effets de la quantité du sorbant, de la présence et de l'absence de l'humidité et de la concentration de  $\text{SO}_2$  à l'entrée sur l'efficacité de la désulfuration. Il est considéré comme un résultat préliminaire montrant que l'humidité peut augmenter considérablement l'efficacité de la désulfuration ; cependant, il n'est pas aussi précis que la deuxième section. Cela est dû au fait qu'il ne reflète pas la physique, ce qui se produit en réalité, exactement.

Dans la deuxième partie, la réaction suit la physique réelle qui se produit. Cette fois, le modèle est capable de tenir compte de la réaction, à la surface des particules, des réactifs (écoulement réactif multiphasique gaz-solide) pour éliminer le  $\text{SO}_2$ . Grâce au couplage bidirectionnel du modèle DPM (modèle à phase discrète), les effets de la phase continue (gaz) et de la phase dispersée (particules) l'une sur l'autre sont pris en compte, illustrant comment les caractéristiques des particules affectent la distribution du gaz, etc. Les conditions évaluées sont à la fois stationnaires et transitoires dans un écoulement isotherme et turbulent, tandis qu'un suivi complémentaire des particules pour deux tailles de particules différentes a été effectué. La vitesse de réaction est introduite dans le modèle en utilisant UDF, comme dans la section précédente. Une étude paramétrique a été réalisée pour étudier les effets de la taille des particules, de la quantité du sorbant (Ca/S) et de l'humidité relative (HR) sur l'efficacité de la désulfuration. Les résultats de cette dernière approche de modélisation qui traite de la réaction gaz-solide montrent que la taille des particules est le paramètre le plus important ; à mesure que la taille des particules diminue, l'efficacité de la désulfuration augmente. Cependant, la production de particules plus fines pourrait engendrer des coûts supplémentaires. L'utilisation de tailles de particules plus grossières entraînerait une réduction de l'efficacité de capture du  $\text{SO}_2$ ; mais, cela pourrait être compensé par une augmentation de l'humidité relative (HR) dans le gaz, qui est un autre paramètre critique du procédé.

## ABSTRACT

Semi-dry desulfurization is one of the methods used for SO<sub>2</sub> removal from the effluent gases of electrolysis cells in aluminum smelters. This method does not require any additional equipment (post-treatment equipment), making it an economical method. It is more efficient than dry desulfurization since the presence of water vapor increases the rate of reaction. As opposed to thermal power plants, the outlet gases of electrolytic cells are at low temperatures and contain a low concentration of SO<sub>2</sub>. In the absence or the presence of humidity, powdered alkaline sorbent (hydrated lime) can be injected into the SO<sub>2</sub>-containing gas (gas phase). The reaction is controlled by the adsorption of SO<sub>2</sub> onto the lime surface. During this project, a mathematical model of a lab-scale scrubber was developed using two different modelling approaches: Eulerian – Eulerian and Eulerian – Lagrangian.

In the first model, a Eulerian-Eulerian modelling was carried out. The laboratory reactor has a filter to separate the lime particles from the gas. It was defined as a porous medium. In this part, lime was assumed as a highly viscous (but Newtonian) liquid; and a multi-phase flow (gas-liquid), including the reaction between lime and SO<sub>2</sub>, were modeled under isothermal and turbulent conditions. The reaction rate was defined using the C language via a user-defined function (UDF) using Ansys-Fluent commercial software. A parametric study was carried out to investigate the effects of the sorbent amount, humidity (with and without), and the inlet SO<sub>2</sub> concentration on the desulfurization efficiency. The results of this model are considered as preliminary results showing that the humidity can significantly increase the desulfurization efficiency. However, the model predictions are not as accurate as the second approach explained below. This is due to the fact that it does not represent the physics that occurs in reality.

In the second part, the representation of the reaction taking place is closer to the actual mechanism. The model which uses Eulerian- Lagrangian approach solves the reaction at the surface of lime particles (gas-solid multi-phase reacting flow) to remove the SO<sub>2</sub> whereas the particles were not represented in the previous model. The solid phase was taken as a viscous liquid. Thus, the reaction took place between the continuous viscous phase and the gas phase and not between individual particles and gas. Through the two-way coupling of the DPM (Discrete phase model) model using Ansys-Fluent software, the effects of both continuous gas phase (SO<sub>2</sub> and air) and dispersed phase (particle phase) on each other were considered such as effect of particle size on the gas flow profile. It is a steady state, transient, and isothermal model. The flow was taken as turbulent and particle trajectories were calculated for two different particle sizes. The reaction rate was introduced into the model using UDF, similar to the previous model. A parametric study was carried out to investigate the effects of particle size, sorbent amount (Ca/S), and relative humidity (RH) on desulfurization efficiency. The results of the latter modelling approach, which deals with gas-solid reactions, showed that particle size is the most important parameter; as the particle size decreases, the desulfurization efficiency increases. However, using finer particles may result in a higher cost due to the additional cost of particle size reduction. Using coarser particle sizes reduced the SO<sub>2</sub> capture efficiency, which could be compensated by increasing relative humidity (RH) in the gas as shown by the model results.

## TABLE OF CONTENTS

Résumé.....	ii
Abstract.....	iii
Table of contents.....	iv
List of tables.....	viii
List of figures.....	ix
List of abbreviations .....	xi
List of symbols.....	xii
DEDICATION.....	xvi
ACKNOWLEDGMENT .....	xvii
Chapter 1: INTRODUCTION .....	1
1.1. Introduction .....	1
1.2. Statement of problems.....	2
1.3. Objectives .....	3
1.4. Originality statement .....	4
1.5. Scope.....	5
1.6. References .....	7
Chapter 2: LITERATURE REVIEW .....	8
2.1. Introduction .....	8
2.1.1. Utilization of low-sulfur petroleum coke .....	13
2.1.2. Pre-calcined coke utilization .....	13
2.1.3. Pre-baked anode utilization .....	14
2.1.4. Reduction in aluminum production capacity.....	14
2.1.5. SO <sub>2</sub> scrubbing technology implementation.....	14
2.2. Wet desulfurization process .....	14
2.2.1. Seawater wet scrubbing.....	15
2.2.2. Sodium-based wet scrubbing.....	17
2.2.3. Limestone wet scrubbing.....	20
2.2.4. Lime-based wet scrubbing.....	22
2.3. Dry desulfurization process .....	24

2.4. Semi-dry desulfurization process .....	27
2.5. Computational Fluid Dynamics.....	43
2.6. Summary.....	44
2.7. References .....	46
Chapter 3: MATHEMATICAL MODELLING OF THE DESULFURIZATION OF ELECTROLYSIS CELL GASES IN A LOW TEMPERATURE REACTOR (ARTICLE 1) .....	48
3.1. Introduction .....	49
3.2. Methodology.....	51
3.2.1. System (Laboratory reactor).....	51
3.2.2. Governing equations.....	52
3.2.3. Filter.....	55
3.2.4. SO <sub>2</sub> -hydrated lime reaction .....	55
3.2.5. Rate of reaction.....	56
3.2.6. Mesh grid study .....	57
3.3. Results and discussion.....	61
3.3.1. Base case.....	61
3.3.2. Parametric study .....	65
3.4. Conclusions .....	68
3.5. References .....	69
Chapter 4: MATHEMATICAL MODELLING OF A SEMI-DRY SO <sub>2</sub> SCRUBBER BASED ON A LAGRANGIAN-EULERIAN APPROACH (ARTICLE 2).....	71
4.1. Introduction .....	73
4.2. Governing equations.....	77
4.2.1. Continuous gas phase mixture.....	79
4.2.2. Dispersed-phase hydrated lime (Ca(OH) <sub>2</sub> ).....	81
4.3. Adsorption process .....	82
4.4. Meshing and boundary conditions.....	83
4.5. Results and discussion.....	85
4.5.1. Steady-state results .....	86
4.5.2. Transient results.....	90

4.6. Conclusions .....	100
4.7. References .....	101
Chapter 5: CONCLUSIONS AND RECOMMENDATIONS .....	103
5.1. General conclusions.....	103
5.2. Recommendations .....	104
APPENDIX: VALIDATION OF THE MATHEMATICAL MODEL .....	106

## LIST OF TABLES

Table 2.1. Effect of scrubbing temperature using NaOH and removal efficiency of SO <sub>2</sub> [10] .....	24
Table 2.2. SO <sub>2</sub> removal efficiency with different sorbent size at various $\Delta T_a$ [15].....	35
Table 3.1. Boundary Conditions .....	56
Table 3.2. Parameters used in the parametric study .....	65
Table 4.1. Dimensions of the scrubber and boundary conditions for gas and solid phases .	77
Table 4.2. Predicted desulfurization efficiency (percentage of SO <sub>2</sub> removed) under different conditions.....	88



## LIST OF FIGURES

Figure 2.1. Schematic process of aluminum production [3].....	9
Figure 2.2. Reduction lines (Hall-Heroult process).....	11
Figure 2.2. Reduction lines (Hall-Heroult process).....	16
Figure 2.2. Reduction lines (Hall-Heroult process).....	18
Figure 2.5. Sodium based absorber at the Alcoa Massena East smelter [3] .....	19
Figure 2.6. Limestone wet desulfurization using forced oxidation process [3] .....	21
Figure 2.7. Lime based wet desulfurization process [3] .....	23
Figure 2.8. Dry desulfurization scrubbing process [3] .....	25
Figure 2.9. Circulating dry scrubbing (CDS) desulfurization process [3] .....	26
Figure 2.10. Schematic process of semi-dry desulfurization using $\text{Ca}(\text{OH})_2$ .....	30
Figure 2.11. Illustration of slurry drying process inside the scrubber .....	31
Figure 2.12. Approach to saturation temperature definition [15] .....	32
Figure 2.13. The effect of the approach to saturation temperature on the $\text{SO}_2$ removal efficiency .....	35
Figure 2.14. Effect of Ca/S ratio on $\text{SO}_2$ removal efficiency .....	37
Figure 2.15. Effect of sorbent size on $\text{SO}_2$ removal .....	39
Figure 2.16. Gas passage through a porous medium .....	40
Figure 2.17. Effect of gas residence time on $\text{SO}_2$ removal.....	40
Figure 2.18. $\text{SO}_2$ removal efficiency as a function of gas inlet temperature at different $W_s$ and $\omega_0$ .....	42
Figure 2.19. Effect of temperature on $\text{SO}_2$ removal: RH = 30%, inlet $\text{SO}_2$ concentration = 2000 ppm .....	43
Figure 3.1. System: laboratory reactor.....	52
Figure 3.2. Mesh Independency Diagram.....	58
Figure 3.3. Mesh used: (a) Side view (b) Front view .....	59
Figure 3.4. Mesh used: (a) Top view (b) Bottom view.....	60
Figure 3.5. Mesh used: Cross-section on the central plane .....	60
Figure 3.6. Air mass fraction contours .....	62

Figure 3.7. SO <sub>2</sub> concentration contours [ppm] .....	63
Figure 3.8. Lime mass fraction contours .....	64
Figure 3.9. Velocity contour .....	65
Figure 3.10. The effect of inlet lime and SO <sub>2</sub> concentrations.....	66
Figure 3.11. The effect of gas humidity on desulfurization for an inlet lime fraction of 0.02 .....	67
Figure 3.12. The effect of gas humidity on desulfurization when the inlet SO <sub>2</sub> concentration is 300 ppm.....	68
Figure 4.1. Scrubber geometry: (a) front view, (b) side view .....	79
Figure 4.2. Meshed domain – front and side views .....	84
Figure 4.3. Meshed domain - Bottom view .....	84
Figure 4.4. Gas phase velocity distribution - Ca/S = 50; RH = 10%; (a) dp = 45 μm (b) dp = 10 μm .....	86
Table 4.5. The effect of particle size and relative humidity on the predicted desulfurization efficiency for the scrubber .....	88
Figure 4.6. Distribution of desulfurization levels at Ca/S = 50 for (a) dp = 10 μm; RH = 10% (b) dp = 45 μm; RH = 30%.....	89
Figure 4.7. Desulfurization efficiency as a function of time .....	91
Figure 4.8. Desulfurization efficiency contours - Ca/S = 50; dp = 45 μm; RH = 30%.....	93
Figure 4.9. Desulfurization efficiency contours - Ca/S = 50; dp = 10 μm; RH = 10 .....	94
Figure 4.10. Particle residence time - Ca/S = 50; dp = 10 μm; RH = 10%.....	96
Figure 4.11. Particle residence time - Ca/S = 50; dp = 45 μm; RH = 30%.....	98
Figure 4.12. DPM volume fraction - Ca/S = 200; dp = 10 μm; RH = 10% .....	99
Figure A 1. The reactor system built by CHIMI group .....	107
Figure A 2. Images of the transparent reactor system before and after the test.....	108
Figure A 3. Images of the reactor system at (a) 5 min, (b) 15 min, and (c) deposited lime on the bottom plate after reaction .....	109
Figure A 4. Comparison of modelling and experimental results for semi-dry conditions (RH ~ 35 %).....	110
Figure A 5. Comparison of modelling and experimental results for dry conditions .....	111

## LIST OF ABBREVIATIONS

BET	Brunauer-Emmett-Teller
CDS	Circulating Dry Scrubber
CFD	Computational fluid dynamics
DEM	Discrete element method
DPM	Discrete phase model
FGD	Flue gas desulfurization
FTC	Fume treatment centre
GTC	Gas treatment centre
OPEX	Operating cost
PAH	Polycyclic aromatic hydrocarbon
PPSB	Powder-particle spouted bed
RH	Relative humidity
RMS	Root mean square
SSA	Specific surface area
UDF	User-defined function
WHB	Waste Heat Boiler

## LIST OF SYMBOLS

$g$	Acceleration of gravity ( $\text{m/s}^2$ )
$\Delta T_a$	Approach to saturation temperature ( $^{\circ}\text{C}$ )
$T_b$	Bed temperature ( $^{\circ}\text{C}$ )
$V_{cell}$	Cell volume ( $\text{m}^3$ )
$L_s$	Characteristic length of system (m)
$u_s$	Characteristic velocity of system (m/s)
$a_i$	Constants for the drag coefficient model
$\rho$	Density ( $\text{kg/m}^3$ )
$\eta_{SO_2}$	Desulfurization efficiency (%)
$J_i$	Diffusion flux of species I ( $\text{kg/m}^2 \text{ s}$ )
$\epsilon$	Turbulent dissipation rate of kinetic energy ( $\text{J/kg.s}$ )
$C_D$	Drag coefficient
$D_{eff}$	Effective diffusivity of $\text{SO}_2$ in air and humidity ( $\text{m}^2/\text{s}$ )
$W_s$	Flowrate of slurry (lit/min)
$u$	Fluid velocity (m/s)
$T$	Gas temperature (K)
$T_0$	Initial gas temperature ( $^{\circ}\text{C}$ )
$C_{in}$	Inlet concentration of $\text{SO}_2$ (ppm)
$\omega_{SO_2}$	Mass fraction of $\text{SO}_2$ in gas phase
$\omega_{SO_2}^0$	Mass fraction of $\text{SO}_2$ in gas phase at the inlet
$\omega_i$	Mass fraction of species i
$\hat{R}_i$	Molar rate of reaction the reaction (species i) ( $\text{kg/m}^3\text{s}$ )
$\mu$	Molecular viscosity (Pa.s)
$M_{w,i}$	Molecular weight of species I (g/mol)
$R_i$	Net source of chemical species I ( $\text{kg/m}^3\text{s}$ )
$C_{out}$	Outlet concentration of $\text{SO}_2$ (ppm)
$A_p$	Particle area ( $\text{m}^2$ )
$\rho_p$	Particle density ( $\text{kg/m}^3$ )
$d_p$	Particle diameter ( $\mu\text{m}$ )
$m_p$	Particle mass (g)

$\dot{m}_{SO_2,k}$	Particle mass source term of SO <sub>2</sub> (kg/m <sup>3</sup> s)
$x_p$	Particle position vector (m)
$t_{res}$	Particle residence time (s)
$u_p$	Particle velocity (m/s)
$\nabla p$	Pressure gradient (Pa/m)
$Re$	Reynolds number
$Sc_t$	Schmidt number
$Y_{SO_2}$	SO <sub>2</sub> molar fraction
$X$	Sorbent molar conversion
$S_{SO_2}$	Source term of SO <sub>2</sub> (kg/m <sup>3</sup> s)
$\omega_0$	Specific water content in slurry
$p$	Static pressure (Pa)
$St$	Stokes number
$\bar{\tau}$	Stress tensor (Pa)
$U_{gas}$	Superficial gas velocity (m/s)
$Ca/S$	The molar ratio of calcium to sulfur
$t$	Time (s)
$D_t$	Turbulent diffusivity (m <sup>2</sup> /s)
$k$	Turbulent kinetic energy (J/kg.s)
$\sigma_k$	Turbulent Prandtl number (for $k$ equation)
$\sigma_\epsilon$	Turbulent Prandtl number (for $\epsilon$ equation)
$\mu_t$	Turbulent viscosity (Pa.s)
$I$	Unit tensor

## **DEDICATIONS**

This thesis is dedicated respectfully to my mother, Elaheh Afrooz, who has enlightened my life path and guided me in the right direction to make a self-directed son, and to my loving father, Alireza Fassadi Chimeh, without whose constant support I would never have been able to be where I am today.

At the same time, my thanks go to my family, especially my grandmother, Tooran Jafarghomi, who always inspire me.

## ACKNOWLEDGEMENT

To begin with, I would like to express my sincere gratitude to my supervisor, Prof. Duygu Kocaefe for her unconditional and continuous supports, guidance, and trusts during my master. She has done everything possible to provide me great opportunities to be a better engineer and researcher with her invaluable skills.

Also, I would like to express my special thanks to my co-supervisor, Prof. Yasar Kocaefe, for his technical and scientific discussions, comments, and guidance in each step of my journey, in spite of his responsibilities as a department chair.

I am also grateful to our industrial partner Rio Tinto, especially, Dr. Yoann Robert, and Mr. Jonathan Bernier for all the support and cooperation they gave for the success of this industrial project.

I am deeply grateful to my jury members, Professor Derek Harvey, Prof. Duygu Kocaefe, Prof. Yasar Kocaefe and Dr. Mounir Baitech for their worthwhile comments, guidance, and support.

I would like to thank Dr. Belkacem Amara and Dr. Karthikeyan Rajan for their countless technical help in every step of my masters.

My appreciation goes to Sylvain Truchon for his great performance as the technician, preparing the set-ups and providing assistance in experimental issues.

I do acknowledge Prof. Emad Elgalad, Prof. Zhan Zhang, Esmail Pourkhorshid, and Siamak Nikzad Khangholi for their suggestions during the optical microscope tests.

In the meantime, I would also like to express my deep gratitude to my colleagues and friends for their fruitful collaboration, scientific discussions, and sharing of their research experiences: MohammadHossein Dabaghi, Armita Rastegari, Julie Bureau, Ali Elasheri, etc.

Last but not least, the support of my close friends – Mohammadreza Basohbatnovinzad, Ali Kodfard, Farnaz Yavari – are greatly appreciated.

# CHAPTER 1

## INTRODUCTION

### 1.1. Introduction

Aluminum electrolysis uses a considerable quantity of electrical energy. If this energy is produced using coal in thermal power plants, it contributes significantly to air pollution. However, aluminum is produced in Quebec using the hydroelectric power, which makes it the greenest aluminum in the world.

Thermal power plants [1, 2] and aluminum smelters [3-5] using power provided by these plants cause significant air pollution. In addition to other gases (CO, CO<sub>2</sub>, NO<sub>x</sub>, etc.), they emit sulfur oxides due to the reaction of sulfur with oxygen (O<sub>2</sub>) present in air [2]. The SO<sub>2</sub>/SO<sub>3</sub> emitted to the atmosphere reacts with water, forming H<sub>2</sub>SO<sub>4</sub> – one of the main sources of acid rain. Acid rain is highly detrimental to both environment as well as animal and human life.

In general, one of the main objectives of these industries is to reduce the concentration of pollutants before discharging into the atmosphere, so that it conforms with environmental regulations such as 88/609/CEE and 2001/80/CEE [6]. The desulfurization process is carried out using a wide range of technologies that will be discussed [1, 7-9].

The process of SO<sub>2</sub> elimination from the contaminated gas streams is known as the desulfurization process. The main objective of this process is to alleviate the concentration of SO<sub>2</sub> from an effluent gas coming from an industrial plant to reduce acid rain [2, 10]. The use of various methods ranging from absorption [10] to adsorption [1, 8] leads to different by-product generation through the desulfurization process.



The desulfurization could be carried out using three different methods depending on how the SO<sub>2</sub> is removed in the process [1]. Due to the acidic nature of SO<sub>2</sub>, an alkaline reagent is used ranging from a calcium-based reagent, e.g. hydrated lime (Ca(OH)<sub>2</sub>), to sodium-based reagent, e.g. sodium hydroxide (NaOH), to achieve acceptable SO<sub>2</sub> removal efficiency (desulfurization efficiency) [2, 10].

The desulfurization efficiency is a function of various parameters; and some of the major ones are given below [8, 11]:

- Relative humidity (RH)
- Sorbent molar ratio (Ca/S)
- Sorbent particle size (d<sub>p</sub>)
- Temperature

The main objective of this project is to develop a mathematical model for a laboratory-scale reactor to determine the effects of major parameters on the desulfurization efficiency. The identification of the most important parameters affecting the desulfurization process will help model the desulfurization in more complicated industrial systems. It is important to represent the phenomena taking place as closely as possible to the actual physical phenomena occurring in the process. For the desulfurization of a gas using lime particles, it is important to account for the reaction taking place on the particle surface.

## **1.2. Statement of the problem**

Increasing SO<sub>2</sub> emissions from any source leads to increased acid rain which results in pollution problems, including but not limited to the events cited below [2]:

- It contaminates the surface waters, leading to the destruction of aquatic life, especially when pH is low ( $\text{pH} < 5$ ).
- Individuals suffering from respiratory diseases such as asthma may lose their lung defense when they are exposed to  $\text{SO}_2$ .
- Agricultural lands get seriously contaminated.
- Irreversible deterioration occurs on historical and ancient buildings.

### **1.3. Objectives**

The principal objective of this study is to develop a mathematical model of an  $\text{SO}_2$  scrubber using hydrated lime in order to treat the effluent gases from the electrolysis process in aluminum industry.

The specific objectives are given below:

- Determination of the factors affecting the desulfurization process and  $\text{SO}_2$  removal efficiency.
- Comparison of the effects of humidity and sorbent size on removal efficiency in order to select an appropriate condition for the desulfurization process.
- Distinguishing the reactant and product particles through the particle surface reaction in the model.
- Developing a general UDF code (Ansys-Fluent) in C language which can be used to model the reaction occurring on the surface of solid particles (gas-solid reaction).

#### **1.4. Originality statement**

Generally, a few studies have been done on the desulfurization of effluent gases from the aluminum smelters. In this project, the focus was on the modelling of a desulfurization process at low temperatures (around 100 °C) as opposed to the thermal power plants where the desulfurization process is carried out at higher temperatures. The concentration of SO<sub>2</sub> from the electrolysis cells (usually within the range of 100 – 400 ppm) is not as high as those emitted from other industries such as the thermal power plants (in thousands of ppm). Even such small sulfur contents must be treated before discharging the gas into the atmosphere, so it makes the process challenging.

In addition, a comparison between the effects of humidity and sorbent size was carried out through a multi-phase (gas – solid) modelling including the particle surface reaction; few studies are available treating such complex reaction systems. The content of the UDF used defines a reaction takes place at the surface of each particle through a kinetic reaction rate. It is possible to use this approach for any other system involving a gas-solid reaction. The coding which considers the gas-solid reaction on the particle surface as well as the impact of the presence of humidity is rare. The reaction rate was obtained from the literature.

In addition, the effects of both continuous phase and dispersed phase (particle phase) on each other are rarely considered due to the complexity of the reaction. During this study, the two-way coupling of solid and gas phases was carried out using the DPM model for the desulfurization of effluent gases from aluminum electrolysis cells. Therefore, the particle size effects on the flow field and other parameters (desulfurization efficiency, particle trajectories) can be determined. It is also rare to find such studies in the literature, as the particle size effect and RH impact on

desulfurization in conjunction with two-way coupling besides particle tracking altogether in one study is entirely novel.

### **1.5. Scope**

This master thesis contains five chapters. Following introduction, a comprehensive literature review on the desulfurization process and the various methods used for this process, including the advantages and drawbacks of each are presented in Chapter 2. Also, the literature review includes the aluminum production and the SO<sub>2</sub> generation in this process. Various methods to reduce the SO<sub>2</sub> emission are discussed.

In Chapter 3, the paper entitled “Mathematical modelling of the desulfurization of electrolysis cell gases in a low temperature reactor” published in *Light Metals 2023* and presented in the TMS 2023 conference is given. This paper is drawn from the first part of the results of this project. It illustrates how the relative humidity (RH) presence and sorbent rate (Ca/S) can affect the desulfurization efficiency using a Eulerian - Eulerian multi-phase reacting flow. It also shows that excessive sorbent utilisation does not further contribute to the removal efficiency.

In Chapter 4, the manuscript entitled “Mathematical modelling of a semi-dry SO<sub>2</sub> scrubber based on a Lagrangian-Eulerian approach” is presented, which is ready for submission to a journal. In this work, the results show how the changes in particle size ( $d_p$ ), relative humidity (RH), and sorbent rate (Ca/S) can affect the desulfurization efficiency. Through the use of two-way coupling in the DPM model, it compares two cases, the use of: 1) smaller sorbent particle size with lower RH and 2) larger sorbent particle size with higher RH, and Ca/S ratio was kept constant. The first case resulted in slightly more efficient desulfurization than the second one. It was found that

increasing RH can compensate for the efficiency reduction when larger sorbent particles are used. This article presents the particle tracks that show the particle residence time, distinguishing the fresh lime particles from those that are reacted and have calcium sulfite (the reaction product on them).

In Chapter 5, conclusions and recommendations are presented. In the Appendix, the validation of the model under a specific condition is presented.

## 1.6. References

1. Ma, X., et al., *Use of limestone for SO<sub>2</sub> removal from flue gas in the semidry FGD process with a powder-particle spouted bed*. Chemical Engineering Science, 2000. **55**(20): p. 4643-4652.
2. Prasad, D.S.N., et al., *Removal of sulphur dioxide from flue gases in thermal plants*. Rasayan Journal of Chemistry, 2010. **3**: p. 328-334.
3. Zettler, S., N. Fortin, and K. Moran, *Feasibility report on technical options to reduce SO<sub>2</sub> emissions Post-KMP*. 2013, Rio Tinto Alcan.
4. Charette, A., Y. Kocaefe, and D. Kocaefe, *Le carbone dans l'industrie de l'aluminium*. 2012: PRAL - Press Aluminium.
5. Maltais, J.-N., et al., *Development, Proof of Concept and Industrial Pilot of the New CHAC Scrubbing Technology: An Innovative and Efficient Way to Scrub Sulfur Dioxide*. 2016. p. 473-478.
6. Gómez, A., N. Fueyo, and A. Tomás, *Detailed modelling of a flue-gas desulfurisation plant*. Computers & Chemical Engineering, 2007. **31**(11): p. 1419-1431.
7. Kang, S.Y., et al., *A comparative evaluation of recarbonated CaCO<sub>3</sub> derived from limestone under oxy-fuel circulating fluidized bed conditions*. Science of The Total Environment, 2021. **758**: p. 143704.
8. Garea, A., et al., *Kinetics of dry flue gas desulfurization at low temperatures using Ca(OH)<sub>2</sub>: competitive reactions of sulfation and carbonation*. Chemical Engineering Science, 2001. **56**: p. 1387-1393.
9. Bausach, M., et al., *Kinetic modelling of the reaction between hydrated lime and SO<sub>2</sub> at low temperature*. AIChE Journal, 2005. **51**: p. 1455-1466.
10. Sharma, R., S. Acharya, and A.K. Sharma, *Effect of Absorption of Sulphur Dioxide in Sodium Hydroxide Solution to Protect Environment : A Case Study at Shree Power, Beawar, Rajasthan*. international journal of chemical sciences, 2010. **8**: p. 1021-1032.
11. Ma, X., et al., *Removal of SO<sub>2</sub> from flue gas using a new semidry flue gas desulfurization process with a powder-particle spouted bed*. The Canadian Journal of Chemical Engineering, 1999. **77**(2): p. 356-362.

## **CHAPTER 2**

### **LITERATURE REVIEW**

#### **2.1. Introduction**

Aluminum is one of the metals widely utilized in construction, transportation, etc. due to its distinct properties [1]. Canada is considered as one of the largest aluminum manufacturing and exporting countries. In 2020, Canada produced approximately 3.2 million tonnes of aluminum and 90% of this amount was produced in Quebec. This province invested more than 3.6 billion dollars in the aluminum industry in 2020 [2]. Rio Tinto is one of the global leaders in aluminum manufacturing. It has six smelters in Quebec and one smelter in British Columbia [3].  $\text{SO}_2$  is present in the outlet gas of electrolysis cells. Previously, researchers focused on  $\text{H}_2\text{SO}_4$  production from this  $\text{SO}_2$ . However, due to a lack of demand for sulfuric acid,  $\text{SO}_2$  had to be disposed in other ways [4]. The amount of  $\text{SO}_2$  production in an aluminum plant is related to the sulfur content in the coke which is used for anode production. Increase in aluminum production, increases the amount of anode used. Thus, it increases the  $\text{SO}_2$  emissions [3]. Figure 2.1, presents the steps of the aluminum manufacturing process.

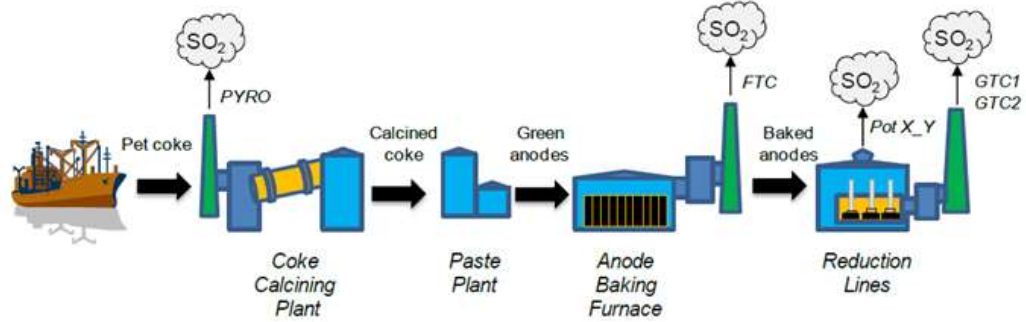


Figure 2.1. Schematic process of aluminum production [3]

The petroleum coke (pet coke) comes from the residue cut of the distillation tower in an oil refinery. Pet coke's sulfur content depends on the source of petroleum. Industry mixes various petroleum cokes from different sources to have the desired sulfur content in green coke. Low sulfur content sources are preferred. But they are rarely available and relatively expensive to use. On the other hand, the sulfur content should not be too low, because it is able to reduce the catalytic effect of the metallic impurities such as Ni and V, and enhance the coke density, leading to a better process in smelters [3].

The petroleum coke contains volatiles. It must be calcined to release the volatiles and obtain a calcined coke with a better structure, which is used in anode production. This calcination process is done in the calcining plant where the petroleum coke is heated in a kiln. It is worth mentioning the emitted  $SO_2$  in the calcining plant originates from two sources; partial combustion of petroleum coke during calcination and the combustion of fuel used for heating the kiln [3].

The next step is the paste production. In this part, the calcined coke is blended with rejected anodes, butts recycled from the reduction lines, and pitch in order to form green anode. There is no sulfur emission at this stage [3].



The anode is baked in a furnace to form hard blocks of carbons (baked anode). There may be a small amount of SO<sub>2</sub> emission during baking if the anodes are heated to temperatures much higher than the coke calcination temperatures. Through the anode baking process, tar (polyaromatic hydrocarbon, PAH), CH<sub>4</sub>, and H<sub>2</sub> are released as volatiles. Tar, H<sub>2</sub>, and CH<sub>4</sub> are used as fuel in the kiln. Unburnt parts of these gases are separated in the fume treatment centre (FTC). When the anode blocks are cooled, they are rodded, and sent to the reduction cells [3].

Last step is the reduction lines. At this stage, the raw material for the aluminum manufacturing process – alumina (Al<sub>2</sub>O<sub>3</sub>) – dissolves in a cryolite (Na<sub>3</sub>AlF<sub>6</sub>) bath and dissociates into aluminum (Al<sup>3+</sup>) and oxygen (O<sub>2</sub><sup>-</sup>) ions through the electrochemical reaction. This process is called Hall-Heroult and illustrated in Figure 2.2. The molten aluminum forms at the cathode and accumulates at the bottom while the oxygen formed collects under the anode. The oxygen reacts with carbon at the hot anode surface and forms mainly CO<sub>2</sub> (and some CO). Meanwhile, the sulfur also reacts with oxygen to form SO<sub>2</sub> which oxidizes to form SO<sub>3</sub>. Then, SO<sub>2</sub> is discharged to the atmosphere from a gas treatment centre (GTC). Anodes are replaced periodically. Unused part of the anode (anode butt) is recycled back to the paste plant [3].

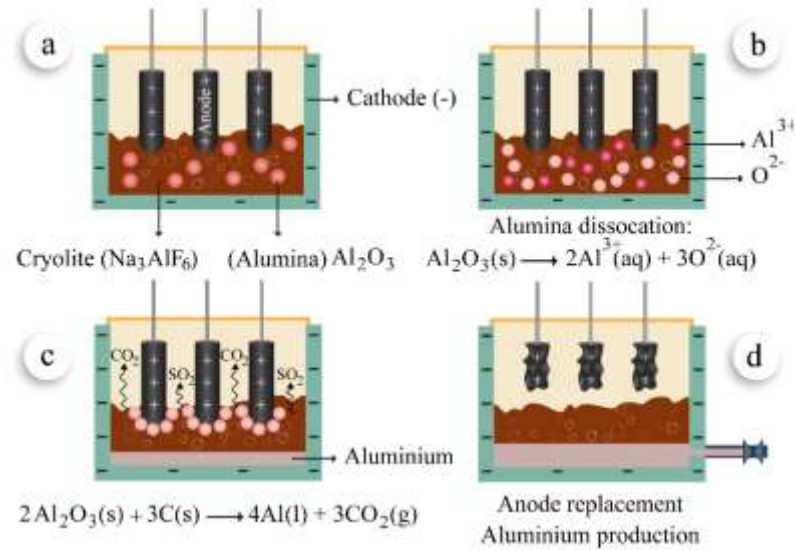


Figure 2.2. Reduction lines (Hall-Heroult process)

© Arash Fassadi Chimeh, 2023

The desulfurization process is the removal or the reduction of sulfur dioxide ( $\text{SO}_2$ ) concentration present in a gaseous stream. There are three different methods of desulfurization known as wet, dry, and semi-dry [5].

A dry desulfurization process involves the contact of  $\text{SO}_2$ -containing gas with a dry solid reagent whereas a wet desulfurization process involves the partial or complete dissolution of reagents in water [6]. During the wet desulfurization process,  $\text{SO}_2$  containing gas passes through a liquor which absorbs the  $\text{SO}_2$  from the gas. This makes the process more complex than the dry process and it is recommended for rich  $\text{SO}_2$  streams. Additionally, the wet desulfurization is a capital-intensive process and is therefore not recommended for high flow rates and/or low concentrations [3]. The presence of a filter in dry (or semi-dry) process requires a larger equipment since the filtration velocity reduces the velocity of gas passing through the equipment [3]. The semi-dry process is carried out with a slurry formed of sorbent and water mixture which

contains a specific amount of water to provide some humidity to enhance the SO<sub>2</sub> reactivity.

In a semi-dry process, no water treatment and reheating energy is required [6]. This process is not as efficient as the wet desulfurization process for industrial applications; however, its lower operating cost compared to that of the wet process and its simplicity have attracted significant attention [7, 8].

The SO<sub>2</sub> removal efficiency ( $\eta$ ) can be determined via Eqn. (2.1):

$$\eta(\%) = \frac{C_{in} - C_{out}}{C_{in}} \times 100 \quad (2.1)$$

where  $C_{in}$  is the SO<sub>2</sub> concentration at the scrubber inlet, and  $C_{out}$  is the SO<sub>2</sub> concentration at the scrubber outlet.

As explained previously, aluminum smelters emit SO<sub>2</sub> similar to other metal manufacturing industries [4]. SO<sub>2</sub> emission control has a significant importance for all the industries, and aluminum is not an exception [3, 9]. The studies focusing on SO<sub>2</sub> emission control in aluminum smelters are quite rare. The source of sulfur is mainly the coke used in anode production, while pitch also contains a small amount of sulfur. These are the main raw materials of anodes which are used in the electrolysis. The stack gas must meet the maximum allowable SO<sub>2</sub> content requirement to protect the eco system [10]. The amount of SO<sub>2</sub>, which must be removed depends on the source it comes from, either from the flue gas of a thermal power plant [10] or the stack gas of an aluminum manufacturing plant [3]. The sources of SO<sub>2</sub> are various types of fuels and coke/pitch, respectively [10, 11]. Compared to the emission from thermal power plants, the gas released to air from the aluminum manufacturing plants contains a

significantly lower amount of SO<sub>2</sub>. The elimination of SO<sub>2</sub> at a very low concentration from a gas is more difficult compared to that at a higher concentration [3, 9].

There are a number of methods for an aluminum manufacturing plant in order to reduce the SO<sub>2</sub> emission. These are categorized below, and each is going to be elaborated in the following sections [3]:

- Utilization of low-sulfur petroleum coke source
- Pre-calcined coke utilization
- Pre-baked anode utilization
- Reduction in aluminum production capacity
- SO<sub>2</sub> scrubbing technology implementation

#### **2.1.1. Utilization of low-sulfur petroleum coke**

One of the means for sulfur content reduction is to choose a low-sulfur pet coke source. Considering the limited petroleum resources, sulfur content of cokes is increasing. The demand of the aluminum manufacturers for low-sulfur coke increased. Consequently, the access to such coke is not easy and it is relatively expensive. Thus, in order to remain competitive, the usage of high-sulfur content coke is necessary, but this requires the removal of SO<sub>2</sub> with scrubbers [3].

#### **2.1.2. Pre-calcined coke utilization**

The option of stopping on-site calcination and purchasing pre-calcined coke from external suppliers could be a potential means of sulfur emission reduction. The calcination process is considered as one of the major sources of SO<sub>2</sub> emission. Thus, the elimination of this step does not lead to a significant decrease in the overall SO<sub>2</sub> emission since the green coke still has to be calcined. Moreover, the shutdown of the

calcination plant results in not only job losses, but also loss of investments in calcination kilns [3].

### **2.1.3. Pre-baked anode utilization**

Another strategy is to purchase pre-baked anodes. The modern aluminum smelters have anode plants to produce pre-baked anodes on site. Thus, they do not buy pre-baked anodes from other suppliers unless it is absolutely necessary [3].

### **2.1.4. Reduction in aluminum production capacity**

Owing to the existence of a relation between the aluminum production capacity and the SO<sub>2</sub> emission, the reduction in capacity is an option to achieve less SO<sub>2</sub> emission. The fewer is the number of anodes utilized, the less SO<sub>2</sub> is expected to be emitted from the stacks. Due to the loss of production capacity, this would be the last option that the industries would resort to [3].

### **2.1.5. SO<sub>2</sub> scrubbing technology implementation**

The SO<sub>2</sub> scrubbing to reduce the sulfur emission is effective to achieve the emission control. Although it requires further investment, it allows the process to use high-sulfur content petroleum coke which is comparatively cheaper and easily available. As a result, not only the feed flexibility but also the valorization of by-products may compensate for the SO<sub>2</sub> scrubbing expenses [3].

## **2.2. Wet desulfurization process**

In this process, the SO<sub>2</sub>-containing gas is scrubbed through a liquid sorbent column or in a spray tower to remove the SO<sub>2</sub> from the gas, achieving a high level of removal. In the spray tower, the liquid sorbent is sprayed downwards to provide a good contact

with the gas flowing upwards. The spray nozzles have been used to atomize the liquid stream, providing a greater surface contact, while mist eliminators have been utilized to ensure the gas leaves the scrubber without any droplets [3].

There are several types of wet desulfurization processes as given below:

- Seawater wet scrubbing
- Sodium based wet scrubbing
- Limestone wet scrubbing
- Lime based wet scrubbing

### **2.2.1. Seawater wet scrubbing**

Seawater consisting of bicarbonate and carbonate compounds is widely used for SO<sub>2</sub> scrubbing, especially when the concentration of SO<sub>2</sub> in the gas is less than 1500 mg/Nm<sup>3</sup>. For SO<sub>2</sub> scrubbing, the main factor in seawater is the alkalinity since this property allows the SO<sub>2</sub> to be neutralized. During this process, sodium bicarbonate (NaHCO<sub>3</sub>) in seawater reacts with SO<sub>2</sub> when they come into contact. In seawater desulfurization applications, a range of alkalinity of about 90-100 mg/lit CaCO<sub>3</sub> is sufficient. Due to the low value of sodium bicarbonate content of seawater, there is a possibility of adding caustic soda (NaOH), to increase the alkalinity and obtain sufficient neutralization [3]. As can be seen in Figure 2.3, to ensure that the seawater contains the desired alkalinity, it must be taken from a sufficient depth. The pH on the surface of ocean is lower (more acidic) due to the acid rain, etc., while the average pH of ocean is 8.0 [3].

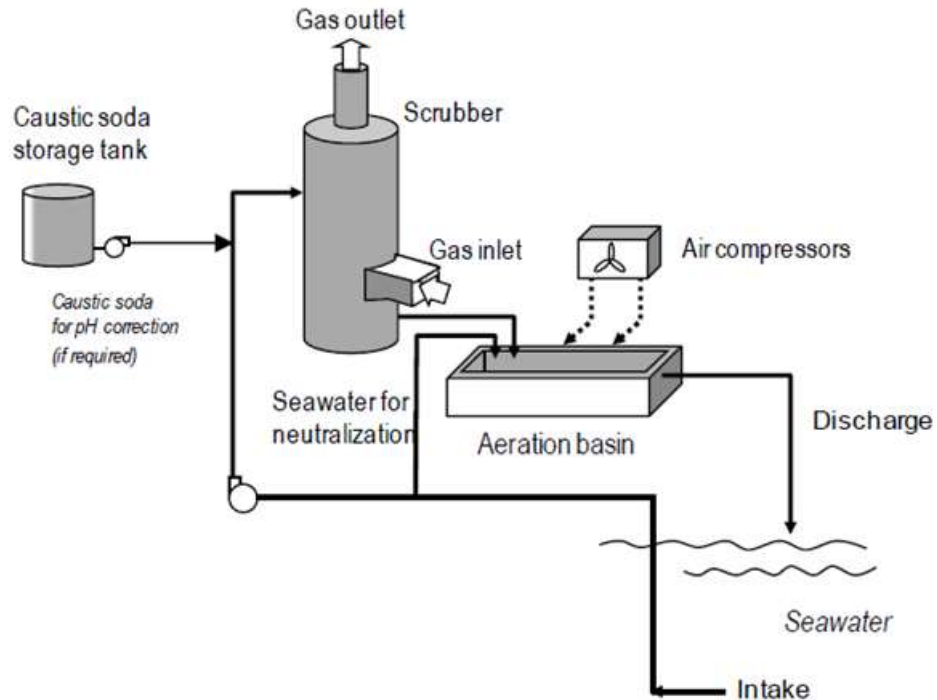


Figure 2.3. Seawater wet desulfurization process [3]

In the tower, the liquor is distributed through spray banks that contain nozzles from various sections of the absorber. Meanwhile, the gas entering the absorber is washed by liquor, and then exhausted from the top. When  $\text{SO}_2$  reacts with sodium bicarbonate ( $\text{NaHCO}_3$ ), sodium sulfate ( $\text{Na}_2\text{SO}_4$ ) is produced. First,  $\text{SO}_2$  converts to sulfite ( $\text{SO}_3^{2-}$ ), and then the oxygen in the gas leads to the conversion of sulfite to sulfate ( $\text{SO}_4^{2-}$ ) via a process known as natural oxidization. Owing to the insufficient oxygen content of the gases, air compressors are also employed to bubble the air in the aeration basin to achieve complete oxidation. Due to the high acid content of the seawater at the outlet of the absorber, it is mixed with the intake seawater in the aeration basin to ensure that the pH of water is safe enough (6.5 or above) to be sent back to the ocean. The control of temperature is also important. Temperature increases must not exceed a few degrees above the actual sea temperature; otherwise, the sea life may be endangered.

Seawater is used once, and no recirculation is done. This is because the recycling can lower pH as well as increase the temperature of discharged seawater, which will have irreversible effects on fish and other marine life. Also, this will increase seawater's sulfate content. Seawater scrubbing is a simple, highly effective, and economical process, even though it is only applicable to coastal plants [3].

### **2.2.2. Sodium-based wet scrubbing**

Sodium salts dissolved in water are considered as an effective method to neutralize  $\text{SO}_2$  and absorb it in the water. The main reagents of sodium based wet scrubbing process are caustic soda ( $\text{NaOH}$ ) and sodium carbonate ( $\text{Na}_2\text{CO}_3$ ). Taking a detailed look to Figure 2.4 reveals that the whole process is more complicated than the configuration of wet scrubbing using seawater. However, it is the most effective one among the wet desulfurization processes [3]. Soda ash, that is stored in the soda ash silo is mixed into the water supply to form soda ash solution. Thereafter, this liquor is blended to the used liquor coming out of absorber and recycled to the spray banks using a pump. Due to the high level of acid content in the exhausted slurry stream, a certain amount of soda ash solution is blended with it in order to elevate the pH. The pH of collected liquor is measured and controlled at the bottom of tower. The process operates in the pH range of 6.5 – 7.0. Above this range, the  $\text{CO}_2$  is also absorbed, which leads to excessive reagent usage. The recycled liquor is atomized via the spray nozzles present at different levels of scrubber [3]. In all spray towers used for  $\text{SO}_2$  scrubbing, the solution is recirculated except in the case of seawater as it is a once-through process.

In such processes, it is desired to minimize the calcium content in order to prevent the uncontrolled gypsum formation. To respond to this demand, a water-softening



system is provided. This system reduces the calcium content of freshwater feed. Due to evaporation taking place inside the spray nozzles, a certain amount of fresh water also enters through the bottom of absorber shown by the level controllers installed inside the tower [3].

Inside the absorber, either  $\text{Na}_2\text{CO}_3$  or  $\text{NaOH}$  are utilized as the reagent. The product is the same. A liquor containing 10 – 15 wt.% sodium sulfate ( $\text{Na}_2\text{SO}_4$ ) is produced through the reactions given in Eqn. (2.2) and Eqn. (2.3) and leaves the tower [3].

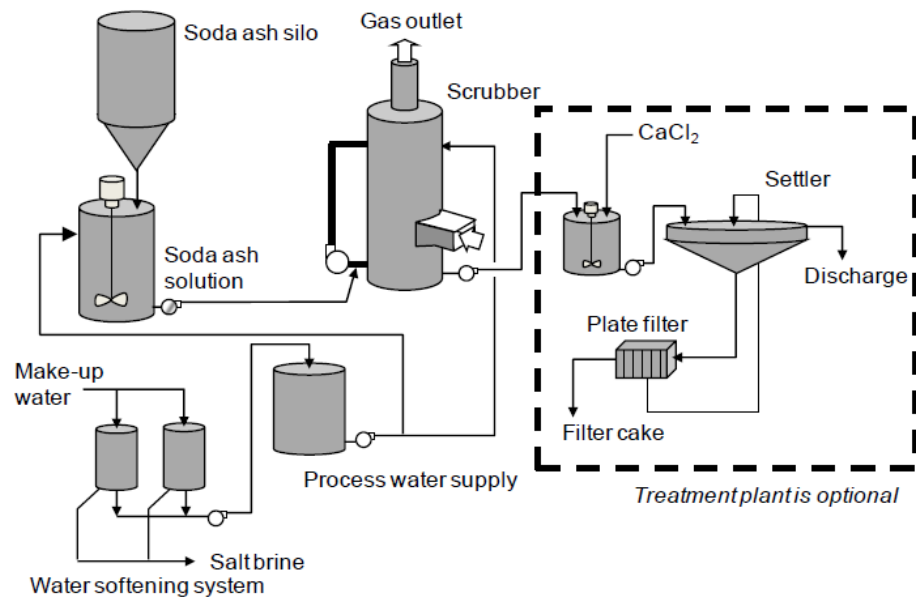
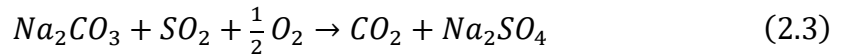
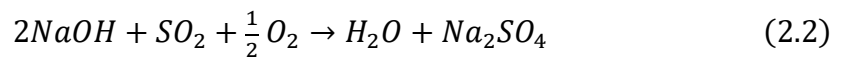
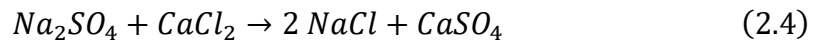


Figure 2.4. Sodium based wet desulfurization scrubbing process [3]

Considering the existence of sodium sulfate at the bottom stream of the absorber, an optional treatment plant can be added to the process although it is a complex unit. It has been widely accepted that the sodium by-products such as  $\text{Na}_2\text{SO}_4$  are more difficult to dispose of compared to lime by-products due to its solubility in water.

Moreover, it is also important to know the quality of by-product in any scrubbing process because they must be either sold or disposed [3]. In the treatment plant, the bottom stream is mixed with calcium chloride ( $\text{CaCl}_2$ ) which converts the majority of  $\text{Na}_2\text{SO}_4$  to calcium sulfate (gypsum) based on the Eqn. (2.4). The filter is used to separate the water from the gypsum which is a highly demanded by-product for wallboard manufacturing and agricultural industries. The water is discharged to the surface waters including but not limited to the local rivers [3].



This process is fairly attractive hence it is used in some industrial plants such as Alcoa Massena East (USA) smelter which can be seen in Figure 2.5 [3].



Figure 2.5. Sodium based absorber at the Alcoa Massena East smelter [3]

### **2.2.3. Limestone wet scrubbing**

This process which uses limestone is considered as the most popular SO<sub>2</sub> scrubbing process in the world. The main by-product generated from this process is gypsum, which is highly demanded for various application ranging from agriculture to wallboards in all continents. As shown in Figure 2.6, the limestone particles of 1 – 5 cm in size, which are stored in the silo, are fed to the mill and mixed with water. Therefore, a slurry forms in the mill with 20 – 25 wt.% limestone. After, the slurry is stored in a storage tank and fed to the absorber at a specific flow rate and pH adjusted with the control system. The range of pH in this process should be 5.5 – 5.8. Limestone dissolves in water very slowly. The final gypsum product must contain only 2 wt.% limestone. If the pH is higher than the maximum pH of the acceptable range, the amount of unreacted limestone in the gypsum becomes too high [3]. A benefit of limestone usage is that not only it is much more available, but also it is 5 to 10 times cheaper compared to hydrated lime. However, the latter provides a better surface contact [6].

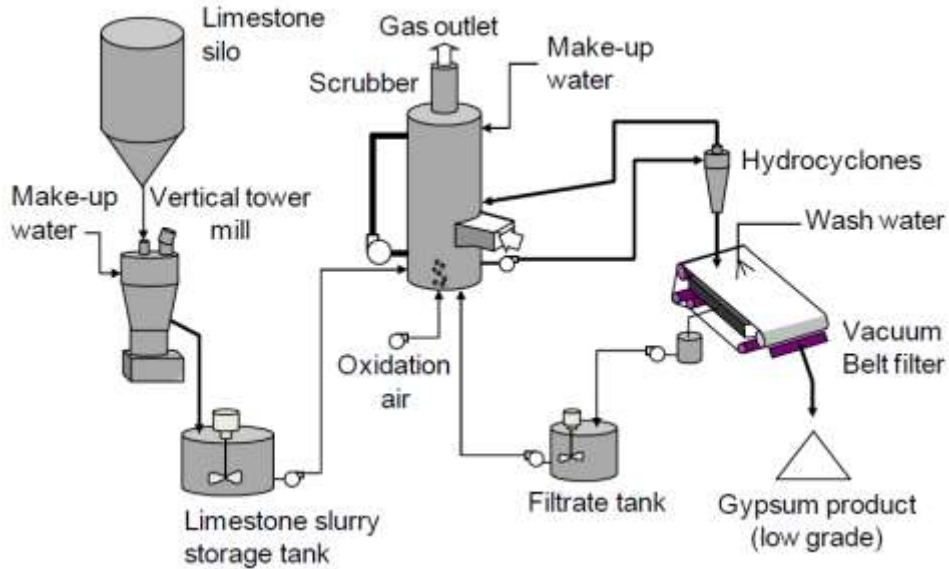


Figure 2.6. Limestone wet desulfurization using forced oxidation process [3]

The process of scrubbing is carried out within the absorber using spray at different levels. In the bottom section of the absorber, air is bubbled through the slurry to oxidize sulfite to sulfate, whilst make-up water is also fed to compensate for the vaporized slurry in the process. It is recirculated in a way similar to wet scrubbing processes (except seawater usage) to increase the process efficiency [3].

A bleed stream is taken to the hydro cyclone where the finer particles are separated from the coarser ones, returning those which are less than 50 – 60 microns in size back to the absorber. The cyclone underflow is a slurry which consists of 30 – 35 wt.% solids dewatered through the vacuum belt filter process to produce gypsum. The filtered water from the slurry is recycled to the absorber [3].

If the concentration of  $\text{SO}_2$  in gas is relatively high, it is possible to produce a high-grade gypsum employed for wallboard application. For the gases with relatively low  $\text{SO}_2$  concentration, the produced low-grade gypsum is only utilized for agricultural processes. Thus, to achieve a high-grade gypsum (wallboard application), a set of water

treatment systems must be considered, which is a more complicated process. Owing to the low SO<sub>2</sub> emitted from the aluminum smelters, the generated gypsum can't be used for wallboard industries. However, it can be used for fertilizer production. Thus, there is no solid waste associated with this process [3].

#### **2.2.4. Lime-based wet scrubbing**

The process of lime-based wet desulfurization is almost similar to the limestone wet desulfurization, although the lime (CaO) – quick lime – has a better SO<sub>2</sub> reactivity and absorption. Consequently, the size of equipment (absorber height, pump capacity, etc.) is smaller compared to limestone case. The main by-product of this process is also the same as that produced with the limestone which is gypsum [3].

In accordance with Figure 2.7, at first, the lime known as quick lime (CaO) coming from the silo is mixed with water, forming Ca(OH)<sub>2</sub> slurry called hydrated lime liquor based on the reaction Eqn. (2.5) [3]:



Considering that the reaction shown in Eqn. (2.5) is exothermic, it requires a particular mixer for mixing with water before sending lime to the lime slurry storage tank, grit and pebbles are also separated from lime. A specific flow of lime slurry is fed to the absorber under a controlled pH condition whilst the pH range should be 6.0 – 6.5 [3].

The SO<sub>2</sub> scrubbing process in lime-based wet desulfurization is similar to the process which uses limestone. The produced gypsum generated from this process is reasonably safe to be put in landfill sites [3].

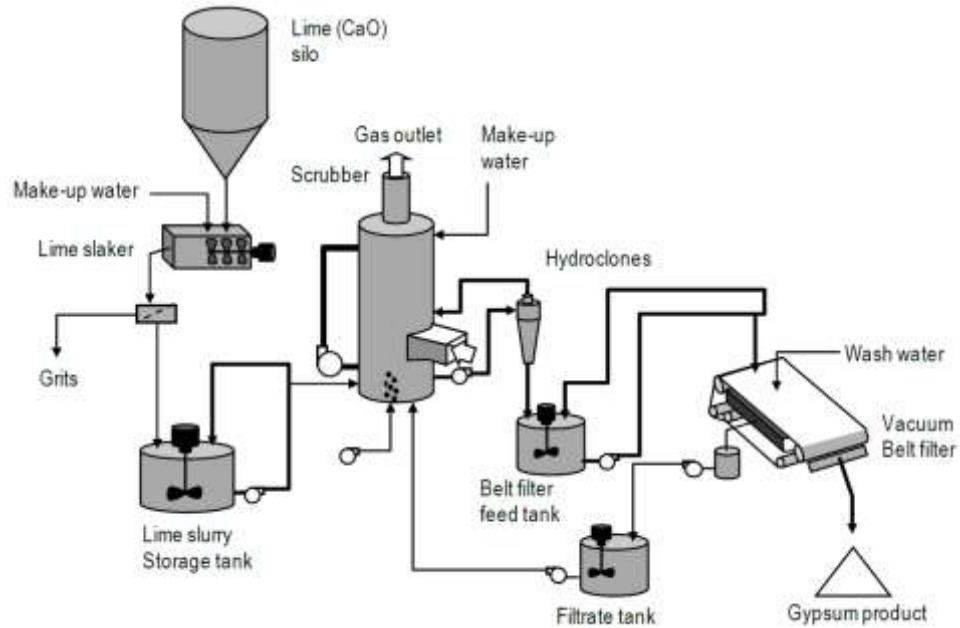


Figure 2.7. Lime based wet desulfurization process [3]

There are various reported research works focusing on wet desulfurization process [10, 12]. These publications are related to the industrial plants emitting  $\text{SO}_2$ , such as the Shree Power Plant – Rajasthan, India or Alcoa Massena East smelter – USA [3, 10].

As shown in Table 2.1 taken from the Shree Power Plant case study with a 3000 ppm  $\text{SO}_2$  load in flue gas [10], using cooler absorbent (approximately 130 °C) resulted in a relatively higher desulfurization efficiency compared to the numbers of Table 2.1. This temperature is close to the temperature of the gas coming out of the electrolysis process in aluminum industries which is 60 °C to 130 °C [13]. It is comparatively lower than flue gas temperatures of other industries, for example, in the range of 150 – 200 °C in the power plants [14].

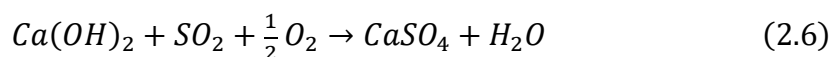
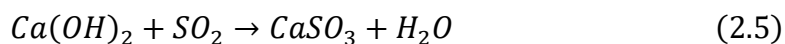
Table 2.1. Effect of scrubbing temperature using NaOH and removal efficiency of SO<sub>2</sub> [10]

NaOH Solution temperature (°C)	SO <sub>2</sub> Removal (%)	Sodium Sulphate (%)
20-25	90.18	1.1
25-30	81.62	0.745
30-35	78.08	0.39

The presence of higher amounts of reagents leads to greater alkalinity and much better SO<sub>2</sub> removal [3, 6, 7] even though there is an optimum value. Feeding excessive reagent (expressed as Na/S in this case) not only is a waste of absorbent, but also does not contribute further to the desulfurization [12].

### 2.3. Dry desulfurization process

In this process, which is efficient for low SO<sub>2</sub> concentrations, a dry reagent, e.g., lime, is injected into the SO<sub>2</sub>-containing gas stream. As soon as the hydrated lime mixes with SO<sub>2</sub>, the reaction shown in Eqn. (2.6) in case of full oxidation and the reaction shown in Eqn. (2.5) in case of partial oxidation take place on the surface of lime particles. The outer surface is covered with a mixture of calcium sulfite (CaSO<sub>3</sub>) and calcium sulfate (CaSO<sub>4</sub>) – gypsum; the latter is formed when a part of the former is oxidized with the oxygen available in the gas stream [3].



If there is no humidity in the sorbent or in the gas during this process, the reaction of SO<sub>2</sub> with dry sorbent is extremely slow. Therefore, it requires a significant amount

of sorbent which increases the operating cost (OPEX) and consequently makes it unattractive even if no precipitation equipment is required [8, 15].

According to Figure 2.8, the dry reagents, e.g., lime, stored in a silo are passed through the water vapor for a short time to form hydrated lime, but the reagents are still solid and dry. Following the injection of lime to the gas stream, lime combined with  $\text{SO}_2$ -containing gas goes through the filter units. The produced solid and reacted lime are captured in the baghouse filters, while the clean gas leaves the filter and discharged into the atmosphere. The solids in the baghouse unit are collected from the bottom of each compartment. A certain amount of the produced solid is taken to the storage, whilst the rest is recycled back to the injection section [3].

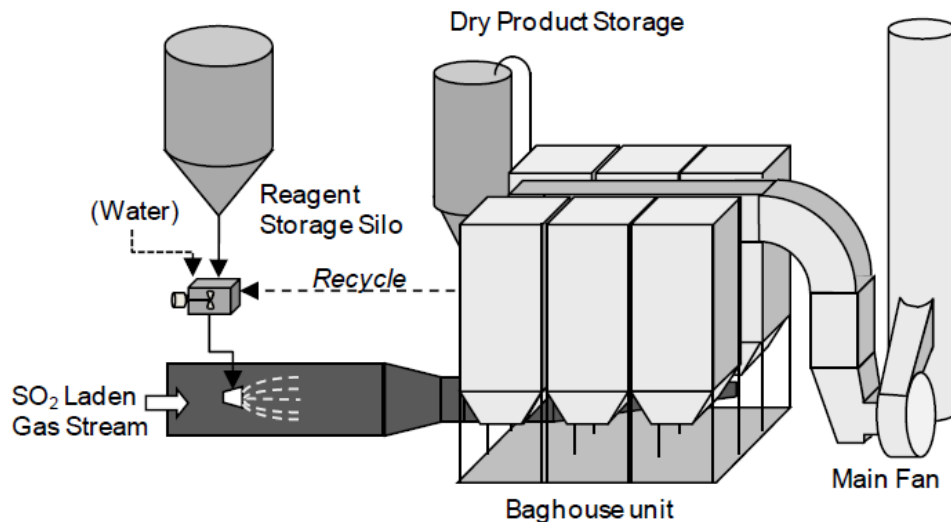


Figure 2.8. Dry desulfurization scrubbing process [3]

The dry scrubbing described above is somewhat costly, since the recycling of produced solid leads to a high usage of lime. To prevent this issue, a fluidized-bed advanced technology of dry desulfurization is also proposed known as the circulating dry scrubber (CDS) [3].



As observed in Figure 2.9, hydrated lime is injected into a vertical scrubber called CDS. Meanwhile, the SO<sub>2</sub>-containing gas is fed to the CDS from the bottom, resulting in an intense mixing with lime, which is considered an advantage. Inside the CDS reactor, the gas mostly contains SO<sub>2</sub>. The amount of lime and produced solid, i.e., calcium sulfite and calcium sulfate, increases and the majority of solids fall down due to gravity. After, the stream is sent to the bag house units. The collected solids are recycled back to the CDS, making a better use of lime. The remaining solid product is stored [3].

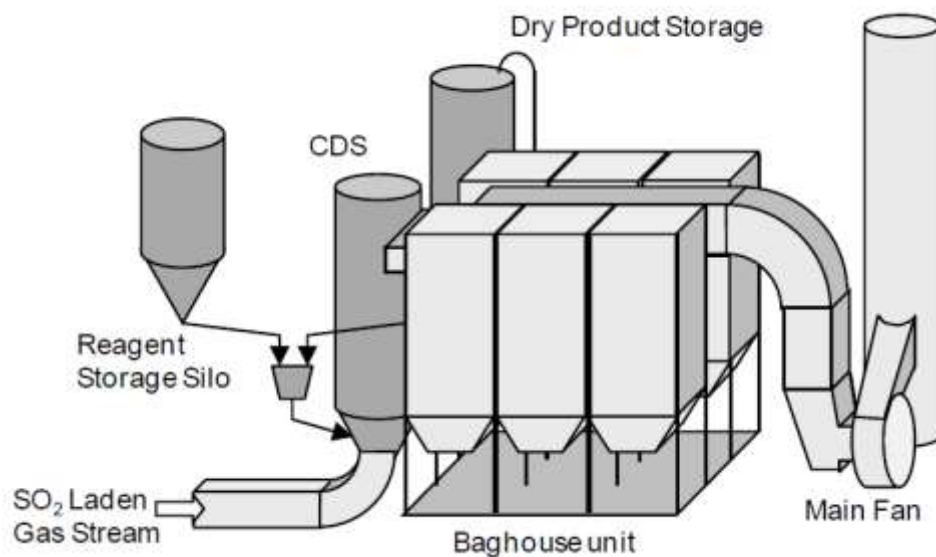


Figure 2.9. Circulating dry scrubbing (CDS) desulfurization process [3]

In order to achieve the required temperature suitable for the SO<sub>2</sub> scrubbing in CDS, a waste heat boiler (WHB) is used to heat the flue gas before entering the CDS reactor. Since the utilization of WHB increases the pressure drop, a centrifugal fan is used to handle both the flow and the pressure drop. The main process in the scrubber is mainly similar to the conventional process, as illustrated in Figure 2.8. Only one compartment

at a time can be shut down for maintenance. The clean gas is withdrawn with fans before being discharged into the stack [3].

On the other hand, instead of using lime, it is possible to inject sodium carbonate ( $\text{Na}_2\text{CO}_3$ ) as the reagent to capture  $\text{SO}_2$ . Sodium sulfite and sodium sulfate are the by-products generated from this method. More common industrial application uses nacholite ( $\text{NaHCO}_3$ ) – sodium bicarbonate. Another form of sodium is Trona [ $\text{Na}_3(\text{CO}_3)(\text{HCO}_3) \cdot 2\text{H}_2\text{O}$ ] which is used as a raw material to produce pure sodium carbonate. These also can be used as reagents for  $\text{SO}_2$  removal [3].

#### **2.4. Semi-dry desulfurization process**

The first semi-dry desulfurization technology was employed in 1980 for a coal-fired power plant in USA; however right now, it accounts for more than 8 % of the world market [16]. Semi-dry is the most preferred choice for incinerators, that are designed to remove multiple pollutants including  $\text{SO}_2$ , HCl, Dioxin [8]. The semi-dry solid product can be considered for the fertilizer production as well.

Considering the disadvantages dominating both the wet and dry desulfurization processes, the use of semi-dry desulfurization as a combination of both wet and dry technologies has been proposed. The wet desulfurization process is commonly commercialized in industrial processes for both aluminum plants [3, 17] and power generation plants [6] with the aim of over 95%  $\text{SO}_x$  removal. However, this technology leads to a high amount of wet solid waste, in conjunction with the requirement of wastewater treatment equipment. Thus, it makes the process more complex [15, 17, 18]. The dry desulfurization process has not been widely utilized due to relatively poor  $\text{SO}_x$  removal as well as excessive sorbent usage despite the lack of water and reheating

energy. This allows a lower operational cost compared to the wet technology [15, 17, 18].

In 2015, a full-scale direct-injection semi-dry scrubber was started to treat gases from the Arvida coke calcination kiln. It was first tested with a mobile pilot scrubber. The process is patented and called CHAC (Chaux Hydratée Aqua-Catalysée /Aqua-Catalyzed Hydrated Lime) which was developed by Rio Tinto. The purpose is to eliminate the SO<sub>2</sub> emitted during the process. The source of sulfur is the raw material (coke) used for anode/cathode production [17]. It treats 120000 Am<sup>3</sup>/h of gas containing approximately 2000 ppm SO<sub>2</sub> at 170 °C. First, sodium bicarbonate (NaHCO<sub>3</sub>) was used as the reagent at a rate of maximum 1000 kg/h. The system also can function with Ca(OH)<sub>2</sub> at the same sorbent rate. Although it has low-cost investment, a relatively high operating cost combined with the CO<sub>2</sub> emission is considered as the drawbacks of this system. It finally achieved the target separation efficiency of 75% SO<sub>2</sub> removal using lime, generating a by-product (calcium sulfate) used in agriculture and the production of wallboard [17].

In semi-dry desulfurization process, a dry reagent is wetted with water to form a slurry, while the rest of the process is mainly similar to dry desulfurization. The difference between the two is that the dry sorbent e.g., lime as well as the recycled solids are wetted with water in the semi-dry desulfurization. The presence of water results in more rapid reaction of the reagent with SO<sub>x</sub> and increases the SO<sub>2</sub> removal efficiency by about 14% compared to dry desulfurization [8]. In a semi-dry process, the slurry is partially dried inside the scrubber. Water enhances the SO<sub>2</sub> removal, improving efficiency; therefore, a lower operating cost and a lower sorbent utilization are achieved [15, 17, 18]. The semi-dry desulfurization process is an adsorption process

due to the presence of solid particles. Various studies focused on the adsorption process since many separation applications ranging from water treatment [19] to industrial practices [6] use this method. The reaction takes place on the surface of the solid particles.

In case of a semi-dry desulfurization process, the reactions take place as given in Eqn. (2.5) and Eqn. (2.6) on the surface of solid in the presence of humidity of the gas. Some water is also produced by the reaction, but its amount is insignificant compared to the humidity of the gas.

A detailed illustration of  $\text{SO}_2$  adsorption is given in Figure 2.10, in which  $\text{Ca}(\text{OH})_2$  is the sorbent. The available specific surface area of particles can be measured using the BET analysis [6]. The contact between  $\text{SO}_2$  and lime leads to the reaction Eqn. (2.5), and  $\text{CaSO}_3$  forms on the solid surface as shown in Figure 2.10(b). The gypsum ( $\text{CaSO}_4$ ) is formed when sufficient oxygen and water vapor is available for the reaction as can be observed in Figure 2.10(c).

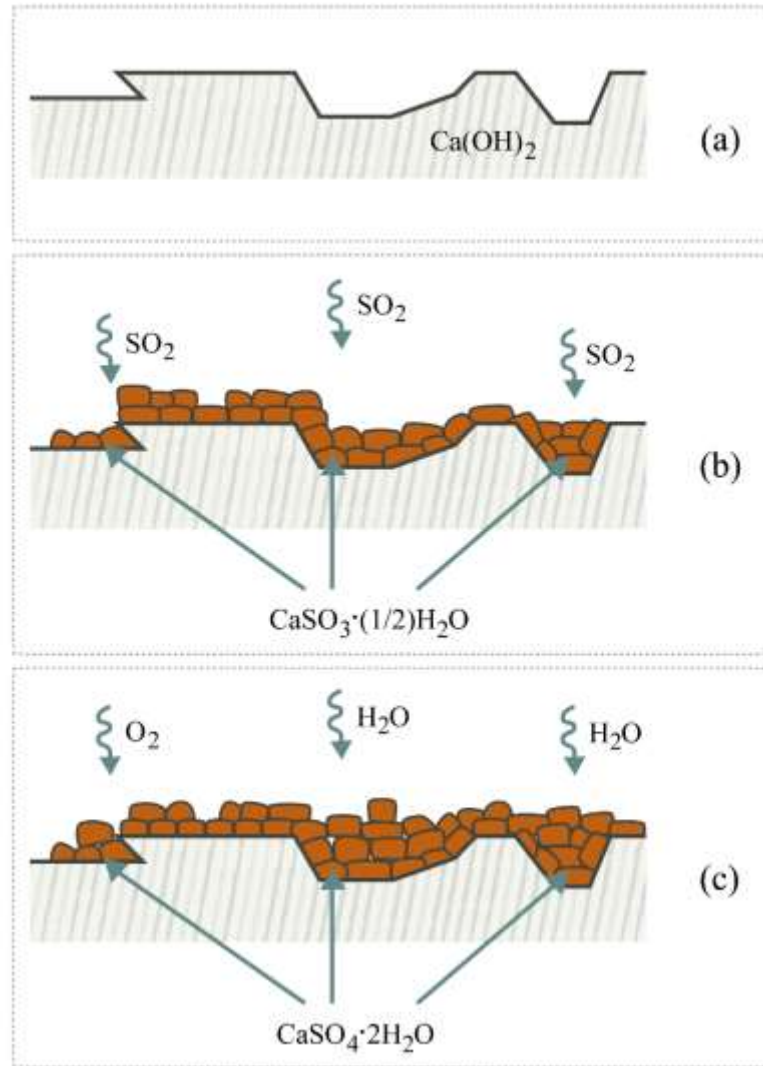


Figure 2.10. Schematic process of semi-dry desulfurization using  $\text{Ca(OH)}_2$

- (a) before the contact of  $\text{SO}_2$  with lime (b) during the contact of  $\text{SO}_2$  with lime to form calcium sulfite powder (c) Providing sufficient water vapor and oxygen to form gypsum

© Arash Fassadi Chimeh, 2023

The water content on the gas is expressed in terms of relative humidity (RH). The actual amount of water vapor present in the gas phase is called absolute humidity. The maximum possible amount of water vapor a gas can hold at a temperature is known as saturation condition. RH can be defined as the division of actual vapor amount to that at saturation at the same temperature according to Eqn. (2.7).

$$RH = \frac{\text{Amount of actual vapor}}{\text{Amount of vapor at saturation at the same temperature}} \quad (2.7)$$

While the process in semi-dry desulfurization scrubber is in progress, the gas temperature is decreased due to the evaporation of water inside the slurry. The evaporated water is transferred to the gas phase, increasing the water content (humidity) of gas. This lowers the temperature and leads to an increase in RH. The higher the RH is, the higher the SO<sub>2</sub> removal efficiency is for a given condition [8, 17]. The slurry feed is atomized to fine particles using an atomizer via an injection through a nozzle. Then, the atomized slurry is rapidly dried into powdered particles as soon as the contact takes place between the gas and the particles. The illustration of slurry drying is shown in Figure 2.11.

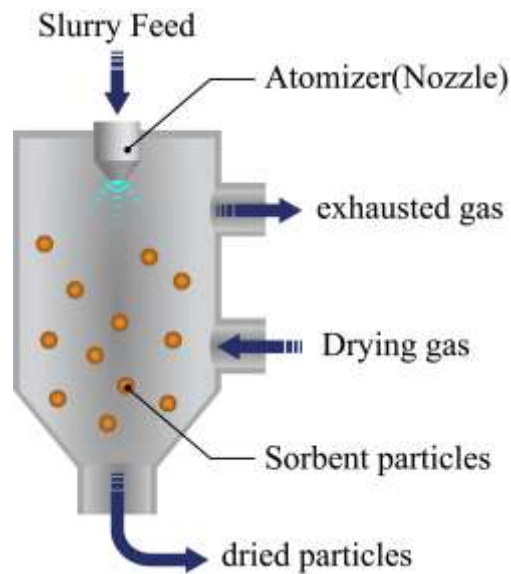


Figure 2.11. Illustration of slurry drying process inside the scrubber

© Arash Fassadi Chimeh, 2023

According to Figure 2.12 taken from the psychrometric chart, on a specific adiabatic line, the gas temperature decreases from the inlet temperature ( $T_0$ ) to the bed temperature ( $T_b$ ) (which is the gas temperature in the reactor) due to the evaporation of

water (assuming an adiabatic system). Thus, RH increases and eventually could reach 100 % (saturation line) at  $T_s$  (saturation temperature). Further cooling of gas results in the condensation of water vapor. In semi-dry processes, usually another factor known as “approach to saturation temperature” ( $\Delta T_a$ ) is used to demonstrate the proximity to the saturation temperature (RH = 100%), according to Eqn. (2.8).

$$\Delta T_a = T_b - T_s \quad (2.8)$$

Despite the fact that the RH cannot be manipulated directly, it is controlled by increasing the water content and/or the temperature using the approach to saturation temperature ( $\Delta T_a$ ).

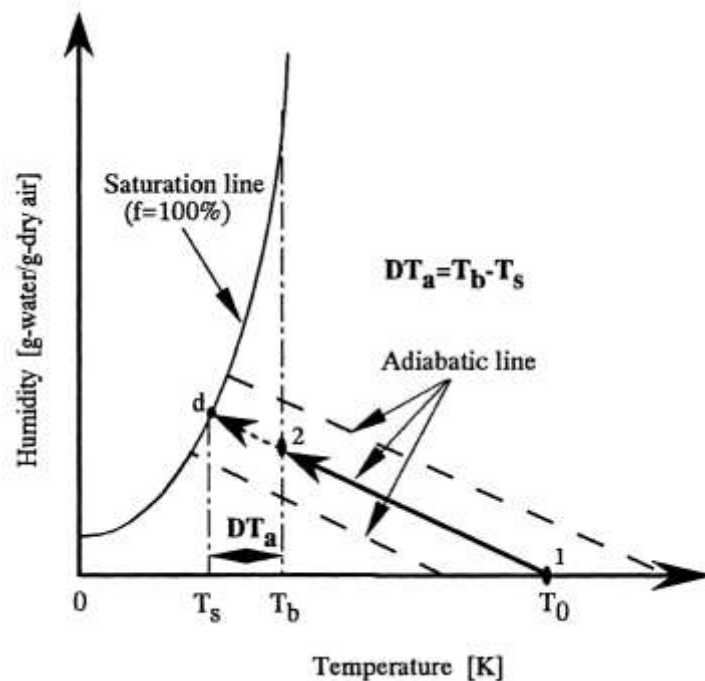


Figure 2.12. Approach to saturation temperature definition [15]

It is observed that if the dry sorbent and humidity are injected together, the  $\text{SO}_2$  removal is better than when they are injected separately to the scrubber. This is probably due to incomplete sorbent mixing with water vapor [18]. However, Wang [8]

reported that injecting them separately with a sufficient distance (6 meters) from slurry nozzle in a duct before the main scrubber resulted in 87% separation efficiency. They reduced the water content in slurry feed and mixed the rest of water at various distances from the slurry atomizer. This study showed that the optimum injection location is where the particles become completely dry. Then, these particles were mixed with additional water. The separation efficiency is also tested without humidity and found as 75%, even though much more sorbent is provided compared to the case with humidity [8]. Other parameters playing important roles in enhancing the SO<sub>2</sub> removal efficiency of semi-dry desulfurization process are reported in a variety of publications such as temperature governing the relative humidity (RH), sorbent ratio Ca/S, sorbent particle size, etc. [6, 8, 20].

It is reported in the literature that increasing humidity (RH) increases the separation efficiency [6, 8, 20, 21]. This factor shows the water present in gas as being one of the most important parameters. The reactivity of dry lime particles with SO<sub>2</sub> is low unless the gas humidity is high. Thus, it accelerates the reaction between the particles and SO<sub>2</sub>. The humidity is indirectly measured using the approach to saturation temperature ( $\Delta T_a$ ) given in Eqn. (2.8). According to this concept, if the  $\Delta T_a$  is lower, the gas is closer to saturation condition leading to higher RH [6, 8, 21]. It seems to be a highly effective factor, especially in case of hydrated lime [20]. Generally, the humidity depends on inlet flue gas temperature and bed temperature ( $T_b$ );  $T_b$  is also affected by the flowrate of slurry and the humidity of gas [6]. For the flue gas at 2000 Nm<sup>3</sup>/h containing 500 ppm SO<sub>2</sub>, a sufficient removal occurred with  $\Delta T_a = 10$  °C [15]. There must be a minimum of 5 °C  $\Delta T_a$  to avoid water condensation leading to water accumulation inside the reactor as well as the agglomeration of particles inside the



scrubbers [15]. It is also possible to change the bed temperature ( $T_b$ ) and consequently  $\Delta T_a$  to improve the  $\text{SO}_2$  removal.

As shown in Figure 2.13, Ma [6] reported that, for the given parameters in a powder-particle spouted bed (PPSB) scrubber, about 65 °C bed temperature and 150 °C inlet temperature with 500 ppm  $\text{SO}_2$  laden flue gas, excessive decrease in  $\Delta T_a$  increased the removal efficiency; however, it was also noted that further decrease in  $\Delta T_a$  did not make a significant change in the removal efficiency. Other researchers obtained higher  $\text{SO}_2$  removal efficiencies under similar conditions. Xu [15] achieved more than 98 % and 86 % efficiency for  $\Delta T_a = 10$  °C and 20 °C, respectively, in a PPSB scrubber under 65 °C bed temperature and 200 °C inlet temperature with 800 ppm  $\text{SO}_2$  as shown in Table 2.2. The main differences between them are Ca/S ratio as well as the sorbent size.

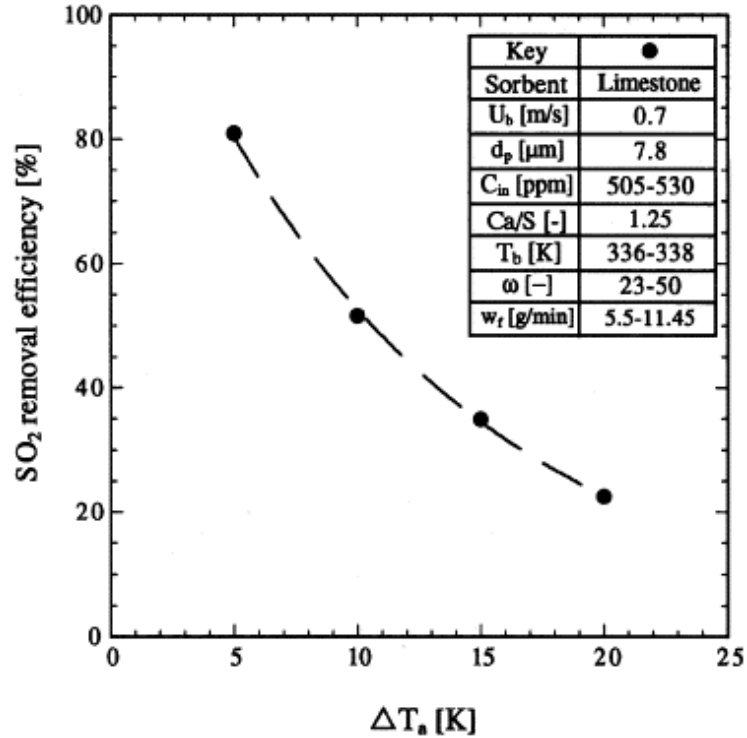


Figure 2.13. The effect of the approach to saturation temperature on the SO<sub>2</sub> removal efficiency

(Authorized by Elsevier and reproduced from [6])

Table 2.2. SO<sub>2</sub> removal efficiency with different sorbent size at various  $\Delta T_a$  [15]

$T_b = 65\text{ }^\circ\text{C}$ ; $C_{in} = 800\text{ ppm}$ ; $\text{Ca/S} = 1.5$		
$\Delta T_a$ ( $^\circ\text{C}$ )	SO <sub>2</sub> removal efficiency (%)	
	$d_p = 4.6\text{ }\mu\text{m}$	$d_p = 28.4\text{ }\mu\text{m}$
10	98	98
20	92	86
30	77	67

An important factor in the desulfurization processes is the ratio of sorbent per mol of SO<sub>2</sub> expressed as Ca/S (mol/mol) in the case of calcium-based reagents. It is preferred not to use this sorbent in a dry desulfurization process due to its relatively

high sorbent utilization and low reactivity with  $\text{SO}_2$  [14]. Houde et al. [14] reported that, in a dry desulfurization process, using both  $\text{CaO}$  and  $\text{CaCO}_3$  as sorbents, only 25% and 20% removal efficiency, respectively, was achieved. It is generally accepted that the wet FGD requires the least amount of  $\text{Ca/S}$ , around 1.2, and it can reach high removal efficiencies (over 95%) easily [7, 15]. According to Figure 2.14, which represents a semi-dry process reported by Ma [6], using more  $\text{Ca/S}$  resulted in more  $\text{SO}_2$  removal up to a point. Further increase of  $\text{Ca/S}$  does not enhance the process. This was also observed by other researchers [15, 20]. Figure 2.14 illustrates that over 90%  $\text{SO}_2$  removal was achieved with  $\text{Ca/S} \sim 1.5$  under the given conditions. It was found that when  $\text{Ca/S}$  is less than 1 (stoichiometric ratio), the process is less efficient, whereas above 2, the sorbent is wasted. Soud [16] also reported that if above 95%  $\text{SO}_2$  removal is targeted,  $\text{Ca/S}$  should be approximately 2.0, which is much greater than the value for the wet desulfurization process. Likewise, Harriot [18] found that the  $\text{SO}_2$  removal efficiency for  $\text{Ca/S}$  of 0.6 to 1 is in the range of 30% - 50%.

Bausache [20] carried out a semi-dry experiment under 60% RH, 70 °C, 1.5 l/min flue gas containing 2000 ppm  $\text{SO}_2$  and 175 ppm  $\text{NO}_2$  resulted in nearly 90% removal for  $\text{Ca/S} = 2$  and 2 hours of contact time. A similar result was obtained without the presence of  $\text{NO}_2$  for  $\text{Ca/S} \sim 5$  in 1 hour [20].

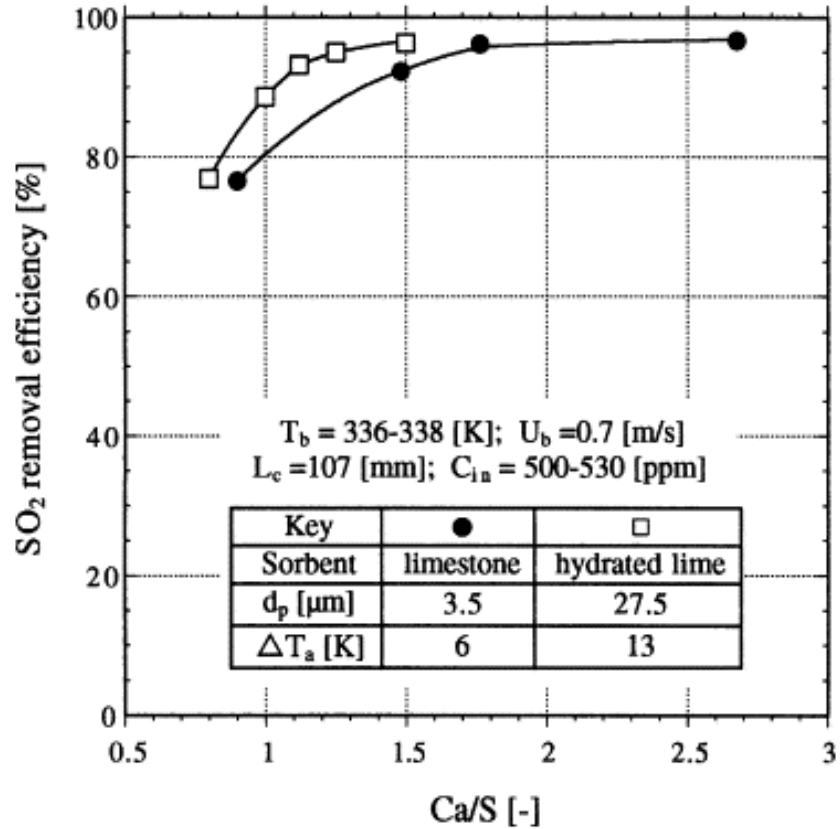


Figure 2.14. Effect of Ca/S ratio on SO<sub>2</sub> removal efficiency

(Authorized by Elsevier and reproduced from [6])

Figure 2.15 shows that the sorbent size ( $d_p$ ) plays a key role in the removal efficiency [6]. This can be also expressed in terms of specific surface area (SSA). The finer sorbents have high specific surface area [6]. It is proved that the finer sorbent utilization enhances SO<sub>2</sub> removal [3, 6, 22]. Harriot [18] and Kligisport [23] similarly reported that the SO<sub>2</sub> removal increased almost linearly as a function of the specific surface area (SSA) of limestone up to 20 m<sup>2</sup>/g, while further increase in the specific surface area (up to 45 m<sup>2</sup>/g) slightly enhanced the removal. The main difference between limestone and hydrated lime is the SSA, making a considerable difference in efficiency. Hydrated lime with even a medium particle size (27.5  $\mu\text{m}$ ) has a threefold SSA compared to a fine limestone (5.4  $\mu\text{m}$ ) [6]. Garea et al. [7] achieved a high SO<sub>2</sub>

removal using  $\text{Ca}(\text{OH})_2$  ( $16 \text{ m}^2/\text{g}$ ) at  $65 \text{ }^\circ\text{C}$  and  $900 \text{ Ncm}^3/\text{min}$  gas flow with  $4000 \text{ ppm}$   $\text{SO}_2$  content during a short period of time. Further, Bausache [20] was able to achieve more than 90% removal with an acceptable sorbent value of  $\text{Ca}/\text{S} = 2$  and the sorbent (limestone) specific surface of  $13 \text{ m}^2/\text{g}$ . Kang [22] compared the reactivity of  $\text{SO}_2$  with commercial limestone and recarbonated limestone for two different particle sizes,  $37.5 \text{ }\mu\text{m}$  and  $750 \text{ }\mu\text{m}$ . The recarbonation process takes place through the calcination and recarbonation reactions according to Eqn. (2.9). The results showed that the conversions of limestone were 25% (at  $37.5 \text{ }\mu\text{m}$ ) and 3.5% (at  $750 \text{ }\mu\text{m}$ ) for the two particle sizes, and those of the recarbonated limestone were 35% (at  $37.5 \text{ }\mu\text{m}$ ) and 5% (at  $750 \text{ }\mu\text{m}$ ) after 60 min. It was also found that the recirculation of limestone using  $\text{O}_2$  and  $\text{CO}_2$  could enhance the  $\text{SO}_2$  removal compared to commercial limestone.

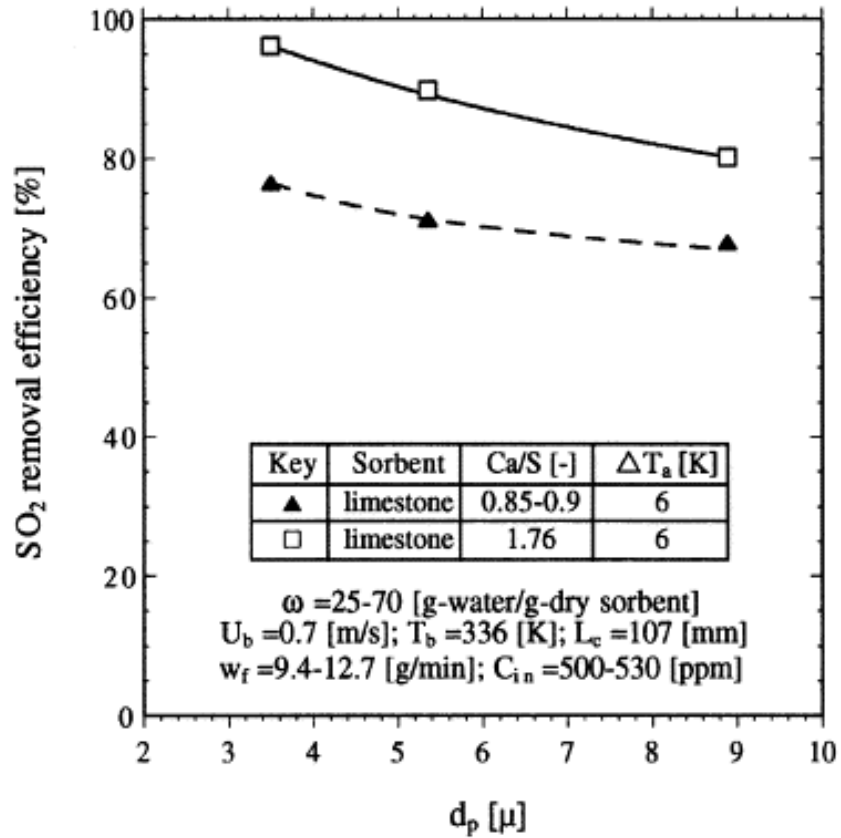
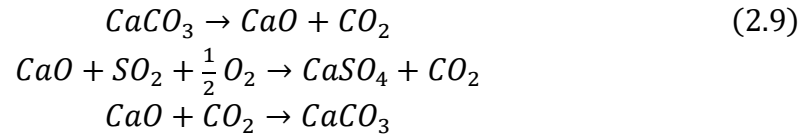


Figure 2.15. Effect of sorbent size on SO<sub>2</sub> removal

(Authorized by Elsevier and reproduced from [6])



Ma et al. [6] compared the effect of different sorbent sizes for SSPB semi-dry process to show its effect on SO<sub>2</sub> removal. Figure 2.16 illustrates a porous medium through which a gas travels a given distance under a particular velocity (pores are represented in a simplified manner such as a cylinder). According to Figure 2.17, lower gas velocity leads to a greater residence time (longer contact time between gas and solid), enhancing the SO<sub>2</sub> removal [15]. It is also possible to obtain a similar residence time by increasing the bed length.

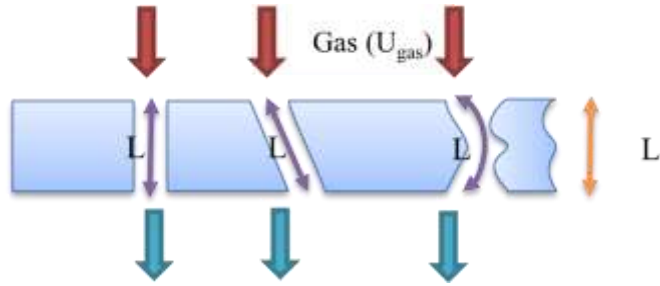


Figure 2.16. Gas passage through a porous medium

© Arash Fassadi Chimeh, 2023

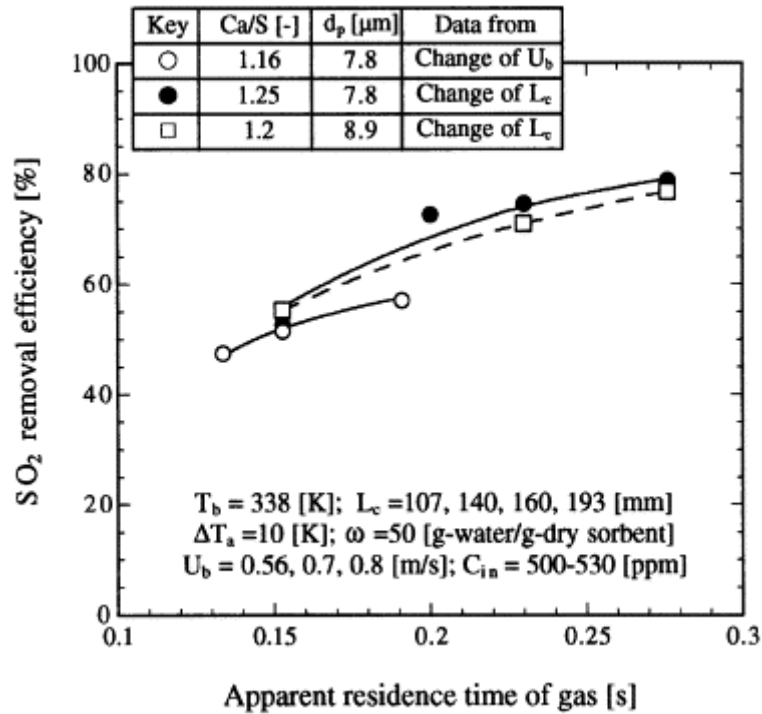


Figure 2.17. Effect of gas residence time on SO<sub>2</sub> removal

(Authorized by Elsevier and reproduced from [6])

Another factor which clearly has an effect on SO<sub>2</sub> removal is the initial SO<sub>2</sub> concentration of the inlet gas stream [3, 7]. Generally, a better desulfurization is expected, when less SO<sub>2</sub> is present in the inlet gas at a fixed amount of sorbent. When the initial SO<sub>2</sub> concentration was doubled, the removal efficiency reduced to only 7% while the other parameters were kept constant [18]. On the other hand, some researchers found an inverse trend for the effect of inlet SO<sub>2</sub> concentration on the

desulfurization efficiency [15, 24]. An increase of nearly 900 ppm SO<sub>2</sub> (from 1100 ppm) at 60% RH and 70 °C allowed less hydrated lime utilization for a given removal efficiency within the same time period [20].

The effect of temperature is not as pronounced as those of RH and Ca/S ratio [20]. Generally, the SO<sub>2</sub> adsorption process takes place more efficiently at lower temperatures [10, 12]. Harriot [18] also reported that a reduction of 12 °C (77 °C to 65 °C) in the outlet flue gas temperature enhanced the removal efficiency nearly two-folds. Xu et al. [15] reported that lowering the inlet temperature of the gas resulted in higher SO<sub>2</sub> removal if other parameters were kept constant. As it can be seen from Figure 2.18, Xu et al. [15] illustrated that if the temperature (above 150 °C) of the semi-dry desulfurization reactor increases, more water ( $\omega_0$ ) content must be available in the slurry while the slurry flowrate ( $W_s$ ) is increased in order to achieve the same SO<sub>2</sub> removal [15]. It is also important to mention that the bed temperature ( $T_b$ ) varies with inlet gas temperature ( $T_0$ ) for a specific water content ( $\omega_0$ ) and flowrate ( $W_s$ ) of slurry [15].

Nevertheless, some research contradicts this trend. As can be seen from the breakthrough curves shown in Figure 2.19, reported by Bausach et al. [20], the temperature slightly affected the SO<sub>2</sub> conversion. At 40 °C, the conversion was only 7.1 %. Increasing the temperature to 80 °C, the conversion was increased to 11.2 %. This may be due to the increase in the desulfurization reaction rate when the  $T_b$  was increased [15]. However, the reaction rate was not affected in all the temperature ranges. A study by Houte et al. supported this result [14]. He worked on the SO<sub>2</sub> removal from high temperature flue gases. His results showed that the desulfurization reaction rate was increased significantly up to 800 °C. After, it decreased up to 900 °C



[14]. Figure 2.19 also shows that reactivity of lime with  $\text{SO}_2$  is significantly high at the earlier times. Then, it decreases but does not stop for a long period of time [20].

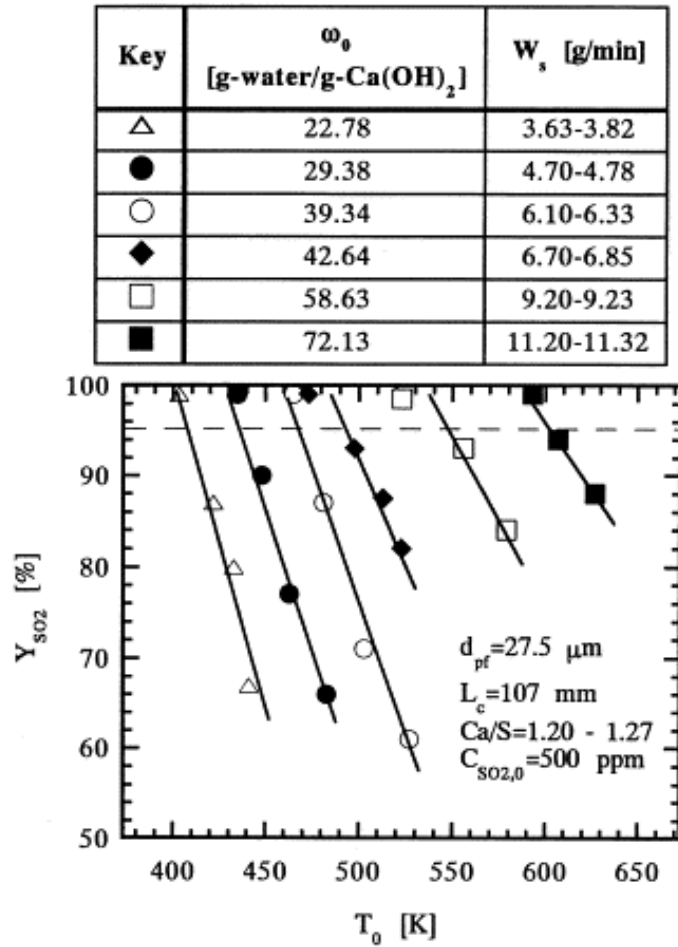


Figure 2.18.  $\text{SO}_2$  removal efficiency as a function of gas inlet temperature at different  $W_s$  and  $\omega_0$  (Authorized by Elsevier and reproduced from [15])

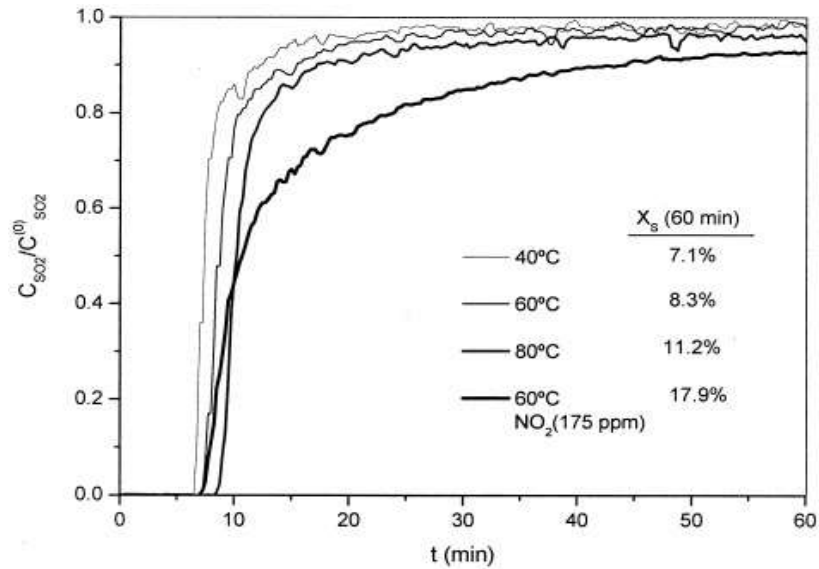


Figure 2.19. Effect of temperature on SO<sub>2</sub> removal: RH = 30%, inlet SO<sub>2</sub> concentration = 2000 ppm

(Authorized by Elsevier and reproduced from [20])

## 2.5. Computational Fluid Dynamics

Considerable attention has been given to computational fluid dynamics (CFD), especially the development and testing of novel technologies that require extensive time, energy, and financial resources [25]. Without the use of modelling, developing new processes can be time-consuming and even impossible in some circumstances, such as those involving hazardous conditions, large-scale equipment, etc. In addition, modelling reveals the results in detail and a parametric study can be easily conducted to determine the effects of various parameters [25]. A wide variety of heat and mass transfer applications specifically in multi-phase condition have been accomplished using CFD. Wang et al. [26] carried out a CFD-DEM numerical investigation focused on the hydrodynamic behavior of gas-solid phases in a semi-dry (PPSB) desulfurization process. Wang et al. [27] used Euler-Euler modelling for a semi-dry desulfurization pilot-scale system considering heat and mass transfer, a reaction model, and the kinetic

particle theory. Marocco and Mora [28] studied a desulfurization process involving a one-way coupled solid-gas interaction using ANSYS Fluent at a RH of 60% to determine and compare the desulfurization rate in two different geometries. The effect of sorbent content and humidity, key parameters for the desulfurization process, was not considered in their studies. A one-way coupling only analyzes the effects of the continuous fluid phase on particles whereas a two-way coupling evaluates the effects of both continuous fluid and solid phases on each other [29].

## **2.6. Summary**

The emission of SO<sub>2</sub> has been a concern for many years due to its irreversible impacts on earth and human life. The SO<sub>2</sub> is one of the contaminants coming from the industrial plants such as aluminum smelters, thermal power generation stations, etc. Thus, the effluent gas must respect a certain maximum limit due to environmental regulations and meet the required criteria to minimize its adverse effects. The processes used to remove SO<sub>2</sub> is known as the desulfurization.

The studies show that widely used Ca-based sorbents for the desulfurization process are quite efficient, leading to high SO<sub>2</sub> removal. Among the three main methods of the desulfurization process, the semi-dry desulfurization is more beneficial since it does not include the drawbacks involved in wet and dry desulfurization processes, e.g., post sludge treatment, high sorbent requirement, etc. Moreover, the utilization of a semi-dry desulfurization process does not result in any waste products since the solid by-products can be converted to high demand materials. In case of Ca(OH)<sub>2</sub> use as the reagent, gypsum is obtained, which is vastly employed in the agriculture. The sorbents used in this process vary such as CaCO<sub>3</sub>, NaOH, NaHCO<sub>3</sub>, etc. Although they may not

be as efficient as hydrated lime, availability and lower cost make them attractive economically if a high removal efficiency is not targeted.

Some operational parameters are also influential for the efficiency of the process. According to the literature, relative humidity (RH) plays a significant role. Increasing RH can significantly enhance the SO<sub>2</sub> removal efficiency. Increasing the amount of sorbent used for a given flue gas flowrate usually leads to a better removal efficiency as well. The sorbent size is also important; smaller particles provide a greater surface area and thus a better contact of SO<sub>2</sub> with sorbent. The influence of temperature and initial SO<sub>2</sub> concentration is also clear although they are not as effective as the parameters mentioned before. The higher temperatures may increase the reaction rate; however, excessive increasing of temperature may result into lower reaction rate followed by lower desulfurization efficiency.

## 2.7. References

1. Charette, A., Y. Kocaefe, and D. Kocaefe, *Le carbone dans l'industrie de l'aluminium*. 2012: PRAL - Press Aluminium.
2. Canada, A.A.o. *PRIMARY ALUMINUM PRODUCTION*. Available from: [https://aac.metrio.net/indicators/economie/autre/production\\_aluminium\\_multi](https://aac.metrio.net/indicators/economie/autre/production_aluminium_multi).
3. Zettler, S., N. Fortin, and K. Moran, *Feasibility report on technical options to reduce SO<sub>2</sub> emissions Post-KMP*. 2013, Rio Tinto Alcan.
4. Semrau, K.T., *Control Of Sulfur Oxide Emissions From Primary Copper, Lead And Zinc Smelters—A Critical Review*. Journal of the Air Pollution Control Association, 1971. **21**(4): p. 185-194.
5. Li, X., et al., *Summary of research progress on industrial flue gas desulfurization technology*. Separation and Purification Technology, 2022. **281**: p. 119849.
6. Ma, X., et al., *Use of limestone for SO<sub>2</sub> removal from flue gas in the semidry FGD process with a powder-particle spouted bed*. Chemical Engineering Science, 2000. **55**(20): p. 4643-4652.
7. Garea, A., et al., *Kinetics of dry flue gas desulfurization at low temperatures using Ca(OH)<sub>2</sub>: competitive reactions of sulfation and carbonation*. Chemical Engineering Science, 2001. **56**: p. 1387-1393.
8. Wang, N. and X. Zhang, *Effect of humidification water on semi-dry flue gas desulfurization*. Procedia Environmental Sciences, 2011. **11**: p. 1023-1028.
9. Ghosh, R., J. Smith, and A. Adams, *Horizontal In-Duct Scrubbing of Sulfur-Dioxide from Flue Gas Exhausts*. 2015. p. 595-601.
10. Sharma, R., S. Acharya, and A.K. Sharma, *Effect of Absorption of Sulphur Dioxide in Sodium Hydroxide Solution to Protect Environment : A Case Study at Shree Power, Beawar, Rajasthan*. international journal of chemical sciences, 2010. **8**: p. 1021-1032.
11. Amara, B., *EFFET DU SOUFRE SUR LA RÉACTIVITÉ DES ANODES EN CARBONE*, in *Applied Science*. 2017, The university of Quebec at chicoutimi (UQAC): Canada.
12. Prasad, D.S.N., et al., *Removal of sulphur dioxide from flue gases in thermal plants*. Rasayan Journal of Chemistry, 2010. **3**: p. 328-334.
13. Environnement, S., et al., *Electrolytic cell gas cooling upstream of treatment center*, in *Light Metals 2012*. 2012, Springer. p. 545-550.
14. Houte, G.V., et al., *Desulfurization of flue gases in a fluidized bed of modified limestone*. Journal of the Air Pollution Control Association, 1978. **28**(10): p. 1030-1033.
15. Xu, G., et al., *A new semi-dry desulfurization process using a powder-particle spouted bed*. Advances in Environmental Research, 2000. **4**(1): p. 9-18.
16. Soud, H., *Suppliers of FGD and NO<sub>x</sub> control systems*. 1995: London, United Kingdom. p. 18-27.
17. Maltais, J.-N., et al., *Development, Proof of Concept and Industrial Pilot of the New CHAC Scrubbing Technology: An Innovative and Efficient Way to Scrub Sulfur Dioxide*. 2016. p. 473-478.

18. Harriott, P., *A simple model for SO<sub>2</sub> removal in the duct injection process*. Journal of the Air & Waste Management Association, 1990. **40**(7): p. 998-1003.
19. Bahmani, E., et al., *Electrospun polyacrylonitrile/cellulose acetate/MIL-125/TiO<sub>2</sub> composite nanofibers as an efficient photocatalyst and anticancer drug delivery system*. Cellulose, 2020. **27**(17): p. 10029-10045.
20. Bausach, M., et al., *Kinetic modelling of the reaction between hydrated lime and SO<sub>2</sub> at low temperature*. AIChE Journal, 2005. **51**: p. 1455-1466.
21. Qimin, G., N. Iwata, and K. Kato, *Process development of effective semi-dry flue gas desulfurization by power-particle spouted bed; Funryu ryudoso ni yoru hankanshiki kokoritsu datsuryu sochi no kaihatsu*. Kagaku Kogaku Ronbunshu, 1996. **22**.
22. Kang, S.Y., et al., *A comparative evaluation of recarbonated CaCO<sub>3</sub> derived from limestone under oxy-fuel circulating fluidized bed conditions*. Science of The Total Environment, 2021. **758**: p. 143704.
23. Klingspor, J.S., *Improved spray dry scrubbing through grinding of FGD recycle material*. JAPCA, 1987. **37**(7): p. 801-806.
24. Irabien, A., et al., *Kinetic model for desulfurization at low temperatures using calcium hydroxide*. Chemical engineering science, 1990. **45**(12): p. 3427-3433.
25. Versteeg, H.K.M., W., *An Introduction to Computational Fluid Dynamics The Finite Volume Method*,. 2007: Pearson Education.
26. Wang, X., et al., *Simulation of the heterogeneous semi-dry flue gas desulfurization in a pilot CFB riser using the two-fluid model*. Chemical Engineering Journal, 2015. **264**: p. 479-486.
27. Wang, X., et al., *Wet flue gas desulfurization using micro vortex flow scrubber: Characteristics, modelling and simulation*. Separation and Purification Technology, 2020. **247**: p. 116915.
28. Marocco, L. and A. Mora, *CFD modelling of the Dry-Sorbent-Injection process for flue gas desulfurization using hydrated lime*. Separation and Purification Technology, 2013. **108**: p. 205-214.
29. ANSYS, *ANSYS FLUENT Theory Guide 2022 R2*. 2022.

**CHAPTER 3**  
**MATHEMATICAL MODELLING OF THE DESULFURIZATION**  
**OF ELECTROLYSIS CELL GASES IN A LOW TEMPERATURE**  
**REACTOR**  
**(ARTICLE 1)**

Arash Fassadi Chimeh<sup>1</sup>, Duygu Kocaefe<sup>1</sup>, Yasar Kocaefe<sup>1</sup>, Yoann Robert<sup>2</sup>, Jonathan  
Bernier<sup>2</sup>

<sup>1</sup>Research Chair on Industrial Materials (CHIMI), University Research Centre on  
Aluminium (CURAL), Aluminium Research Center (REGAL), University of Quebec  
at Chicoutimi, 555 University Blvd., Chicoutimi, Quebec, Canada G7H 2B1

<sup>2</sup> Arvida Research and Development Centre (ARDC), Rio Tinto, 955 boulevard  
Mellon, Jonquière, Québec, G7S 4K8, Canada

This article is published in Light Metal 2023 and presented in TMS 2023  
conference.

**Abstract**

SO<sub>2</sub> is one of the main sources of acid rain and air pollution. Semi-dry sorbent injection, using powdered alkaline sorbents, is an effective means of removing SO<sub>2</sub>. Since no costly additional equipment is needed, the operating cost is lower, and it is a more economical and efficient process compared to wet and dry desulfurization processes. The reaction between sorbent (hydrated lime, Ca(OH)<sub>2</sub>) and SO<sub>2</sub> is dominated by the adsorption step. In this study, a mathematical model has been developed to simulate the lab-scale desulfurization reactor employed for the low temperature gases containing low SO<sub>2</sub> concentration coming from the electrolysis cells used for aluminum production. A parametric study was carried out in order to examine

the effects of certain parameters, such as inlet SO<sub>2</sub> concentration, sorbent flowrate, and relative humidity of the gas on the desulfurization efficiency. The model and some of the results are presented in this article.

Keywords: SO<sub>2</sub> removal, Semi-dry desulfurization, Aluminum electrolysis, Computational fluid dynamics (CFD).

### 3.1. Introduction

The aluminum demand is expected to grow by 4.2% per year till 2050 due to increased demand in the construction, transport, and renewable energy sector [1]. The sulfur-containing gases (SO<sub>2</sub> and SO<sub>3</sub>) are emitted from aluminum smelters. These gases may react with water vapor in air and produce H<sub>2</sub>SO<sub>3</sub> and H<sub>2</sub>SO<sub>4</sub>, which are major contributors to acid rain [1]. In addition to being detrimental for the environment, acid rain is extremely harmful to the health of humans and animals. Also, it affects the aquatic life because it contributes to the toxicity of water resources. Another severe consequence of acid rain is the deterioration of historical and ancient buildings [1].

The environmental laws restrict the total emission of contaminants through certain regulations. For instance, 88/609/CEE and 2001/80/CEE aim to control the emissions from fossil fuels coming from the industrial plants [2]. Therefore, the industries have to meet the maximum allowable concentration of SO<sub>2</sub> present in the gases exhausted from the stacks [3].

Aluminum is a metal widely used in a large number of applications, including transportation, construction, etc. due its distinct properties [4]. Canada is one of major aluminum manufacturing and exporting countries. In 2020, Canada produced approximately 3.2 million tonnes of aluminum and 90% of this was produced in



Quebec [5]. The source of sulfur in gases emitted from the electrolysis cells is the raw materials, especially coke, used in anode production. Since the quality of anode raw materials is decreasing, their sulfur content is increasing [6]. Rio Tinto, which has six smelters in Quebec and one in British Columbia, is one of the major aluminum producers in the world. It continuously searches for ways to further reduce its emissions [3].

There are three types of desulfurization processes: dry, wet, and semi-dry [3, 4]. In a wet process, sulfur oxides are scrubbed by passing the gas through a large quantity of solution containing a solute (mostly Na). This process is capital-intensive. Its operation and maintenance costs are high. The solvent has to be neutralized and recovered [7], and the process creates low-quality by-products [6]. In the dry process, the solid particles are injected into the gas stream. The dry process has also some disadvantages, including the low desulfurization efficiency and excessive sorbent utilization [7]. In the semi-dry process, particles suspended in water are injected into the gas. It is reported in the literature that the presence of humidity in gas increases the reaction rate of the sorbent (solid particles) with  $\text{SO}_2$ . An increase of 14% in  $\text{SO}_2$  removal efficiency compared to that of the dry process was observed by some researchers [8].

Contrary to the emissions in thermal plants, gases released from the aluminum smelters contain a much lower  $\text{SO}_2$  concentration at somewhat lower temperatures. The elimination of  $\text{SO}_2$  at such a low concentration level is complex and requires further attention [3, 9]. Studies focusing on the removal of  $\text{SO}_2$  from effluent gases in the smelters are quite rare.

Modelling is an effective tool to determine the design and operational conditions of a process as it reduces the cost. Industrial processes ranging from a simple water air pipe [10] to the complex absorbers and reactors [11] mostly contain more than one phase (multi-phase systems), which is the case for the current system.

In this study, a mathematical model of a desulfurization reactor is developed under semi-dry conditions.  $\text{SO}_2$  is removed using hydrated lime  $\text{Ca}(\text{OH})_2$ , therefore, it is a multi-phase system. The main objective is to remove  $\text{SO}_2$  from the gas stream as efficiently as possible. The system is isothermal and turbulent. The commercial code Ansys-Fluent was used to solve the governing equations. The kinetic equation was introduced via a UDF (user-defined function). The effect of gas relative humidity on  $\text{SO}_2$  removal is demonstrated, which enhanced the removal efficiency by 8 % in some cases.

## 3.2. Methodology

### 3.2.1. System (Laboratory reactor)

Figure 3.1 presents the geometry and shows the three domains: filter and the two domains on both sides. Gas inlet, gas outlet, and the filter are indicated on the figure as well.

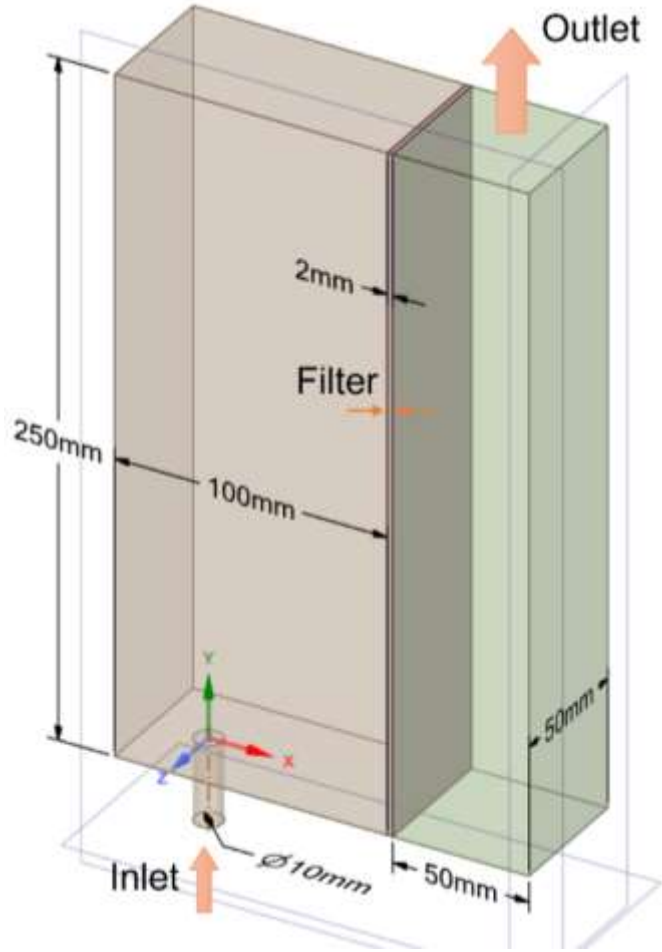


Figure 3.1. System: laboratory reactor

### 3.2.2. Governing Equations

The model is based on the two-phase Eulerian-Eulerian strategy. Each of the existed phases i.e. continuous phase (gas mixture of air and SO<sub>2</sub>) and dispersed phase (hydrated lime and the reaction product) considered as separate flow domains. The system is isothermal. The temperature is taken as 70 °C. A porous domain is defined to represent the filter. The continuity and momentum equations are shown in Eqn. (3.1) and Eqn. (3.2), respectively.

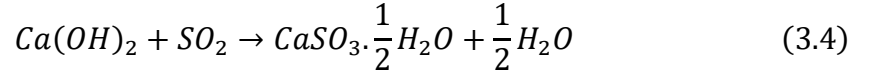
$$\frac{\partial \rho}{\partial t} + \nabla \cdot (\rho \vec{u}) = 0 \quad (3.1)$$

$$\frac{\partial(\rho\vec{u})}{\partial t} + \nabla \cdot (\rho\vec{u}\vec{u}) = -\nabla p + \nabla \cdot (\vec{\tau}) + \rho\vec{g} + \vec{F} \quad (3.2)$$

where,  $\rho$  is the fluid density (kg/m<sup>3</sup>),  $u$  is the fluid velocity (m/s), and  $p$  is the static pressure (Pa).  $\rho\vec{g}$  and  $\vec{F}$  describe the gravitational body forces and external body forces (N), respectively.  $\vec{F}$  is the source term representing porous media or any other model dependant source terms. Stress tensor ( $\vec{\tau}$ ) is defined as shown in Eqn. (3.3).

$$\vec{\tau} = \mu \left[ (\nabla\vec{u} + \nabla\vec{u}^T) - \frac{2}{3}\nabla \cdot \vec{u}I \right] \quad (3.3)$$

where,  $\mu$  is the molecular viscosity and  $I$  is the unit tensor [12]. In this process, hydrated lime is injected into the SO<sub>2</sub>-containing gas stream. When the hydrated lime mixes with SO<sub>2</sub>, the reaction shown in Eqn. (3.4) takes place [3, 11].



In reality, part of the calcium sulfite (CaSO<sub>3</sub>) oxidizes to form calcium sulfate (CaSO<sub>4</sub>). Thus, the product is a mixture of the two. But it is taken as sulfite in order to simplify the problem. Species transport equation shown in Eqn. (3.5) and Eqn. (3.6) are used for simulating the reacting flow in a volumetric reaction model. It was assumed that the reaction takes place in a single phase [12].

$$\frac{\partial(\rho\omega_i)}{\partial t} + \nabla \cdot (\rho\omega_i\vec{u}) = -\nabla \cdot (\vec{J}_i) + R_i + S_i \quad (3.5)$$

$$\vec{J}_i = -\left(\rho D_{i,m} + \frac{\mu_t}{Sc_t}\right)\nabla\omega_i - D_{T,i}\frac{\nabla T}{T} \quad (3.6)$$

where,  $\omega_i$  is the mass fraction of species  $i$  participating in the reaction.  $\vec{J}_i$  is the diffusion flux of species  $i$ , generated due to the concentration gradient.  $Sc_t = \frac{\mu_t}{\rho D_t}$  is the

turbulent Schmidt number taken as 0.7.  $\mu_t$  and  $D_t$  are the turbulent viscosity and turbulent diffusivity, respectively, used in turbulent Schmidt number formulation.  $R_i$  is the net source of chemical species  $i$  due to the reaction and defined as given in Eqn. (3.7). There is only one reaction in this process, where  $M_{w,i}$  is the molecular weight of the species  $i$ , and  $\widehat{R}_i$  is the molar rate of the reaction of species  $i$  [12].

$$R_i = M_{w,i}\widehat{R}_i \quad (3.7)$$

The turbulence model used is a two-equation model called standard  $k - \epsilon$  [13]. The transport equations for both turbulent kinetic energy ( $k$ ) and dissipation rate ( $\epsilon$ ) are presented in Eqn. (3.8) and Eqn. (3.9), respectively. These equations were proposed by Launder and Spalding [13]. They are applicable to a wide range of turbulent flow systems, especially to those requiring a simple and accurate enough model to prevent high computational loads. The turbulent (eddy) viscosity term  $\mu_t$  consists of  $k$  and  $\epsilon$  as shown in Eqn. (3.10) where  $C_\mu$  is a constant [12].

$$\frac{\partial}{\partial t}(\rho k) + \frac{\partial}{\partial x_i}(\rho k u_i) = \frac{\partial}{\partial x_j} \left[ \left( \mu + \frac{\mu_t}{\sigma_k} \right) \frac{\partial k}{\partial x_j} \right] + G_k + G_b - \rho \epsilon - Y_M + S_k \quad (3.8)$$

$$\frac{\partial}{\partial t}(\rho \epsilon) + \frac{\partial}{\partial x_i}(\rho \epsilon u_i) = \frac{\partial}{\partial x_j} \left[ \left( \mu + \frac{\mu_t}{\sigma_\epsilon} \right) \frac{\partial \epsilon}{\partial x_j} \right] + C_{1\epsilon} \frac{\epsilon}{k} (G_k + C_{3\epsilon} G_b) - C_{2\epsilon} \rho \frac{\epsilon^2}{k} + S_\epsilon \quad (3.9)$$

$$\mu_t = \rho C_\mu \frac{k^2}{\epsilon} \quad (3.10)$$

where,  $G_k$  and  $G_b$  represent the generation of turbulence energy due to mean velocity gradient and buoyancy, respectively.  $Y_M$  represents the effect of compressibility on the turbulence model which can be neglected.  $S_k$  and  $S_\epsilon$  are both user-defined source terms which are taken as zero in this study.  $\sigma_\epsilon$  and  $\sigma_k$  are as the turbulent Prandtl numbers

for  $k$  and  $\epsilon$ , respectively [13]. The model constants are taken as suggested by Launder and Spalding since they apply to a wide range of flows [12].

$$\sigma_\epsilon = 1.3; \sigma_k = 1.0; C_{1\epsilon} = 1.44; C_{2\epsilon} = 1.92; C_\mu = 0.09$$

### 3.2.3. Filter

There are three different domains in this system. The filter, which is located between two fluid domains, is defined as a porous medium. It is used to capture the unreacted lime and the reaction product (calcium sulfite) from the gas stream. The porosity of the filter was estimated as 0.6 using optical microscope. High viscosities are assigned to hydrated lime calcium sulfite (dispersed phase) in order to represent their behavior. The resistivity of the porous filter medium was estimated from  $\vec{u}/-\nabla p$ , and the pressure drop was determined using the Ergun equation [12].

### 3.2.4. SO<sub>2</sub>-hydrated lime reaction

In this study, a two-phase Eulerian-Eulerian model under turbulent conditions was developed assuming that a reaction with volumetric species transport model takes place in a single phase as mentioned previously [12]. Hydrated lime (Ca(OH)<sub>2</sub>) constitutes 5 % of the total inlet mass flow. This reacts with SO<sub>2</sub> of the continuous gas phase. The inlet concentration of SO<sub>2</sub> is 300 ppm. The outlet boundary condition is taken as the atmospheric pressure, and the no-slip condition is applied on the walls. The boundary conditions for the base case are presented in Table 3.1; also, the temperature is taken as 70 °C, and there is no humidity in the gas. It should be mentioned here that even if no humidity is injected into the reactor, a certain amount of water forms due to the desulfurization reaction (Eqn. (3.4)). The goal is to remove the SO<sub>2</sub>, as calcium

sulfite/sulfate, which can be used in the production of valuable by-products such as fertilizer, wallboard, etc.

Table 3.1. Boundary Conditions

Boundary Conditions			
	Parameter	Value	Unit
Inlet	SO <sub>2</sub> mass concentration	300	ppm
	Ca(OH) <sub>2</sub> mass fraction	0.05	-
	H <sub>2</sub> O mass fraction (Humidity)	0	-
	Air mass fraction	Balance	
	Velocity	1	m/s
Outlet	Gauge pressure	0	Pa

### 3.2.5. Rate of reaction

The kinetic expression for the rate of reaction is introduced to the model based on Eqn. (3.11) using a user-defined function (UDF). This kinetic equation is obtained by Gutierrez and Orello [14] for an in-duct desulfurization process at low temperatures. They have used pilot plant experimental data to derive the equation:

$$\frac{dX}{dt} = 0.0768 \left( \frac{BET}{12.9} \right) \exp \left( - \frac{12.9 * 0.0019 X}{(RH/100)(BET)Y_{SO_2}} \right) \quad (3.11)$$

where, BET is the specific surface area of the sorbent which is 15 (m<sup>2</sup>/g) in this study. Y<sub>SO<sub>2</sub></sub> is the molar fraction of SO<sub>2</sub>, and X is the sorbent molar conversion. RH represents the relative humidity in percent.

### 3.2.6. Mesh Grid Study

Mesh grid analysis was carried out with a focus on the mesh independency and mesh quality. The examination of mesh independency was considered for various cell elements. The number of elements selected based on the verification of the results which did not further vary with the number of mesh cells, as illustrated in the Figure 3.2. The selected mesh has approximately 500 000 elements. The majority of elements are tetrahedral and wedge shaped. The element size is about 4 mm.

The convergence criterion was set as  $RMS = 10^{-6}$ . Outlet  $SO_2$  concentration was also monitored. Once this parameter no longer changed with subsequent iterations and the condition set for the Root Mean Square (RMS) was satisfied, the results were taken as final. The finer elements were used near the walls to represent the boundary layers appropriately, and a certain mesh inflation using ANSYS Meshing was applied near the walls and the filter. The mesh is presented in Figure 3.3, Figure 3.4, and Figure 3.5.



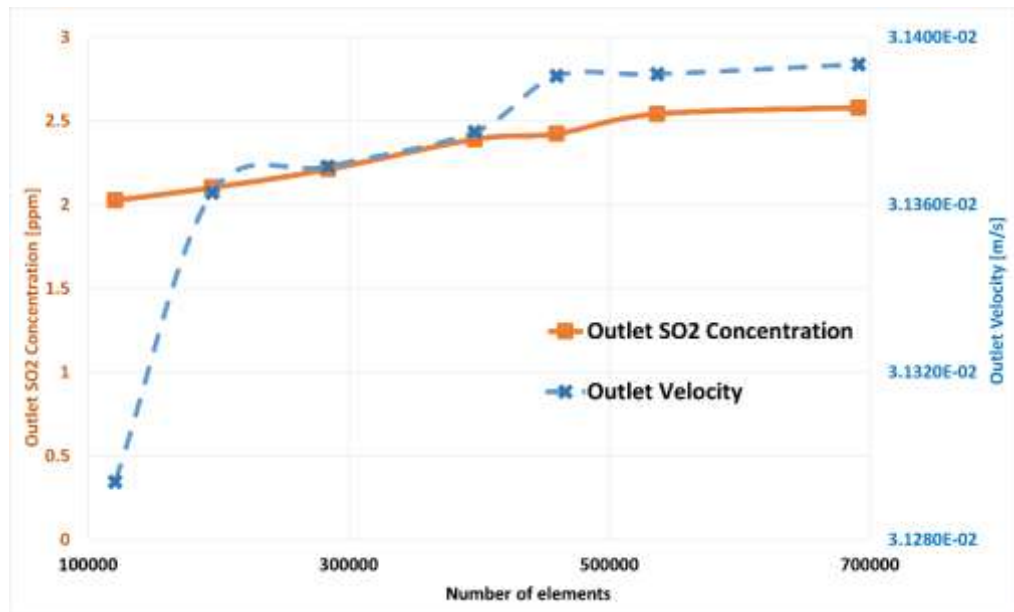


Figure 3.2. Mesh Independence Diagram

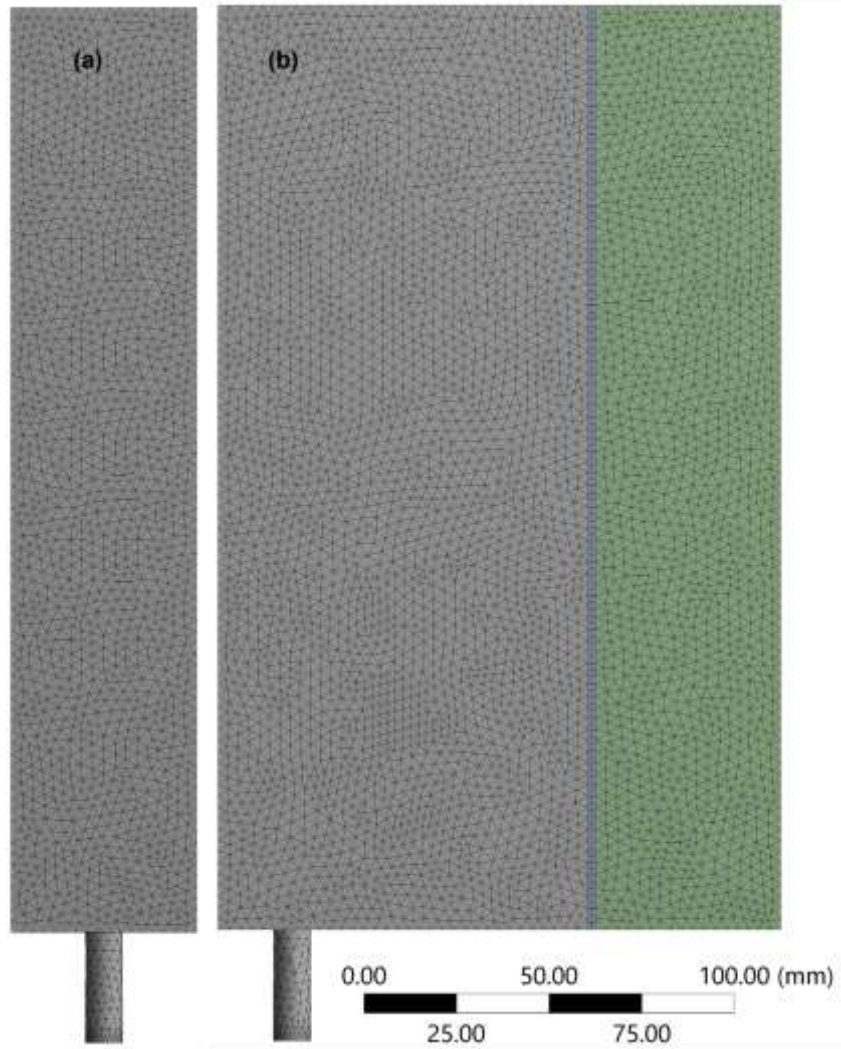


Figure 3.3. Mesh used: (a) Side view (b) Front view

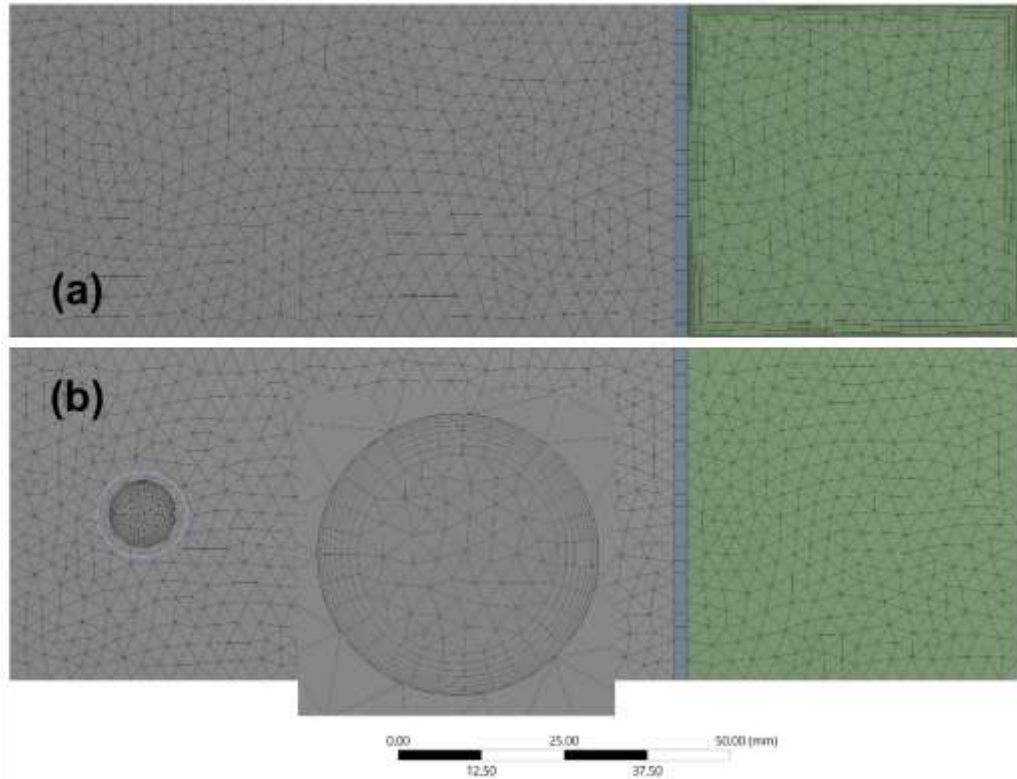


Figure 3.4. Mesh used: (a) Top view (b) Bottom view

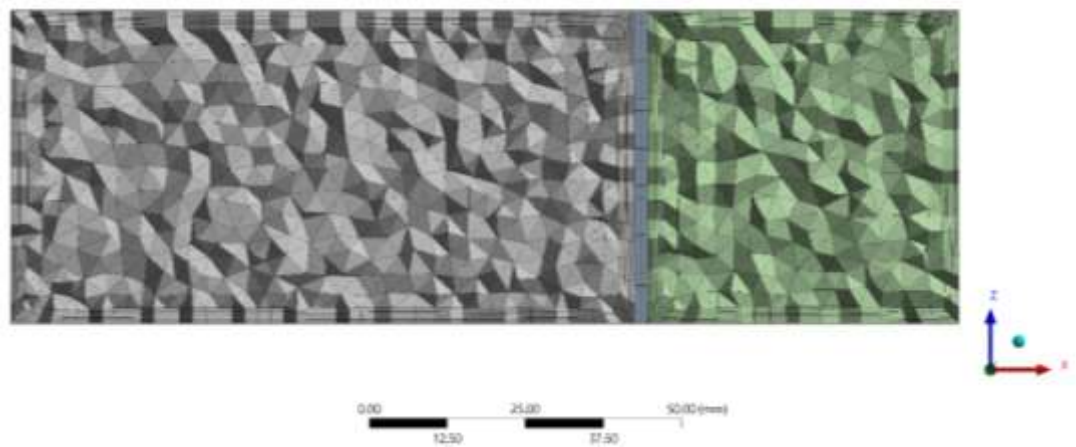


Figure 3.5. Mesh used: Cross-section on the central plane

The mesh quality is another important issue to ensure the reliability of the predictions. It is defined by maximum skewness, minimum orthogonality, and aspect ratio. The maximum skewness, which is suggested to be less than 0.85, is 0.65. The orthogonality is 0.7, which is greater than the minimum suggested value of 0.25.

Maximum aspect ratio is 10, which is recommended to be less than 20 to obtain a smooth convergence [12].

### 3.3. Results and discussion

#### 3.3.1. Base case

The results show that the  $\text{SO}_2$  is efficiently removed under the conditions presented in Table 3.1. It decreased from 300 ppm to 2 ppm when 5.0 wt.% hydrated lime is used as the sorbent. There is no humidity in the gas for the base case. Also, a parametric study was carried out and the results are presented. The parameters considered are the inlet sorbent (hydrated lime) concentration, inlet  $\text{SO}_2$  concentration, and relative humidity of gas on the outlet  $\text{SO}_2$  concentration ( $\text{SO}_2$  removal).

Figure 3.6 shows that the air concentration distribution in the reactor, and the variation is negligibly small as expected since it is inert. Its mass fraction is approximately 0.95 in the whole domain when no humidity is injected into the system.

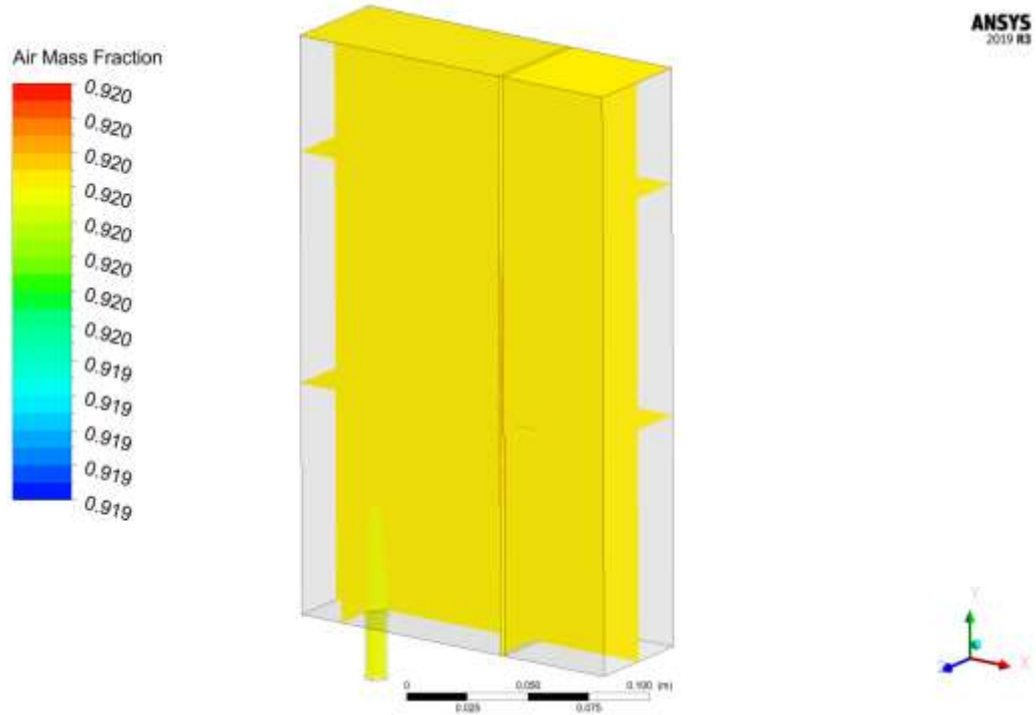


Figure 3.6. Air mass fraction contours

Figure 3.7 presents the  $\text{SO}_2$  mass concentration distribution (in ppm). It decreases from 300 ppm at the inlet to 2 ppm at the outlet under the conditions of the base case as it can be seen in the figure. This shows that it is possible to desulfurize the gas efficiently if the reaction rate equation properly represents the actual reaction. The experimental work is underway. The rate expression will be verified based on the experimental results and will be modified if necessary.

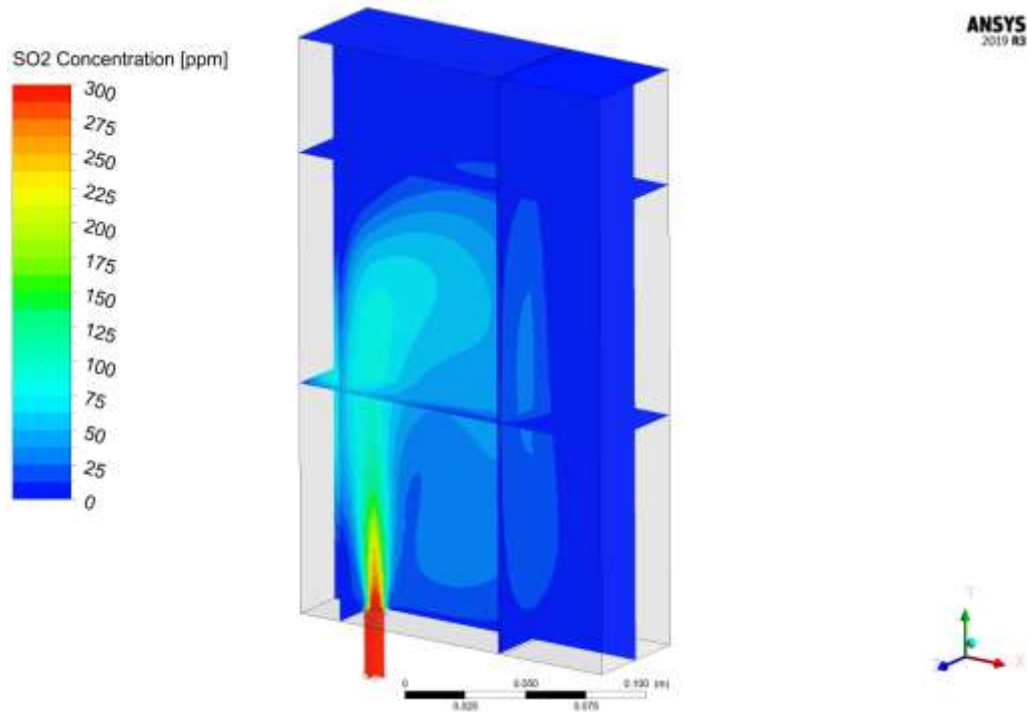


Figure 3.7 SO<sub>2</sub> concentration contours [ppm]

The distribution of the lime mass fraction is shown in Figure 3.8. The amount of lime is highest at the inlet and reduces as the reaction proceeds in the reactor. The trend is similar to that of SO<sub>2</sub> since they are both reactants. The hydrated lime is mostly retained on the filter as it can be seen in the figure. Normally, all particles should be retained, and none should exist after the filter. However, this part is still under development.

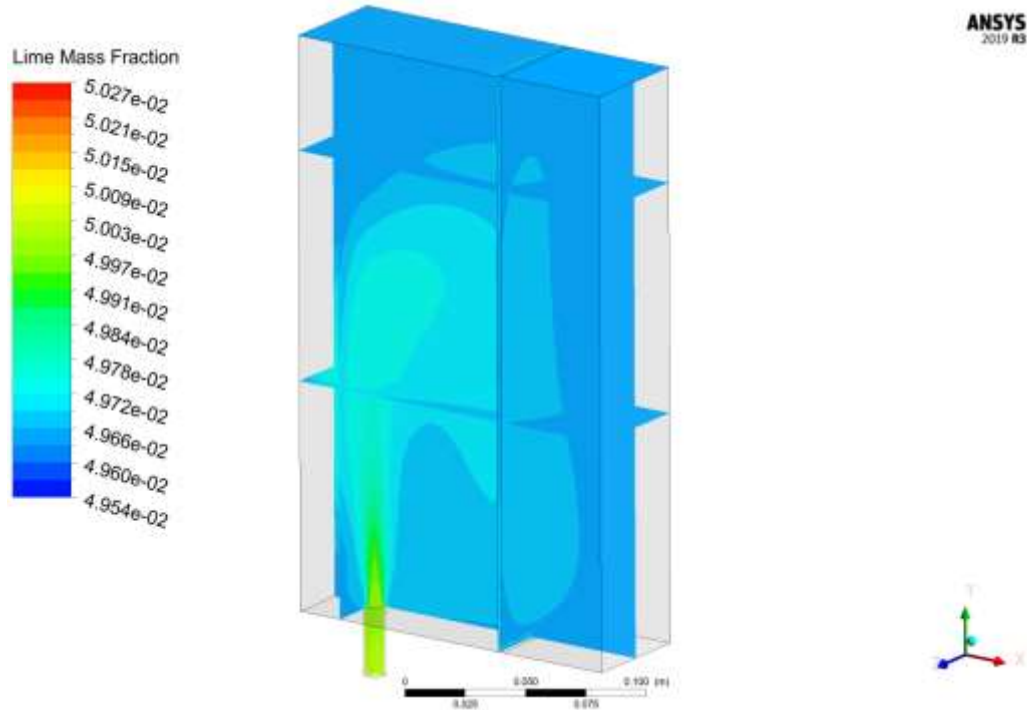


Figure 3.8. Lime mass fraction contours

The product calcium sulfite forms on/within the lime particles, and the amount formed can be calculated according to the stoichiometry of the reaction (Eqn. (3.4)) and the total amount of  $\text{SO}_2$  removed through the reaction. The  $\text{H}_2\text{O}$  is the other product of the reaction (Eqn. (3.4)) that shows the same trend as that of calcium sulfite, but the  $\text{H}_2\text{O}$  concentrations are also very low due to the small  $\text{SO}_2$  levels.

Figure 3.9 presents the velocity contours, showing the flow distribution. A fully developed flow is observed immediately in the inlet section and the centre of inlet line possesses the maximum velocity. Velocities are higher near the filter which shows that the hydrated lime and the product will be carried by the gas to the zone near the filter surface.

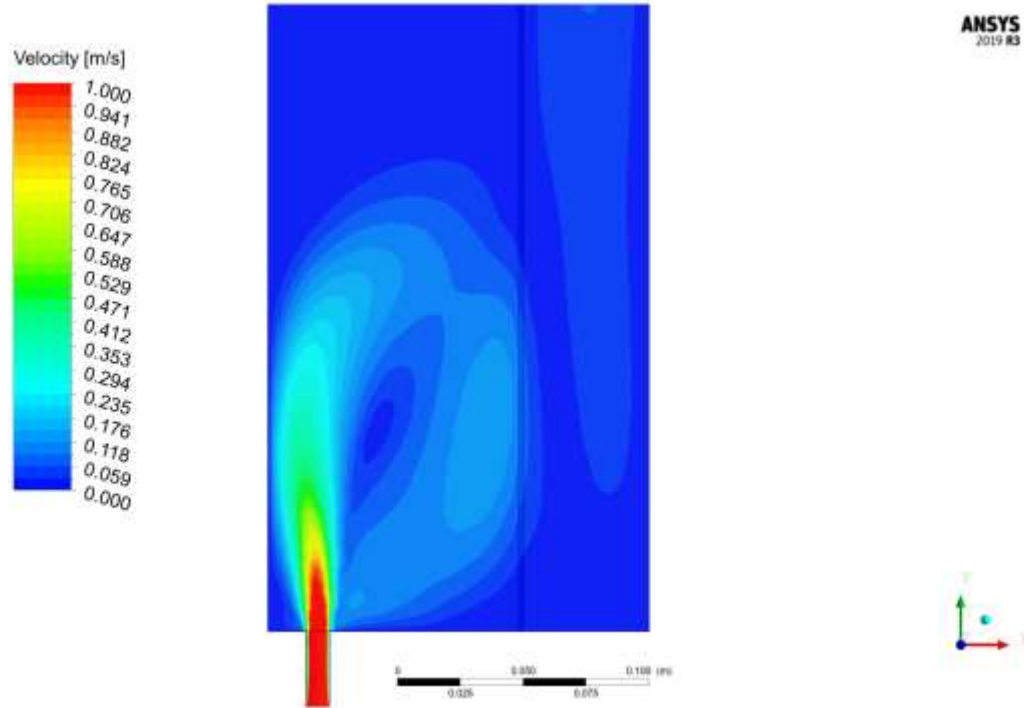


Figure 3.9. Velocity contour

### 3.3.2. Parametric Study

A parametric study was carried out to study the impact of some parameters on the SO<sub>2</sub> removal: inlet sorbent amount, inlet SO<sub>2</sub> concentration, and relative humidity, as shown in Table 3.2.

Table 3.2. Parameters used in the parametric study

	Base case	Parametric study
Inlet Ca(OH) <sub>2</sub> concentration, mass fraction	0.05	0.01, 0.02
Inlet SO <sub>2</sub> concentration, ppm	300	100, 200
Relative humidity (RH), %	0	15



Figure 3.10 shows the effect of the inlet concentrations of sorbent (hydrated lime) and SO<sub>2</sub> inlet concentration on the desulfurization of the gas. Increasing lime content increases the SO<sub>2</sub> removal at a given inlet SO<sub>2</sub> concentration. The higher the inlet SO<sub>2</sub> concentration is, the higher the outlet SO<sub>2</sub> concentration is for the same hydrated lime content. A slight increase in sorbent (hydrated lime) in the low sorbent ranges has a substantial impact on the removal process as shown in this figure. However, increasing the concentration of the sorbent further affects the removal of SO<sub>2</sub> to a lesser extent, especially when its inlet concentration is low. The results are in agreement with those of Ma et al. [15]. They found that an increase in the amount of calcium-based sorbent leads to a higher SO<sub>2</sub> removal. However, the excessively high Ca/S ratio does not substantially contribute to the removal process [16, 17]. The SO<sub>2</sub> concentration at the inlet affects the desulfurization process as observed by other research [3, 18, 19].

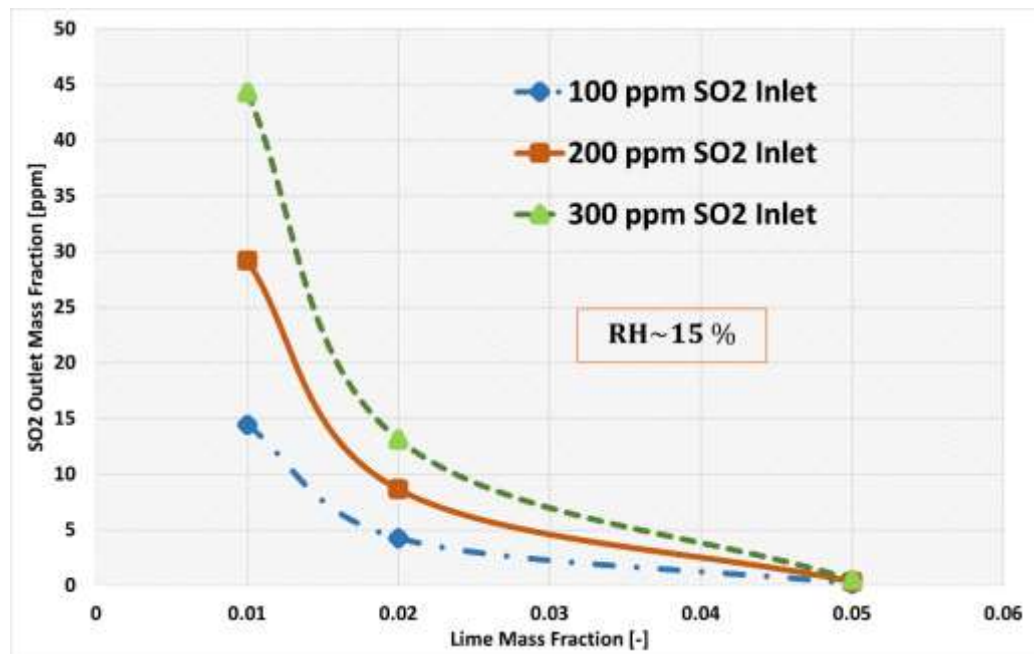


Figure 3.10. The effect of inlet lime and SO<sub>2</sub> concentrations

The presence of humidity also improves the desulfurization process [8, 15] as shown in Figure 3.11. The humidity of the gas at the inlet enhances the removal of SO<sub>2</sub> for a given lime mass fraction. The model results have demonstrated that humidity (15 % RH, Table 3.2) can increase the removal efficiency by 3 % (92 % to 95 %) for an inlet lime mass fraction of 2 %. The presence of humidity in gas is more influential when the inlet SO<sub>2</sub> concentration is high.

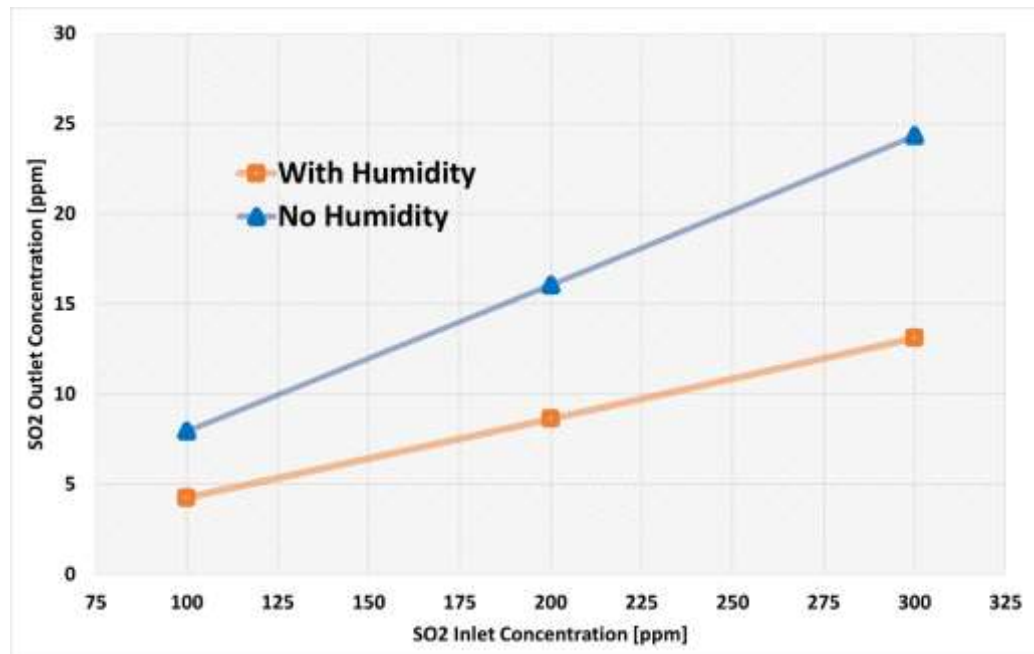


Figure 3.11. The effect of gas humidity on desulfurization for an inlet lime fraction of 0.02

Humidity plays an important role in SO<sub>2</sub> removal when low amount of sorbent is used as illustrated in Figure 3.12. For an inlet SO<sub>2</sub> concentration of 300 ppm, the presence of humidity improves the desulfurization process, resulting in a lower SO<sub>2</sub> concentration at the outlet. For example, it increases the removal efficiency by 8 % (77 % to 85 %) when the inlet lime mass fraction is 0.01.

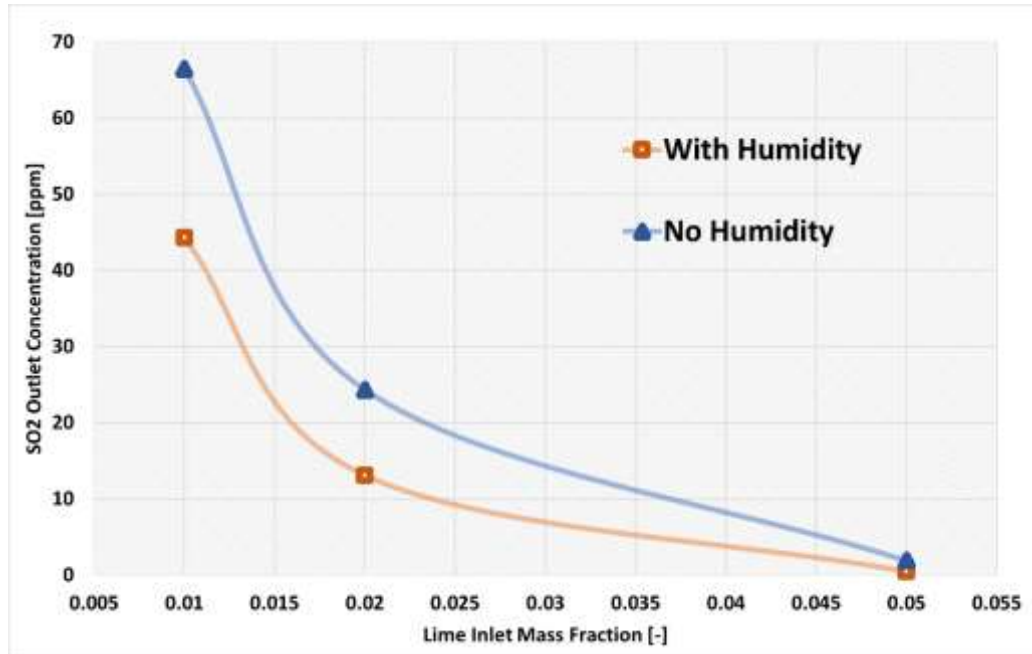


Figure 3.12. The effect of gas humidity on desulfurization when the inlet SO<sub>2</sub> concentration is 300 ppm

### 3.4. Conclusions

A multi-phase Eulerian-Eulerian and turbulent CFD model was developed and used to simulate the SO<sub>2</sub> removal from the gas in a lab-scale reactor.

Model solves the continuity, Navier-Stokes, species transport, and  $k - \epsilon$  turbulence model equations to determine the flow field and the species distributions in the system. The mesh was assessed in terms of both quality and independence of the results. In addition, inflation meshing is employed near the walls to well-represent the boundary layers. The process is isothermal (70 °C here, which can be changed) since the impact of reaction is minimal due to the low SO<sub>2</sub> concentration. A kinetic reaction rate is incorporated into the model using a UDF (user defined function). The reaction rate was taken from the literature. Based on this rate expression, it was possible to remove SO<sub>2</sub>

effectively. This will be verified using the experimental system and the necessary modifications will be made depending on the results.

The results showed that the SO<sub>2</sub> mass concentration of dry gas (0 % RH) is reduced from 300 ppm to 2 ppm, when 5.0 wt.% hydrated lime is used as the sorbent. Injection of humidity (RH = 15 %) into the gas improved the removal efficiency, resulting in lower SO<sub>2</sub> concentration at the outlet (about 0.5 ppm).

The parametric study showed that increasing the inlet SO<sub>2</sub> concentration results in a higher outlet concentration of SO<sub>2</sub> if all the other conditions are kept the same. Furthermore, increasing the sorbent concentration at the reactor inlet without any other change leads to a higher SO<sub>2</sub> removal. The presence of humidity in the inlet gas can increase the removal efficiency, enhancing as much as 8% in some cases depending on the inlet SO<sub>2</sub> and lime concentrations. The results are entirely consistent with those found in the literature. All these findings will be further assessed based on the results of the experimental work currently being undertaken.

### Acknowledgements

The financial and technical support of the NSERC, Rio Tinto, Graymont, the University of Quebec at Chicoutimi (UQAC), and REGAL is greatly appreciated.

### 3.5. References

1. Prasad, D.S.N., et al., *Removal of sulphur dioxide from flue gases in thermal plants*. Rasayan Journal of Chemistry, 2010. **3**: p. 328-334.
2. Gómez, A., N. Fueyo, and A. Tomás, *Detailed modelling of a flue-gas desulfurisation plant*. Computers & Chemical Engineering, 2007. **31**(11): p. 1419-1431.
3. Zettler, S., N. Fortin, and K. Moran, *Feasibility report on technical options to reduce SO<sub>2</sub> emissions Post-KMP*. 2013, Rio Tinto Alcan.
4. Charette, A., Y. Kocaefe, and D. Kocaefe, *Le carbone dans l'industrie de l'aluminium*. 2012: PRAL - Press Aluminium.

5. Canada, A.A.o. *PRIMARY ALUMINUM PRODUCTION*. Available from: [https://aac.metrio.net/indicators/economie/autre/production\\_aluminium\\_multi](https://aac.metrio.net/indicators/economie/autre/production_aluminium_multi).
6. Masterson, L., *Refinery run cuts reduce anode-grade coke supply*. 2020.
7. Maltais, J.-N., et al., *Development, Proof of Concept and Industrial Pilot of the New CHAC Scrubbing Technology: An Innovative and Efficient Way to Scrub Sulfur Dioxide*. 2016. p. 473-478.
8. Wang, N. and X. Zhang, *Effect of humidification water on semi-dry flue gas desulfurization*. *Procedia Environmental Sciences*, 2011. **11**: p. 1023-1028.
9. Ghosh, R., J. Smith, and A. Adams, *Horizontal In-Duct Scrubbing of Sulfur-Dioxide from Flue Gas Exhausts*. 2015. p. 595-601.
10. Lotfi, M., et al., *Computational Fluid Dynamics Modelling of the Pressure Drop of an Iso-Thermal and Turbulent Upward Bubbly Flow Through a Vertical Pipeline Using Population Balance Modelling Approach*. *Journal of Energy Resources Technology*, 2022. **144**(10).
11. Marocco, L. and A. Mora, *CFD modelling of the Dry-Sorbent-Injection process for flue gas desulfurization using hydrated lime*. *Separation and Purification Technology*, 2013. **108**: p. 205-214.
12. ANSYS, *ANSYS FLUENT Theory Guide 2022 R2*. 2022.
13. Launder, B.E. and D.B. Spalding, *Mathematical Models of Turbulence*. *Journal of Applied Mathematics and Mechanics* 1973. **53**(6): p. 424-424.
14. Gutiérrez Ortiz, F.J. and P. Ollero, *A realistic approach to modelling an in-duct desulfurization process based on an experimental pilot plant study*. *Chemical Engineering Journal*, 2008. **141**: p. 141–150.
15. Ma, X., et al., *Use of limestone for SO<sub>2</sub> removal from flue gas in the semidry FGD process with a powder-particle spouted bed*. *Chemical Engineering Science*, 2000. **55**(20): p. 4643-4652.
16. Xu, G., et al., *A new semi-dry desulfurization process using a powder-particle spouted bed*. *Advances in Environmental Research*, 2000. **4**(1): p. 9-18.
17. Bausach, M., et al., *Kinetic modelling of the reaction between hydrated lime and SO<sub>2</sub> at low temperature*. *AIChE Journal*, 2005. **51**: p. 1455-1466.
18. Garea, A., et al., *Kinetics of dry flue gas desulfurization at low temperatures using Ca(OH)<sub>2</sub>: competitive reactions of sulfation and carbonation*. *Chemical Engineering Science*, 2001. **56**: p. 1387-1393.
19. Harriott, P., *A simple model for SO<sub>2</sub> removal in the duct injection process*. *Journal of the Air & Waste Management Association*, 1990. **40**(7): p. 998-1003.

**CHAPTER 4**  
**MATHEMATICAL MODELLING OF A SEMI-DRY SO<sub>2</sub>**  
**SCRUBBER BASED ON A LAGRANGIAN-EULERIAN**  
**APPROACH**  
**(ARTICLE 2)**

Arash Fassadi Chimeh<sup>1</sup>, Duygu Kocaefe<sup>\*1</sup>, Yasar Kocaefe<sup>1</sup>, Yoann Robert<sup>2</sup>, Jonathan  
Bernier<sup>2</sup>

<sup>1</sup>Research Chair on Industrial Materials (CHIMI), University Research Centre on Aluminium (CURAL),  
Aluminium Research Center (REGAL), University of Quebec at Chicoutimi, 555 University Blvd., Chicoutimi,  
QC G7H 2B1, Canada

<sup>2</sup>Arvida Research and Development Centre (ARDC), Rio Tinto, 955 Boulevard Mellon, Jonquière, QC G7S 4K8,  
Canada

This article is ready to be submitted to a journal.

Abstract

Semi-dry desulfurization is an efficient means of SO<sub>2</sub> removal from the effluent gases from electrolysis cells in aluminum smelters. These gases are at low temperature and contain low concentrations of SO<sub>2</sub>, as opposed to thermal power plants. The removal is carried out by injecting powdered alkaline sorbent, hydrated lime (solid particles), into the SO<sub>2</sub>-containing gas (gas phase) in the presence of humidity. The reaction is controlled by the adsorption of SO<sub>2</sub> onto the surface of lime. This study involves the mathematical modelling of a lab-scale scrubber using a Lagrangian-Eulerian approach in order to analyze the desulfurization efficiency. A parametric study was carried out to investigate the effects of particle size, sorbent amount, and relative humidity (RH) on the desulfurization efficiency. The results show that the particle size

is the most important parameter; as the particle size decreases, the desulfurization efficiency increases. However, using finer particles may increase the process cost. The loss in SO<sub>2</sub> capture efficiency due to the use of coarser particle size could be compensated by increasing the relative humidity (RH) of the gas, another key parameter of the process.

**Keywords:** Semi-dry desulfurization; Computational fluid dynamics (CFD); Aluminum electrolysis; Particle surface reaction; Lagrangian-Eulerian method.

### Nomenclature

$A_p$	Particle area (m <sup>2</sup> )	$V_{cell}$	Cell volume (m <sup>3</sup> )
$a_i$	Constants of drag coefficient model	$x_p$	Particle position vector (m)
$BET$	Specific surface area (m <sup>2</sup> /g)	$X$	Ca(OH) <sub>2</sub> molar conversion (mol/mol)
$Ca/S$	Calcium to sulfur ratio (mol/mol)	$Y_{SO_2}$	SO <sub>2</sub> molar concentration in gas phase (mol/mol)
$d_p$	Particle diameter (m)		
$D_{eff}$	Effective diffusivity of SO <sub>2</sub> in air and humidity (m <sup>2</sup> /s)		
$g$	Acceleration of gravity (m/s <sup>2</sup> )		
$k$	Turbulent kinetic energy (m <sup>2</sup> /s <sup>3</sup> )		
$L_s$	Characteristic length of system (m)		<i>Greek letters</i>
$m_p$	Particle mass (kg)	$\eta_{SO_2}$	SO <sub>2</sub> removal efficiency
$\dot{m}_{SO_2,k}$	Particle mass source term of SO <sub>2</sub> (kg/s)	$\epsilon$	Energy dissipation rate (m <sup>2</sup> /s <sup>3</sup> )
$M_i$	Molecular weight of i-th species (kg/mol)	$\mu$	Gas dynamic viscosity (Pa s)
$P$	Pressure (Pa)	$\rho$	Gas density (kg/m <sup>3</sup> )

$P_{op}$	Operating pressure (Pa)	$\rho_p$	Particle density (kg/m <sup>3</sup> )
$RH$	Relative Humidity (%)	$\omega_{SO_2}$	Mass fraction of SO <sub>2</sub> in gas phase
$Re$	Reynolds number	$\omega_{SO_2}^0$	Mass fraction of SO <sub>2</sub> in gas phase at inlet
$S_{SO_2}$	Source term of SO <sub>2</sub> species (kg/m <sup>3</sup> s)		
$t$	Time (s)		
$t_{res}$	Particle residence time (s)		Acronyms
$T$	Gas temperature (K)	CFD	Computational fluid dynamics
$\vec{u}$	Gas velocity vector (m/s)	DPM	Discrete phase model
$\vec{u}_p$	Particle velocity vector (m/s)	RMS	Root mean square
$u_s$	Characteristics velocity of the system (m/s)		

#### 4.1. Introduction

The emissions of sulfur dioxide (SO<sub>2</sub>) from industrial plants and other sources are a major source of air pollution through the acid rain [1]. It is harmful for human health and wild and aquatic life; it also corrodes the buildings, ancient structures, and monuments [1, 2]. The removal of SO<sub>2</sub> from the effluent gas before discharging it to atmosphere is called desulfurization.

As one of the most widely used metals, demand for aluminum is expected to increase by 4.2 percent annually until 2050 as a result of its unique properties [3]. Aluminum is used in a variety of applications, including construction, transportation, etc. [4]. As one of the world's largest aluminum producers and exporters, Canada produced approximately 3.2 million tonnes of aluminum in 2020, with 90% of that amount



coming from Quebec [5]. Aluminum is electrolytically produced through the Hall-Heroult process, and the atmospheric emissions include sulfur dioxide (SO<sub>2</sub>) [6].

The desulfurization process can be carried out using three different methods: wet, dry, and semi-dry processes [7]. Dry desulfurization involves the interaction of SO<sub>2</sub> containing gas with a solid sorbent such as lime [2]. The process is generally used when the sulfur content of gas stream is low or medium. There are several different technologies for dry desulfurization, including lime spray dryer (LSD) and circulating fluidized bed (CFB) which are mostly used [7].

The disadvantages associated with the dry and wet desulfurization processes led to the development of semi-dry desulfurization technology in the 1980s. In dry desulfurization, the process is dominated by a large sorbent demand and a low desulfurization rate. The desulfurization efficiency in the wet process is high, but the capital cost is also high. In addition, it requires reheating and post-treatment facilities [8]. The semi-dry process does not require such facilities, and it is less costly and requires less space than the wet desulfurization process [7]. The semi-dry desulfurization process is widely used for low to medium sulfur content (< 2.5 %) [9]. Lime powder with water is atomized into fine droplets and sprayed into the reactor. Water vaporizes rapidly increasing the relative humidity of the gas. SO<sub>2</sub> is adsorbed onto the Ca(OH)<sub>2</sub> particles, and this is followed by the reaction of SO<sub>2</sub> with lime. In the industrial scrubbers, the solid particles are collected in the baghouse [2, 8].

In recent years, continuous research has been conducted to improve and optimize the semi-dry desulfurization process. Karlsson and Klingsspor [10] found that the SO<sub>2</sub> content in the gaseous stream has no direct impact on the desulfurization rate. Ma et al. [9] determined experimentally the key parameters that affect the desulfurization

rate: relative humidity (RH), sorbent Ca/S molar ratio, sorbent particle size ( $d_p$ ). They achieved 96% desulfurization efficiency using Ca/S = 1.5 for hydrated-lime and Ca/S = 1.75 for limestone with a particle size of 3.5  $\mu\text{m}$ . Zhou et al. [11] were able to increase the desulfurization rate by humidifying the adsorbent using water and hydrogen peroxide ( $\text{H}_2\text{O}_2$ ) solutions. Based on the sorbent value and the “approach to adiabatic saturated temperature” (difference between the gas temperature and saturated temperature through the adiabatic line of humidity chart), the desulfurization efficiency varied from 25% to 40% when water was used. The utilization of  $\text{H}_2\text{O}_2$  increased the desulfurization efficiency from 45% to 56%. Ma et. al. [12] showed when the Ca/S ratio is greater than 1.2 and the approach to adiabatic saturation temperature is less than 13 K, the desulfurization efficiency can be increased up to 95 %.

The field of computational fluid dynamics (CFD) has received considerable attention, especially with regard to new technologies which require extensive time, energy, and financial resources to develop and test [13, 14]. Development of new processes without using modelling can be time-consuming, and almost impossible in some cases, such as those involving hazardous conditions, large-scale equipment, etc. In addition, the modelling reveals the results in detail and a parametric study can be easily conducted to determine the effects of various parameters [14].

A wide variety of heat and mass transfer applications specifically in multi-phase condition have been accomplished using CFD. Lotfi et al. [13] investigated a multi-phase Euler-Euler single species (water) flow in order to estimate the pressure drop and void fraction using ANSYS CFX. Wang et. al. [15] carried out a CFD-DEM numerical investigation focused on the hydrodynamic behavior of gas-solid phases in a semi-dry (PPSB) desulfurization process. Wang et. al. [16] used Euler-Euler modelling for a

semi-dry desulfurization pilot-scale system considering heat and mass transfer, a reaction model, and the kinetic particle theory. Marocco and Mora [17] studied a desulfurization process involving a one-way coupled solid-gas interaction using ANSYS Fluent at a RH of 60% to determine and compare the desulfurization rate in two different geometries. The effect of sorbent content and humidity, key parameters for the desulfurization process, was not considered in their studies. A one-way coupling only analyzes the effects of the continuous fluid phase on particles whereas a two-way coupling evaluates the effects of both continuous fluid and solid phases on each other [18]. Fassadi Chimeh et al. [19] evaluated the desulfurization efficiency in a similar geometry using the Euler-Euler method, assuming a volumetric reaction and a high viscosity liquid for sorbent instead of particle surface reactions, which is the subject of the current article.

In this study, both steady-state and transient CFD multi-phase (gas-solid) models were developed under isothermal (70 °C) condition using an Eulerian-Lagrangian method to determine the desulfurization efficiency of a lab-scale reactor (scrubber) under different relative humidities (RH). User Defined Function (UDF) was used to introduce the kinetic reaction rate in the model (ANSYS Fluent 2022 R1) using the C language. A two-way coupling was employed to determine the mutual effects of both gas and solid phases. A parametric study was carried out to investigate the effect of the sorbent particle size, sorbent molar ratio (Ca/S), and relative humidity (RH) on the desulfurization efficiency. A comprehensive understanding of the impact of key parameters that control the desulfurization process under the conditions of low temperatures and low SO<sub>2</sub> concentrations is not yet available. However, these are the conditions encountered during aluminum production. The outcomes of this study give

an insight into the impact of key parameters that result in the desulfurization process. The predicted results are in agreement with those found in the literature [12, 17, 19-21].

#### 4.2. Governing equations

The continuous gas phase, which consists of air, SO<sub>2</sub>, and humidity, is considered as the Eulerian framework while the Lagrangian approach is used for the dispersed solid phase containing sorbent particles. A two-way coupling is employed to determine the mutual influence of discrete and continuous phases [18]. Discrete phase model (DPM) is used to treat the sorbent solid particles. The dimensions of the scrubber and the boundary conditions are given in Table 4.1. The geometry, shown in Figure 4.1, is prepared using Space claim. To prevent particles from escaping to the atmosphere, a filter is used in the scrubber domain. It allows the gas phase to exit the scrubber without particles.

Table 4.1. Dimensions of the scrubber and boundary conditions for gas and solid phases

Geometry of the scrubber	
Inlet diameter	10 (mm)
Height	250 (mm)
Width	150 (mm)
Depth	50 (mm)
Characteristic length	~ 18.5 (mm)
Gas phase	
Temperature	70 °C
Relative humidity	10, 30 (%)

SO <sub>2</sub> inlet concentration	200 ppm
Inlet velocity	1 m/s
Outlet pressure	0 Pa (atmospheric)
Viscosity	$\sim 1.8 \times 10^{-5}$ (Pa.s)
Solid phase (Ca(OH) <sub>2</sub> )	
Mass flowrate (molar Ca/S ratio)	Ca/S = 10, 50, 200
Specific surface area, BET	38.25, 11.80 (m <sup>2</sup> /g)
Mean particle diameter	10, 45 (μm)
Density	2300 kg/m <sup>3</sup>

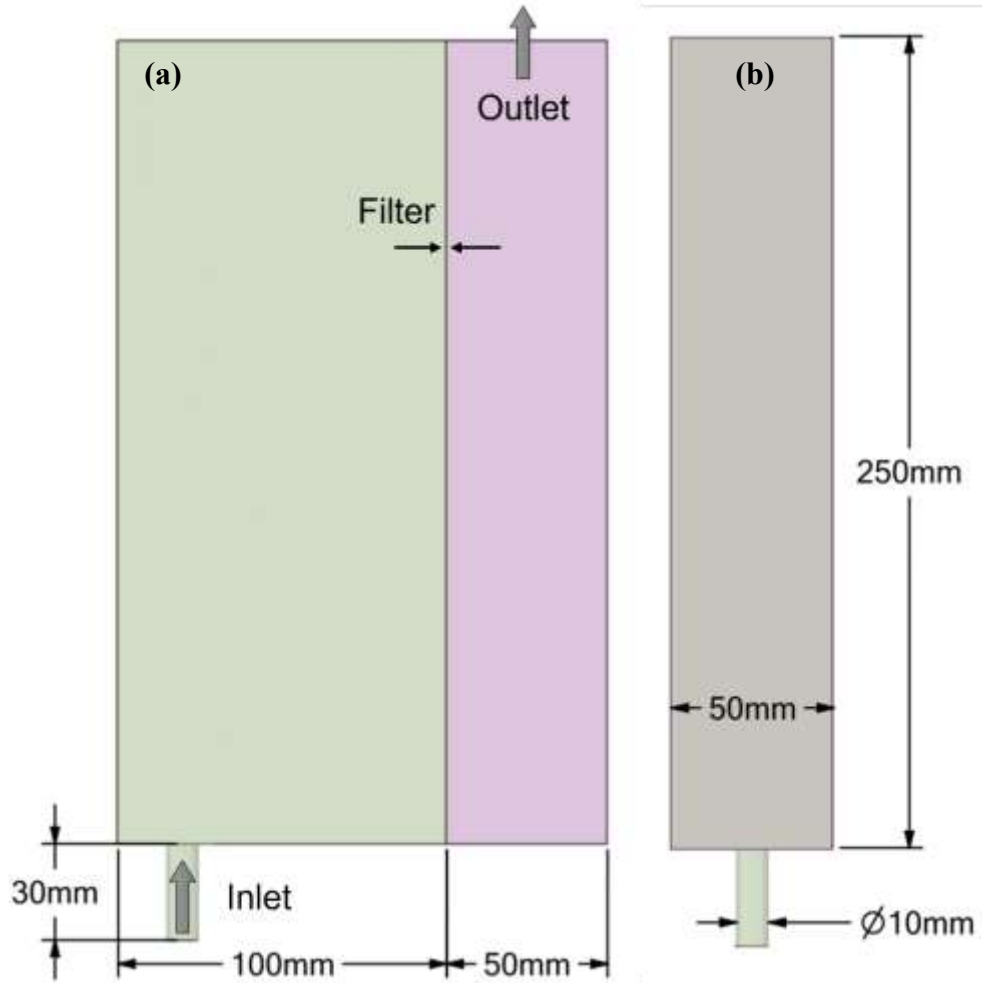


Figure 4.1. Scrubber geometry: (a) front view, (b) side view

© Arash Fassadi Chimeh, 2023

#### 4.2.1. Continuous gas phase mixture

The mass and momentum equations are solved for the continuous gas phase (Eqns (4.1)-(4.3)). The species transport equation is solved for each of the species (Eqn (4.3)), and  $S_i$  is the source term. The source term of  $\text{SO}_2$  in the continuity equation can be neglected due to the low content of  $\text{SO}_2$  compared to the total gas flowrate.

$$\frac{\partial \rho}{\partial t} + \nabla \cdot (\rho \vec{u}) = 0 \quad (4.1)$$

$$\frac{\partial(\rho\bar{u})}{\partial t} + \nabla \cdot (\rho\bar{u}\bar{u}) = -\nabla p + \nabla \cdot (\tau + \tau_R) + \rho\bar{g} \quad (4.2)$$

$$\frac{\partial(\rho\omega_i)}{\partial t} + \nabla \cdot (\rho\omega_i u) = \nabla \cdot (\rho D_{eff} \nabla \omega_i) + S_i \quad (4.3)$$

The source term for SO<sub>2</sub> in Eqn. (4.3) is defined as the volume average of the contributions to the SO<sub>2</sub> capture by all the individual particles within the cell volume according to Eqn. (4.4).

$$S_{SO_2} = -\frac{1}{V_{cell}} \sum_k S_{SO_2,k} = -\frac{1}{V_{cell}} \sum_k \dot{m}_{SO_2,k} \quad (4.4)$$

The standard  $k - \epsilon$  turbulence model is selected due to its accuracy in simulating heat and mass transfer in a wide range of engineering applications. The reasonable accuracy in addition to the relatively short calculation time makes this semi-empirical, two-equation model a good choice for the current study [18]. This model is proposed by Launder and Spalding [22]. The turbulent viscosity (eddy) term is a function of  $k$  and  $\epsilon$  which are turbulent kinetic energy and dissipation rate of energy, respectively. Eqn. (3.5) to Eqn. (3.7) represent the standard  $k - \epsilon$  turbulence equations.

$$\frac{\partial}{\partial t}(\rho k) + \frac{\partial}{\partial x_i}(\rho k u_i) = \frac{\partial}{\partial x_j} \left[ \left( \mu + \frac{\mu_t}{\sigma_k} \right) \frac{\partial k}{\partial x_j} \right] + G_k + G_b - \rho \epsilon \quad (4.5)$$

$$\frac{\partial}{\partial t}(\rho \epsilon) + \frac{\partial}{\partial x_i}(\rho \epsilon u_i) = \frac{\partial}{\partial x_j} \left[ \left( \mu + \frac{\mu_t}{\sigma_\epsilon} \right) \frac{\partial \epsilon}{\partial x_j} \right] + C_{1\epsilon} \frac{\epsilon}{k} (G_k + C_{3\epsilon} G_b) - C_{2\epsilon} \rho \frac{\epsilon^2}{k} \quad (4.6)$$

$$\mu_t = \rho C_\mu \frac{k^2}{\epsilon} \quad (4.7)$$

The model constants are given below, which are suggested by Launder and Spalding [22].

$$\sigma_\epsilon = 1.3; \sigma_k = 1.0; C_{1\epsilon} = 1.44; C_{2\epsilon} = 1.92; C_\mu = 0.09$$

#### 4.2.2. Dispersed phase – hydrated lime (Ca(OH)<sub>2</sub>)

When the flow field is known, the particle trajectories can be calculated. The dispersed solid phase is calculated using the Lagrangian approach by Discrete Phase Model (DPM). Stokes number ( $St$ ), representing the relation between the particle response time and the system response time, can help select the most appropriate model. For the particle phase, DPM would be an acceptable and suitable choice if the Stokes number is close to 1 [18].

$$St = \frac{\tau_p}{t_s} = \frac{\left(\rho_p d_p^2 / 18\mu\right)}{\left(L_s / u_s\right)} \quad (4.8)$$

The characteristic length of the system ( $L_s$ ) is the ratio of the system volume to the surface area of the system in contact with the gas phase. It is assumed that the particles have a uniform size distribution that is the same as the one at the inlet. It must be noted that the particle-particle interaction is negligible since the volume fraction of discrete phase is less than 10% [18]. The continuity and momentum equations for individual and non-rotating particles are given in Eqns. (4.9) to (4.11).

$$\frac{dx_p}{dt} = u_p \quad (4.9)$$

$$\frac{dm_p}{dt} = S_{SO_2,k} = \dot{m}_{SO_2,k} \quad (4.10)$$

$$m_p \frac{du_p}{dt} = \frac{1}{2} \rho C_D |u - u_p| (u - u_p) A_p + m_p g \quad (4.11)$$

The particles are considered spherical to determine the drag coefficient,  $C_D$ , which is calculated using Eqn. (12). The constants, proposed by Morsi and Alexander [23], are applicable in a wide range of Reynolds number.

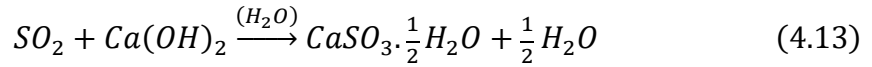


$$C_D = a_1 + \frac{a_2}{Re} + \frac{a_3}{Re^2} \quad (4.12)$$

The flowrate of particles is defined according to the Ca/S molar ratios of 10 (=  $2.3 \times 10^{-7}$  kg/s), 50 (=  $1.15 \times 10^{-6}$  kg/s), and 200 (=  $4.6 \times 10^{-6}$  kg/s).

### 4.3. Adsorption process

The reaction between SO<sub>2</sub> and hydrated lime (Ca(OH)<sub>2</sub>) in the presence of humidity takes place according to Eqn. (4.13). SO<sub>2</sub> is adsorbed on the surface of lime particles and the reaction occurs producing a mixture of calcium sulfite and sulfate on the particle surface [7]. To simplify the calculations in this study, it is assumed that only calcium sulfite forms as the reaction product.



Ortiz and Ollero [24] developed a kinetic model as a function of relative humidity (RH), BET, and other factors for the reaction between SO<sub>2</sub> and hydrated lime. They found that the model results are in good agreement with the experimental results obtained from their pilot plant. Thus, this model is used in this study to calculate the reaction rate. According to Eqn. (4.14), the key variables are the amount of sorbent utilized, SO<sub>2</sub> concentration in the gas, specific surface area, and relative humidity (RH).

$$\frac{dX}{dt} = 0.0768 \left( \frac{BET}{12.9} \right) \exp \left( - \frac{12.9 * 0.0019 X}{\frac{RH}{100} \cdot BET \cdot Y_{SO_2}} \right) \quad (4.14)$$

where X is the sorbent conversion defined as the molar ratio of the lime reacted to its initial value, BET is the BET surface area (m<sup>2</sup>/g) of the particles, and RH represents the relative humidity (%). Y<sub>SO<sub>2</sub></sub> is the SO<sub>2</sub> molar concentration in the gas phase (mol/mol).

#### 4.4. Meshing and boundary conditions

In ANSYS Fluent 2022 R1, the kinetic reaction rate is integrated into the model using a user-defined file (UDF). It must be noted that only the mass transfer of SO<sub>2</sub> between the gas and solid phases is simulated in the presence of humidity.

The structured mesh used in this study is of high quality, providing a smoother convergence during the calculation. Maximum skewness and minimum orthogonal quality are 0.25 and 0.7, respectively. The aspect ratio is obtained as 10. The o-grid mesh type is used for the inlet section of the scrubber, and all the cells are hexahedral. There are 350 000 elements, which is the optimum number of elements obtained from a sensitivity analysis of grid independence. Finer mesh is used near the walls ( $y^+ = 5.0$ ) and a filter is used to capture the high gradient factors. Figure 4.2 and Figure 4.3 illustrate the front, side, and bottom views of the meshed domain.

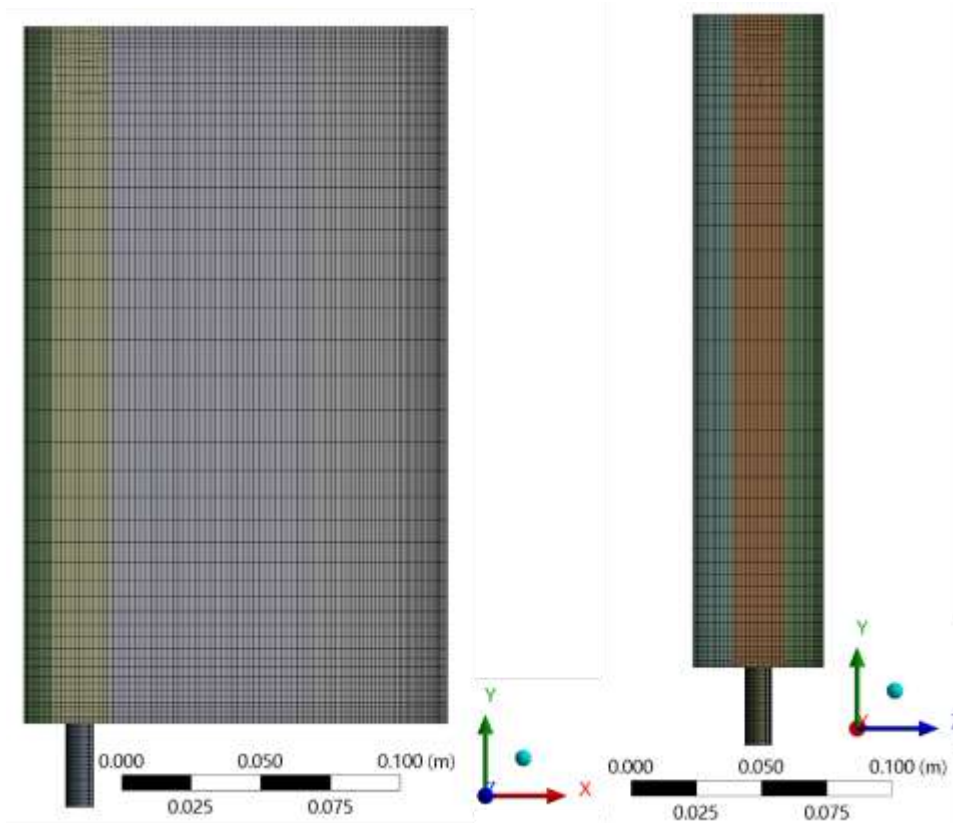


Figure 4.2. Meshed domain – front and side views

© Arash Fassadi Chimeh, 2023

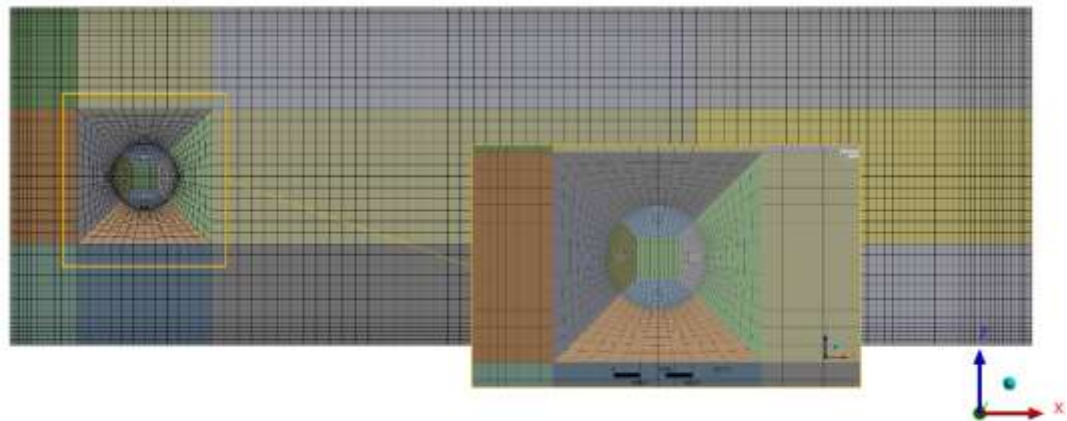


Figure 4.3. Meshed domain - Bottom view

© Arash Fassadi Chimeh, 2023

As it can be seen from Eqn. (13), for each mole of reacted  $\text{SO}_2$ , half a mole of water is produced, which increases the humidity. This humidity, however, is negligible due

to the small SO<sub>2</sub> concentration (about 200 ppm). The water produced by the reaction does not affect the relative humidity significantly because the amount of water vapor in the system (humidity injected) is three orders of magnitude greater than the amount of water produced during the reaction. All cells are considered to have the same relative humidity value. No-slip and adiabatic boundary conditions are applied at the walls. Filter is represented by the *porous-jump* boundary condition with a 2-mm thickness, and the discrete phase boundary condition type has been selected as *trap*. It prevents the particles from passing through the filter and traps them on the surface of the filter. This paper presents a mathematical model for a semi-dry gas desulfurization scrubber, including the simulation of a filter [17], a subject on which there are very few publications.

A converged solution is obtained when both of the following conditions are satisfied: (a) root mean square (RMS) of all equations is less than 10<sup>-6</sup>, and (b) the concentration of SO<sub>2</sub> (ppm) at the outlet remains constant.

Stokes number is estimated using Eqn. (3.8) as  $\approx 0.77$  which is close to unity. Therefore, DPM can be considered a suitable choice for the simulation of this system if the volume fraction of dispersed phase is less than 10%.

#### 4.5. Results and discussion

After carrying out the simulation of the reactor, the volume fraction of dispersed phase was verified. It was found that its value in every cell is less than 10 %. Thus, the utilization of DPM was justified. Various cases were simulated. The results of the simulations are presented, and the removal efficiencies, defined by Eqn. (3.15), for different cases were compared.

$$\eta_{SO_2}(x) = 1 - \frac{\omega_{SO_2}(x)}{\omega_{SO_2}^0} \quad (3.15)$$

where,  $\omega_{SO_2}^0$  is the inlet  $SO_2$  mass fraction in the gas fed to the scrubber.

#### 4.5.1. Steady-state results

Figure 4.4 demonstrates the velocity vectors and contours for the gas phase using two different particle sizes. The hydrodynamic boundary layer (velocity gradient) at the inlet can be clearly seen in this figure. The impact of the interaction between the continuous gas phase and the solid dispersed phase on the velocity field is evident. The velocities are somewhat higher near the top for the smaller particles, which indicates that they can be carried further compared to the larger particles, as expected.

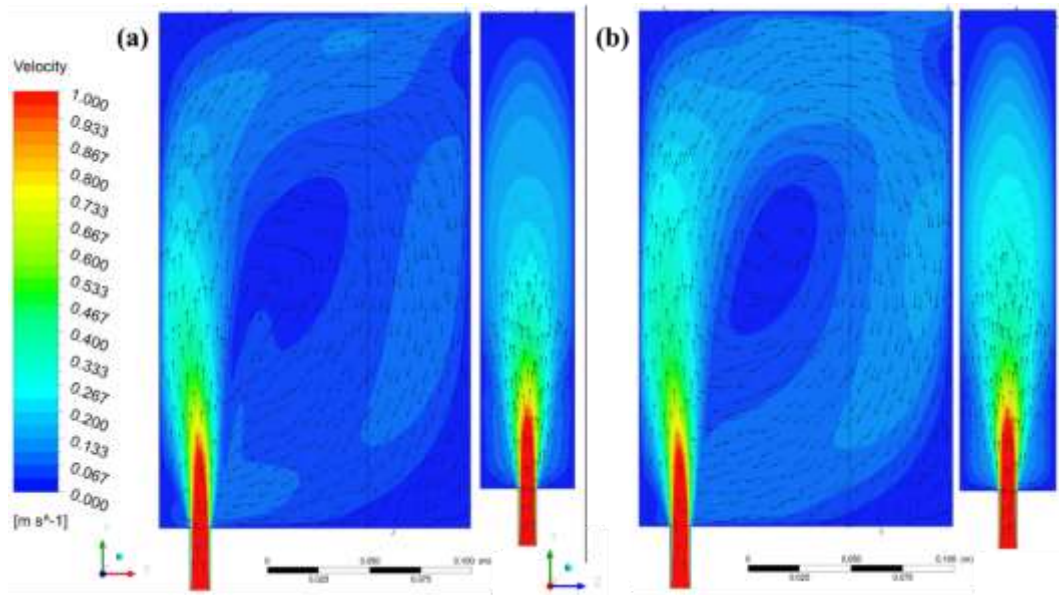


Figure 4.4. Gas phase velocity distribution - Ca/S = 50; RH = 10%; (a)  $d_p = 45 \mu m$  (b)  $d_p = 10 \mu m$

© Arash Fassadi Chimeh, 2023

Table 4.2 presents the conditions used in the simulations and the calculated desulfurization efficiency values for the scrubber. The results show that a higher sorbent amount (Ca/S ratio) improves desulfurization when other parameters are kept

constant. Higher ratio means that there is more lime available to capture the sulfur. Also, increasing RH, increases the desulfurization rate when all the other parameters are kept the same (see Eqn. (3.14)). Particle size is another key parameter which influences the desulfurization rate. Smaller particles lead to better SO<sub>2</sub> removal. First of all, the smaller particles have a greater surface area compared to the larger particles. In addition, the small particles used in this study were obtained by crushing the larger particles in order to have higher BET specific surface area (38,25 m<sup>2</sup>/g compared to 11.81 m<sup>2</sup>/g). This means that the area where SO<sub>2</sub> and lime can come into contact and react is greater for the smaller particles, and this increases the desulfurization rate (see Eqn. (3.14)).

Figure 4.5 shows the effect of relative humidity and particle size on the desulfurization rate. The dashed lines illustrate the behavior of 45-micron particles while solid lines show that of the 10-micron particles. It is observed that in lower sorbent ranges, RH plays a more significant role than the particle size for the desulfurization efficiency; however, as the sorbent (Ca/S) value increases, the effect of particle size becomes more significant, especially at lower RH values. As can be seen in Figure 4.5, increasing relative humidity for finer particles is not as effective as it is for coarser particles, especially for values greater than Ca/S = 50. Therefore, the relative humidity is an important parameter if the coarser particles ( $d_p = 45 \mu\text{m}$ ) are used. Increasing the relative humidity improves the desulfurization efficiency more when larger particles are used, especially around Ca/S = 50.

Table 4.2. Predicted desulfurization efficiency (percentage of SO<sub>2</sub> removed) under different conditions © Arash Fassadi Chimeh, 2023

Inlet SO <sub>2</sub> concentration = 200 ppm			
	$Ca/S = 10$	$Ca/S = 50$	$Ca/S = 200$
RH = 10 %	$d_p = 10 \mu m$ 0.357	$d_p = 10 \mu m$ 0.853	$d_p = 10 \mu m$ 0.974
	$d_p = 45 \mu m$ 0.214	$d_p = 45 \mu m$ 0.624	$d_p = 45 \mu m$ 0.885
RH = 30 %	$d_p = 10 \mu m$ 0.676	$d_p = 10 \mu m$ 0.951	$d_p = 10 \mu m$ 0.993
	$d_p = 45 \mu m$ 0.413	$d_p = 45 \mu m$ 0.835	$d_p = 45 \mu m$ 0.963

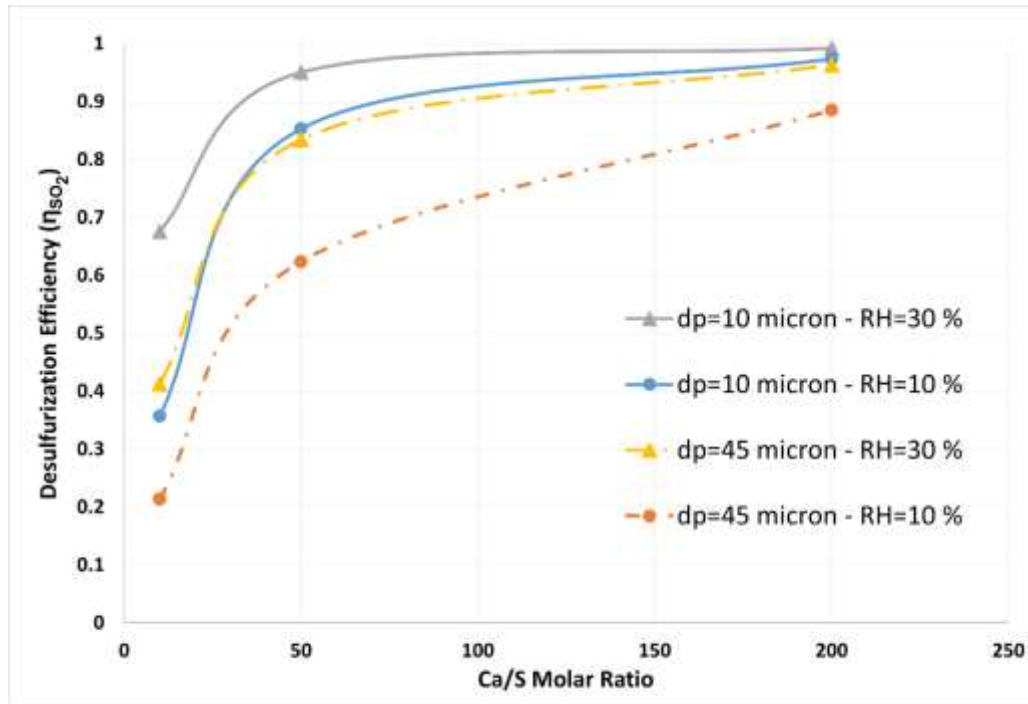


Figure 4.5. The effect of particle size and relative humidity on the predicted desulfurization efficiency for the scrubber

© Arash Fassadi Chimeh, 2023

Figure 4.6 compares the distributions of desulfurization contours in the scrubber for two different cases with a Ca/S ratio of 50. The particle fraction remains less than 10 %, and the particle-particle interaction can be neglected for this case as well. The first case is for low RH and smaller particles (Figure 8b) while the second case is for high RH and larger particles. At this sorbent value, smaller particles and lower RH give a slightly better desulfurization efficiency (0.853) than coarser particles and higher RH (0.835). Although the rate of desulfurization is quite similar, the difference in particle size and RH has a significant impact on the desulfurization pattern. This particle size effect can only be observed if the two-way coupling approach (particles affect the gas phase and the gas phase affects the particles) is used.

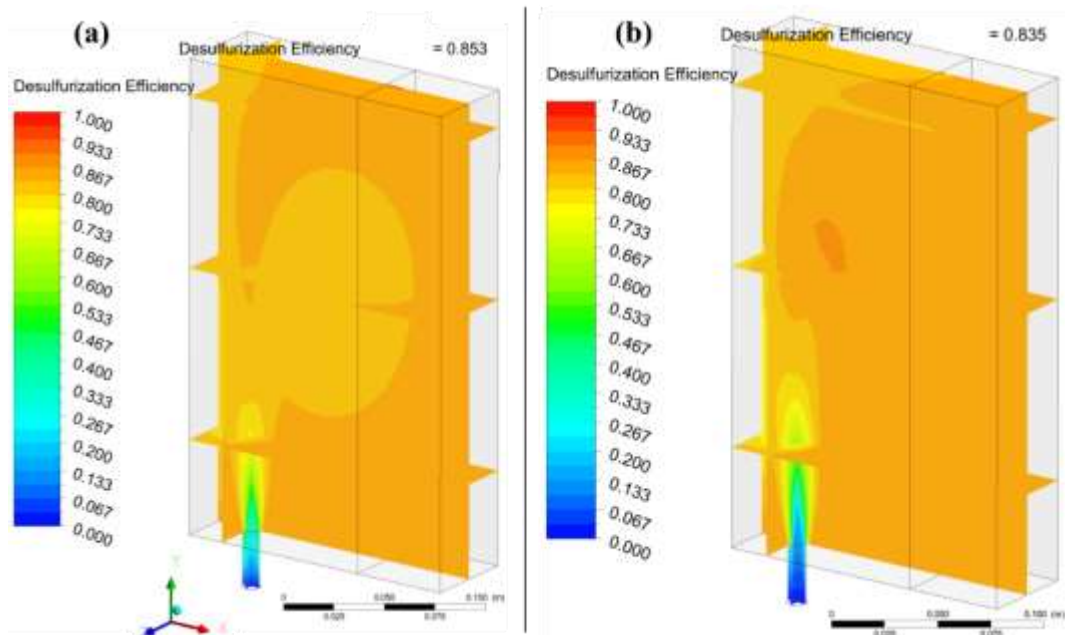


Figure 4.6. Distribution of desulfurization levels at Ca/S = 50 for (a)  $d_p = 10 \mu m$ ; RH = 10%

(b)  $d_p = 45 \mu m$ ; RH = 30%

© Arash Fassadi Chimeh, 2023



#### 4.5.2. Transient results

A number of cases were analyzed under transient conditions to compare the effects of RH, sorbent size, and Ca/S ratio on the desulfurization efficiency as a function time. A time step of 0.2 second was found appropriate and the total number of time steps is 300. The first minute of the desulfurization process was modelled. The desulfurization efficiency of the scrubber – the parameter of interest – as a function of time is shown in Figure 4.7 for a number of cases to determine the time it takes to reach the steady-state condition. It takes approximately 10 seconds to approach the steady-state condition for the highest sorbent ratio ( $\text{Ca/S} = 200$ ). For other Ca/S ratios, RH, and particle sizes, the steady-state condition is reached somewhat later. The desulfurization efficiency results show that the influence of the BET specific surface area (particle size) is greater than that of the relative humidity since increasing the BET area three times (11.80 to 38.25  $\text{m}^2/\text{g}$ ) increases desulfurization more than the case where the relative humidity is increased three times (10% to 30%). The effect of RH on the desulfurization efficiency is less than that of the particle size. If the larger particles are used, increasing the RH could compensate for the loss of the desulfurization efficiency in industrial applications; this would lead to almost a similar desulfurization efficiency if smaller particles were used under low RH conditions. In addition, almost similar desulfurization efficiency can be obtained by using higher RH, instead of increasing the Ca/S ratio of 10-micron particles, as it can be seen in Figure 4.7 and Table 4.2.

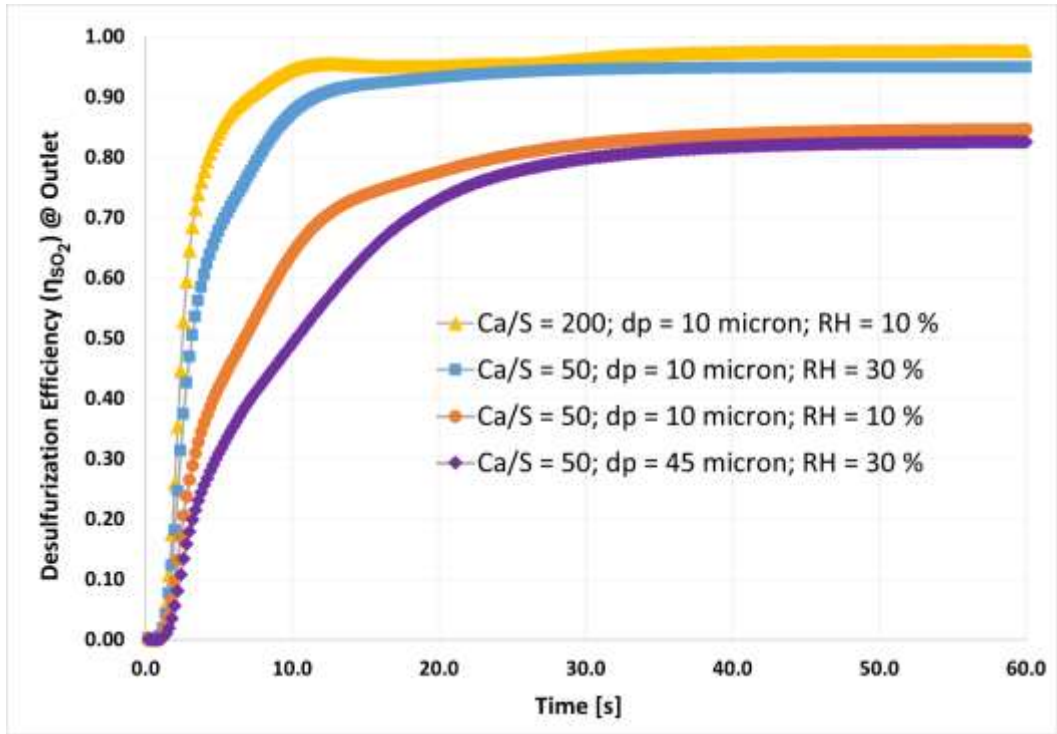


Figure 4.7. Desulfurization efficiency as a function of time

© Arash Fassadi Chimeh, 2023

Figure 4.8 and Figure 4.9 compare the desulfurization efficiency contours of two cases:  $dp = 45$  micron,  $RH = 30\%$ ; and  $dp = 10$  micron,  $RH = 10\%$  at different times (1, 5, 10, and 55 seconds). As shown in these figures, after the injection of sorbent particles, the reaction starts to take place and the desulfurization efficiency increases near the inlet where the particles are fed to the system (1 s). The particles continue to pass through the domain (5 s), and the desulfurization efficiency in upper part of the scrubber increases since the particles become present there, reducing the  $SO_2$  concentration. As the time increases (10 s), the lower part of the scrubber reaches  $SO_2$  concentrations similar to those of the upper side of the scrubber. Finally, the steady state is reached, and the outlet  $SO_2$  concentration does not change further with increasing time. It is observed that a better desulfurization efficiency is reached after

10 s using smaller particles under low RH condition compared to the other cases. After 55 s, the outlet SO<sub>2</sub> concentrations are almost similar for both cases.

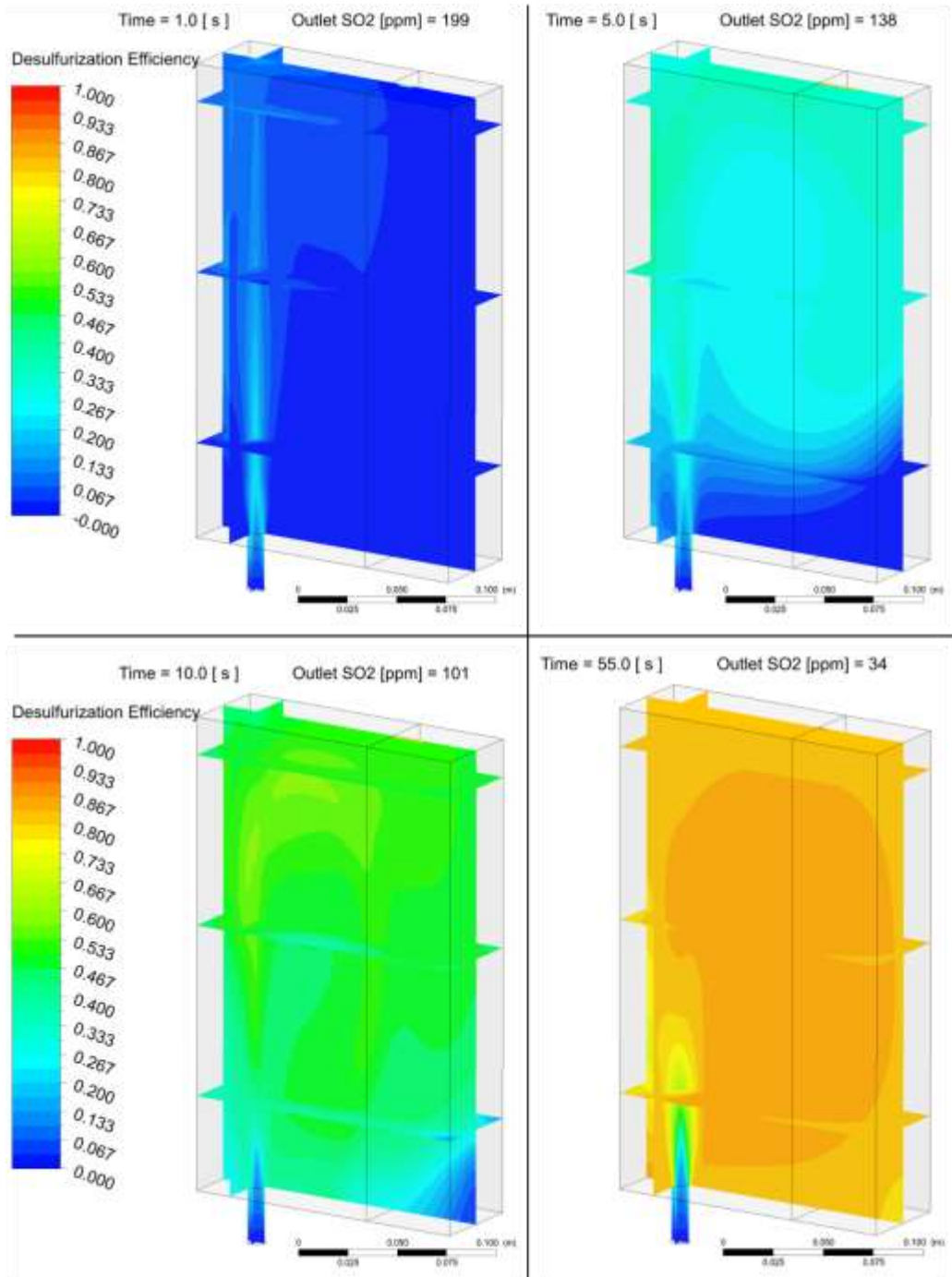


Figure 4.8. Desulfurization efficiency contours -  $Ca/S = 50$ ;  $d_p = 45 \mu m$ ;  $RH = 30\%$

© Arash Fassadi Chimeh, 2023

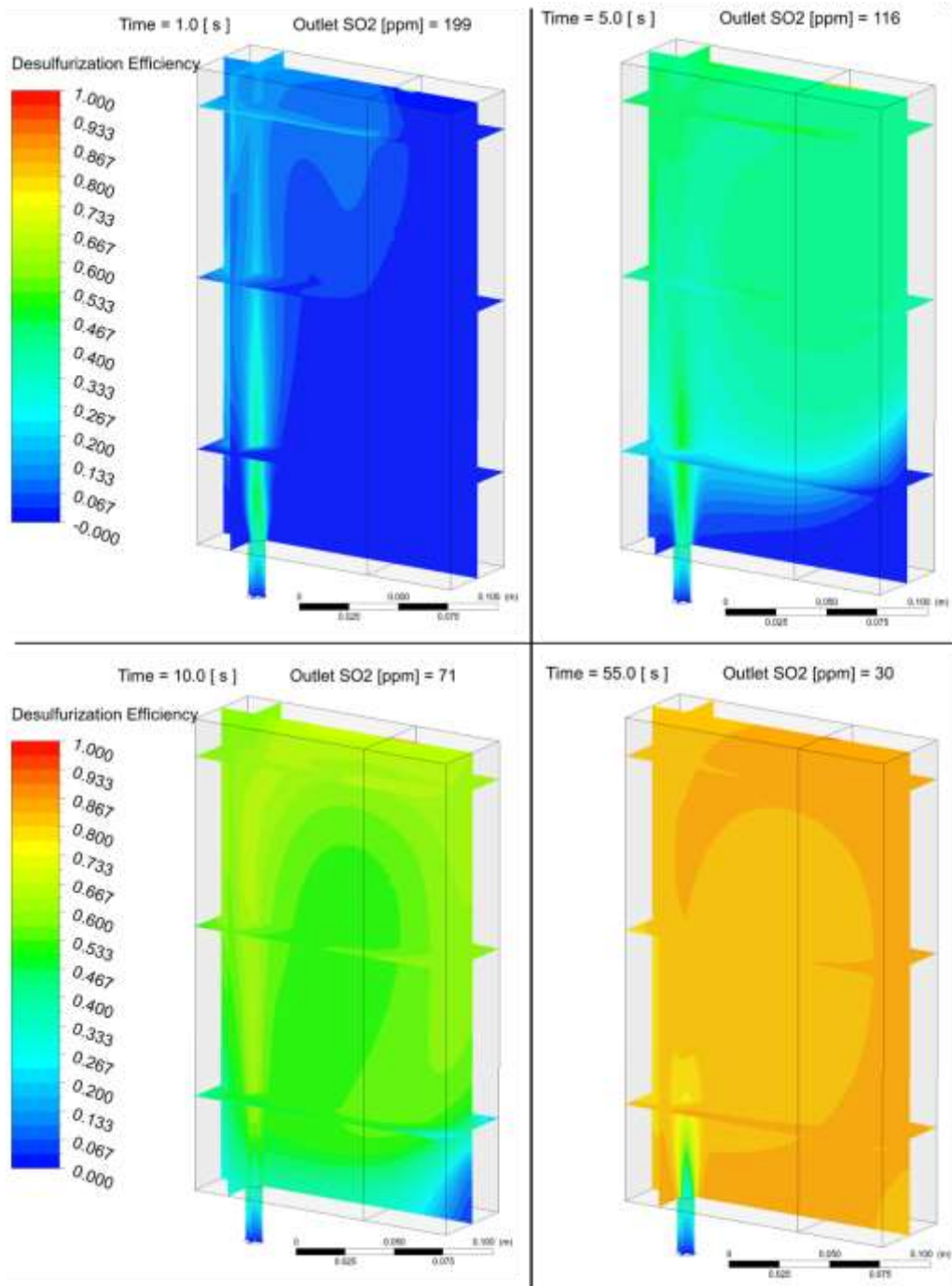


Figure 4.9. Desulfurization efficiency contours -  $Ca/S = 50$ ;  $dp = 10 \mu m$ ;  $RH = 10\%$

© Arash Fassadi Chimeh, 2023

Figure 4.10 illustrates the particle tracks and the residence times for the case with smaller particles and lower relative humidity at different times during the process. These results provide a good insight in terms of the desulfurization product ( $CaSO_3$ )

formation and the presence of fresh hydrated lime since the product is formed on the surface of the fresh hydrated lime. The particles colored nearly red (indicating high residence time) are the calcium sulfite, and those colored nearly blue (indicating low residence time) are the fresh hydrated lime. The SO<sub>2</sub> concentration at the scrubber outlet shows that the outlet SO<sub>2</sub> concentration decreases as the time increases and more particles are injected into the system.

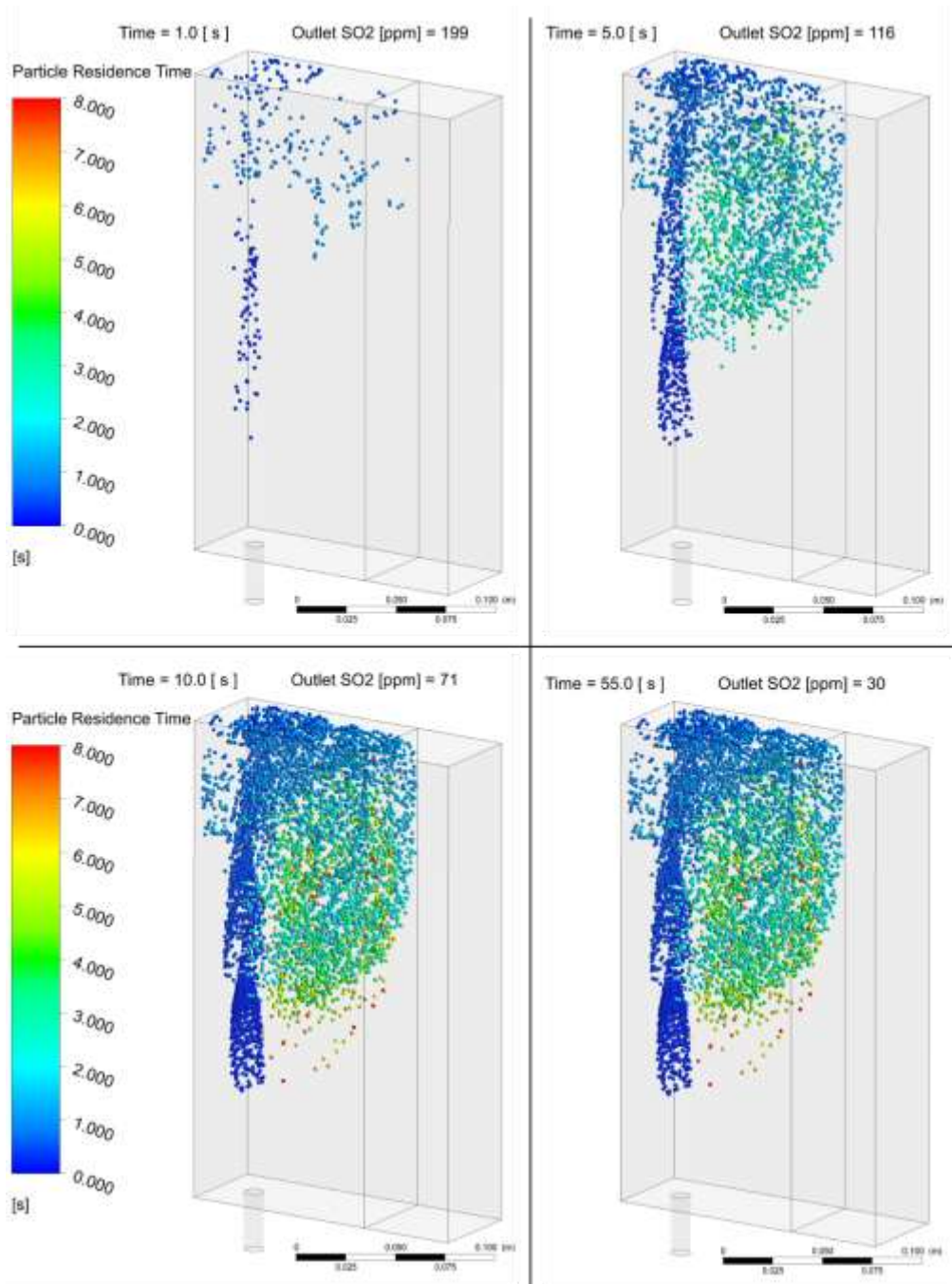


Figure 4.10. Particle residence time -  $Ca/S = 50$ ;  $d_p = 10 \mu m$ ;  $RH = 10\%$

© Arash Fassadi Chimeh, 2023

Figure 4.11 illustrates the particle tracks and the residence times for the case with larger particles and higher relative humidity (RH) at different times. If Figure 4.10 and 11 are compared, it can be seen that the heavier 45-micron particles tend to fall more

quickly compared to 10-micron particles, as expected. Similar to the results seen in Figure 4.10, the particle residence time helps identify the fresh lime and the calcium sulfite ( $\text{CaSO}_3$ ). The particles of 45-micron size settle more quickly compared to 10-micron particles. The larger particles may be easier to handle in industry, for example for scrubber cleaning.



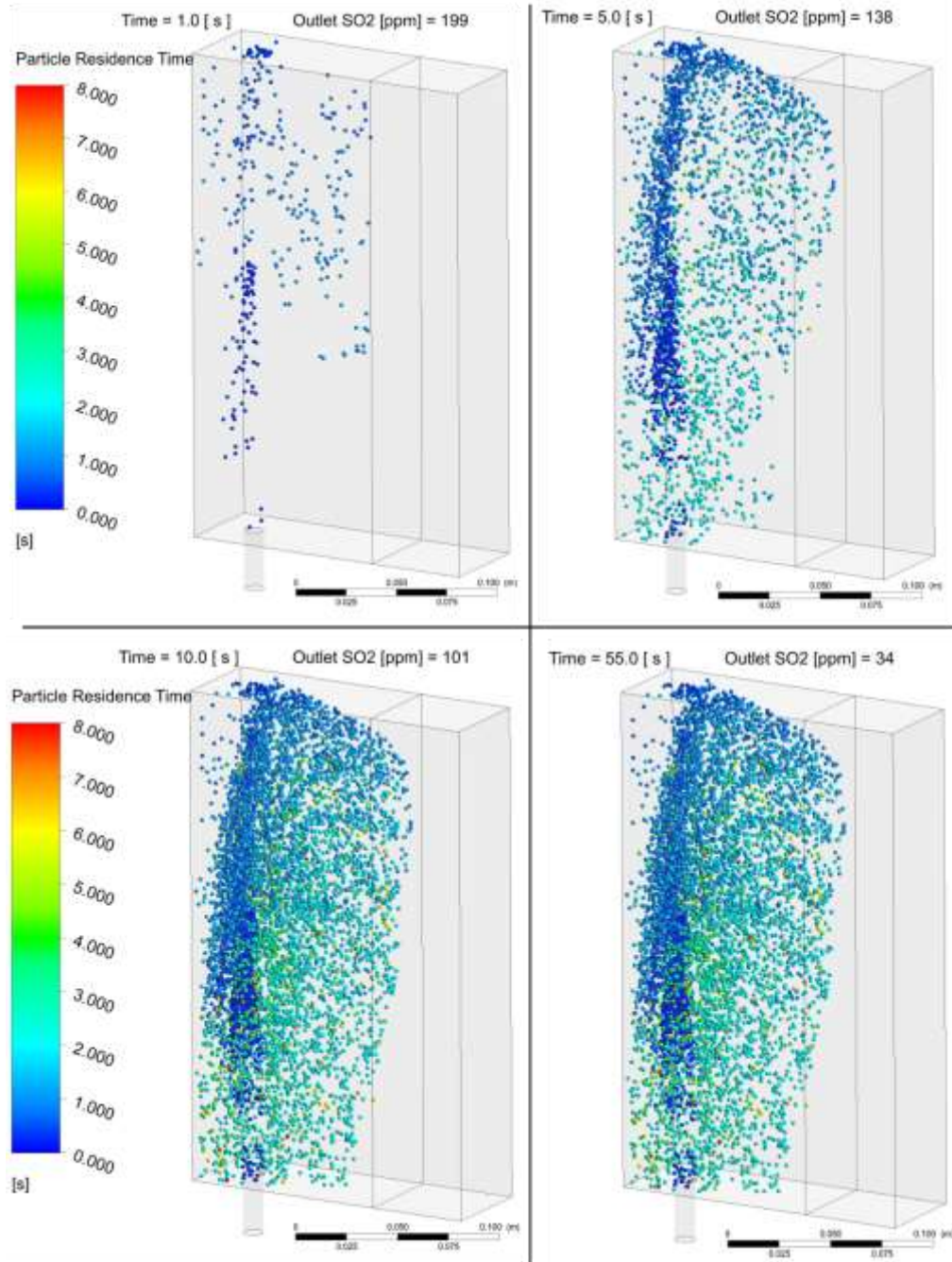


Figure 4.11. Particle residence time -  $Ca/S = 50$ ;  $d_p = 45 \mu m$ ;  $RH = 30\%$

© Arash Fassadi Chimeh, 2023

Figure 4.12 demonstrates the volume fraction of particle phase (DPM volume fraction) for a case with the highest amount of sorbent presented in this study ( $Ca/S = 200$ ) at different times. As can be seen from this figure, the DPM volume fraction is

significantly less than 10% which justifies the utilization of this model. The DPM volume fractions are smaller in the other cases since lower sorbent amounts are used.

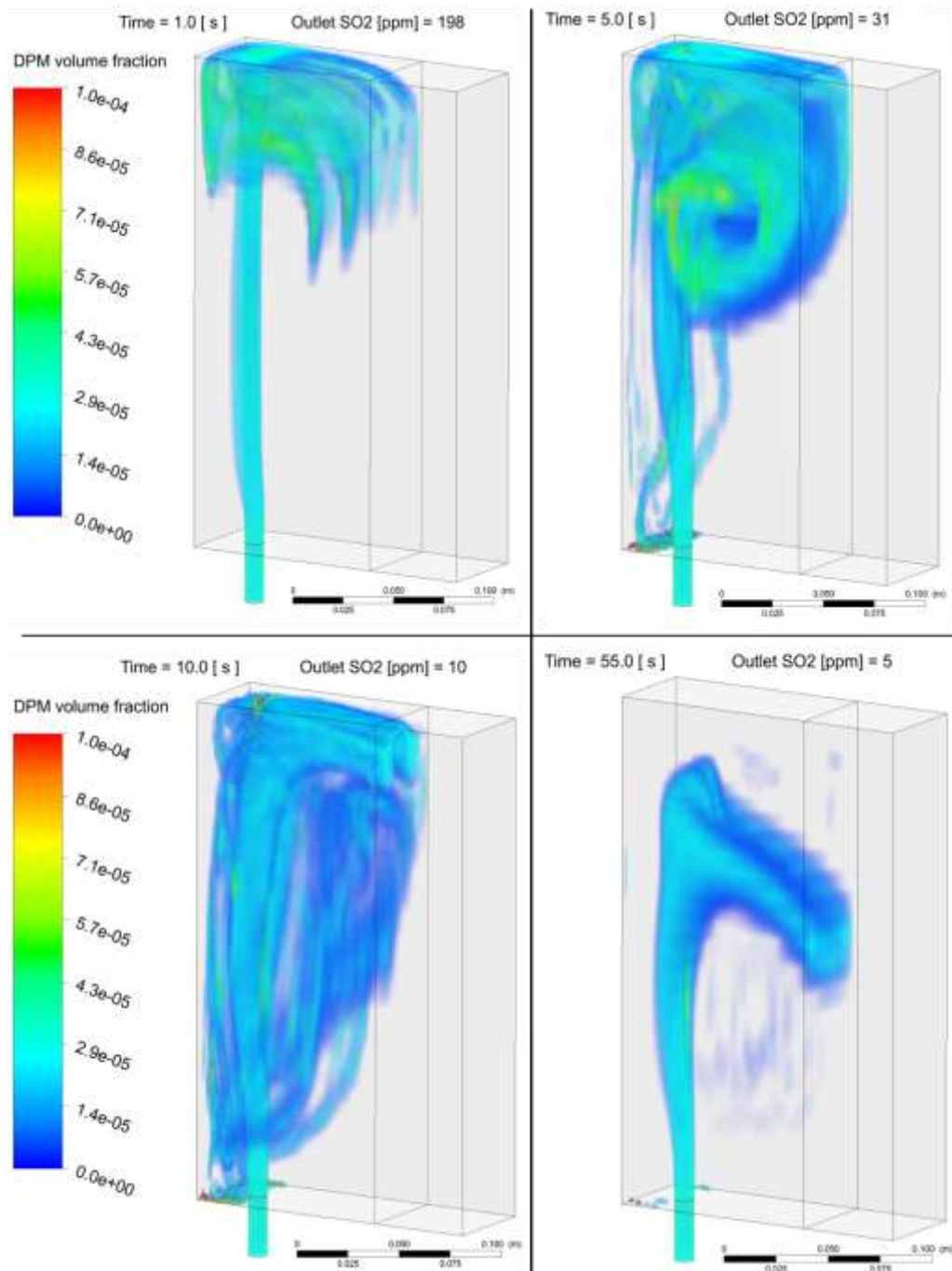


Figure 4.12. DPM volume fraction - Ca/S = 200;  $d_p = 10 \mu\text{m}$ ; RH = 10%

© Arash Fassadi Chimeh, 2023

#### 4.6. Conclusions

The aluminum production process generates effluent gases containing SO<sub>2</sub> which contributes to air pollution. Aluminum industry is committed to reducing such gases to produce greener aluminum. The semi-dry desulfurization process is an effective way of SO<sub>2</sub> removal before discharging the effluent gases coming from the electrolysis cells into the atmosphere. An alkaline powder – hydrated lime – is used to remove SO<sub>2</sub>. The kinetic rate expression proposed by Ortiz and Ollero which represents their experimental data well was incorporated into the model. A mathematical model using an Eulerian-Lagrangian approach was developed, and it was found to be an appropriate model for the simulation of a scrubber in which a gas-solid reaction is occurring in the presence of humidity. The smaller particles lead to a better desulfurization efficiency even under low relative humidity conditions. The results indicate that high desulfurization efficiencies could be achieved with larger particles under high relative humidity conditions. It was also seen that the larger particles settle more quickly compared to smaller particles; thus, the use of larger particles may be more practical for industrial applications because this could be helpful in terms of the cleaning of the scrubber units.

Experiments are underway for the validation of the model. Once validated, this model will be used as a tool to design an industrial scrubber and test its performance under different conditions.

#### Acknowledgements

The financial and technical support of Natural Sciences and Engineering Research Council of Canada (NSERC), Rio Tinto, Graymont, Centre québécois de recherche et

de développement de l'aluminium (CQRDA), CURAL, REGAL, and University of Québec at Chicoutimi (UQAC) is greatly appreciated.

#### 4.7. References

1. Semrau, K.T., *Control Of Sulfur Oxide Emissions From Primary Copper, Lead And Zinc Smelters—A Critical Review*. Journal of the Air Pollution Control Association, 1971. **21**(4): p. 185-194.
2. Zettler, S., Fortin, N., and Moran, K., *Feasibility report on technical options to reduce SO<sub>2</sub> emissions Post-KMP*. 2013, Rio Tinto Alcan.
3. *An assessment of global megatrends and regional and market sector growth outlook for aluminium demand, February 2020, CM group*.
4. Charette, A., Kocafe, Y., and Kocafe, D., *Le carbone dans l'industrie de l'aluminium*. 2012: PRAL - Press Aluminium.
5. *Aluminium Association of Canada, Primary aluminum production*.
6. Masterson, L., *Refinery run cuts reduce anode-grade coke supply*. 2020.
7. Li, X., Han, J., Liu, Y., Dou, Z., and Zhang, T.-a., *Summary of research progress on industrial flue gas desulfurization technology*. Separation and Purification Technology, 2022. **281**: p. 119849.
8. Sargent. and Lundy., *Flue Gas Desulfurization Technology Evaluated Dry Lime vs. Wet Limestone FGD*, in *project number 11311-001*. 2007. p. 1-63.
9. Ma, X., Kaneko, T., Tashimo, T., Yoshida, T., and Kato, K., *Use of limestone for SO<sub>2</sub> removal from flue gas in the semidry FGD process with a powder-particle spouted bed*. Chemical Engineering Science, 2000. **55**(20): p. 4643-4652.
10. Karlsson, H.T. and Klingspor, J., *Tentative modelling of spray-dry scrubbing of SO<sub>2</sub>*. Chemical engineering & technology, 1987. **10**(1): p. 104-112.
11. Zhou, Y., Zhu, X., Peng, J., Liu, Y., Zhang, D., and Zhang, M., *The effect of hydrogen peroxide solution on SO<sub>2</sub> removal in the semidry flue gas desulfurization process*. Journal of Hazardous Materials, 2009. **170**(1): p. 436-442.
12. Ma, X., Kaneko, T., Guo, Q., Xu, G., and Kato, K., *Removal of SO<sub>2</sub> from flue gas using a new semidry flue gas desulfurization process with a powder-particle spouted bed*. The Canadian Journal of Chemical Engineering, 1999. **77**(2): p. 356-362.
13. Lotfi, M., FassadiChimeh, A., Dabir, B., and Mohammadi, A.H., *Computational Fluid Dynamics Modelling of the Pressure Drop of an Iso-Thermal and Turbulent Upward Bubbly Flow Through a Vertical Pipeline Using Population Balance Modelling Approach*. Journal of Energy Resources Technology, 2022. **144**(10).
14. Versteeg, H.K.M., W., *An Introduction to Computational Fluid Dynamics The Finite Volume Method*,. 2007: Pearson Education.

15. Du, J., Yue, K., Wu, F., Ma, X., and Hui, Z., *Numerical investigation on the water vaporization during semi dry flue gas desulfurization in a three-dimensional spouted bed*. Powder Technology, 2021. **383**: p. 471-483.
16. Wang, X., Li, Y., Zhu, T., Jing, P., and Wang, J., *Simulation of the heterogeneous semi-dry flue gas desulfurization in a pilot CFB riser using the two-fluid model*. Chemical Engineering Journal, 2015. **264**: p. 479-486.
17. Marocco, L. and Mora, A., *CFD modelling of the Dry-Sorbent-Injection process for flue gas desulfurization using hydrated lime*. Separation and Purification Technology, 2013. **108**: p. 205-214.
18. ANSYS, *ANSYS FLUENT Theory Guide 2022 R2*. 2022.
19. Chimeh, A.F., Kocafe, D., Kocafe, Y., Robert, Y., and Bernier, J., *Mathematical Modelling of the Desulfurization of Electrolysis Cell Gases in a Low-Temperature Reactor*, in *Light Metals 2023*. 2023, Springer. p. 749-756.
20. Xu, G., Guo, Q., Kaneko, T., and Kato, K., *A new semi-dry desulfurization process using a powder-particle spouted bed*. Advances in Environmental Research, 2000. **4**(1): p. 9-18.
21. Garea, A., Herrera, J.L., Marques, J.A., and Irabien, Á., *Kinetics of dry flue gas desulfurization at low temperatures using Ca(OH)<sub>2</sub>: competitive reactions of sulfation and carbonation*. Chemical Engineering Science, 2001. **56**: p. 1387-1393.
22. Launder, B.E. and Spalding, D.B., *Mathematical Models of Turbulence*. Journal of Applied Mathematics and Mechanics 1973. **53**(6): p. 424-424.
23. Morsi, S.A. and Alexander, A.J., *An investigation of particle trajectories in two-phase flow systems*. Journal of Fluid Mechanics, 1972. **55**(2): p. 193-208.
24. Gutiérrez Ortiz, F.J. and Ollero, P., *A realistic approach to modelling an in-duct desulfurization process based on an experimental pilot plant study*. Chemical Engineering Journal, 2008. **141**: p. 141–150.

## CHAPTER 5

### CONCLUSIONS AND RECOMMENDATIONS

#### 5.1 General conclusions

In this project, it has been shown that humidity is a key factor in the desulfurization process and increasing the relative humidity (RH) leads to the improvement of the desulfurization efficiency. The particle size of sorbent ( $d_p$ ) and the ratio (Ca/S) also have impact on the desulfurization process. A summary of general conclusions is given below:

1. The mathematical model, which uses Eulerian – Eulerian approach (Volumetric model), represents the solid particles as a viscous fluid. It gives quick results which give a good idea about the overall view. However, reactant and product are in the same viscous phase and their distribution in the reactor cannot be identified. The mathematical model which uses Eulerian – Lagrangian approach (Discrete Phase Modelling (DPM)) takes longer time but it can precisely calculate the distribution of all the components separating fresh hydrated lime particles from those with product accumulation at their surfaces.
2. The predictions of the DPM model showed that increasing sorbent value (Ca/S) leads to an increase in the desulfurization efficiency, while the presence of humidity improves the desulfurization up to 8 % in certain cases depending on the sorbent rate used.
3. Comparing the predictions of the model for two cases, one with a higher relative humidity (30 %) and coarser sorbent size ( $d_p=45$  micron) and the other one with a lower relative humidity (10 %) and finer sorbent size ( $d_p=10$  micron), indicated that the latter case is slightly more efficient than the former one, achieving 85.3 %

and 83.5 % desulfurization efficiency, respectively. Thus, increasing sorbent specific surface area three times (11.80 to 38.25 m<sup>2</sup>/g) by decreasing the particle size improves the desulfurization process slightly more compared to increasing RH three times.

4. In addition, due to the two-way coupling used in DPM, it was possible to see that the smaller particles can be carried to the top of the system easier than the larger particles as expected. Particle tracking of two particle groups showed that the larger particles (45 micron) tend to fall down, and the smaller particles (10 micron) stay suspended in the gas.
5. The transient particle tracking can distinguish between fresh hydrated-lime particles and those covered with product using residence time. Those particles containing solid product on their surfaces have a higher residence time, while the lower residence time refers to the fresh hydrated lime. This can be considered as a means to find the positions of reactant and product particles inside the scrubber domain.

## **5.2 Recommendations**

There are several additional issues that are worth investigating. Several suggestions are proposed below for the future work.

1. Analyse the effects of CO<sub>2</sub> presence in the gas phase during the desulfurization process and compare the results with this study where the gas contains only air, SO<sub>2</sub>, and humidity.

2. Model the pulse injection of sorbent into the scrubber and compare the results with those of the current study to determine if this type of feeding could improve the desulfurization.
3. Simulate the particle deposition on the surface of the filter to determine when the performance of the filter becomes ineffective due to increasing pressure drop and the length of the period after which the filter has to be cleaned.
4. Model the filter cleaning process, for example using high-pressure air in the reverse flow direction, and determine how the filter is cleaned from the deposited particles.



## APPENDIX

### VALIDATION OF THE MATHEMATICAL MODEL

Figure A 1 illustrates the custom-built experimental reaction system (by CHIMI group), providing details for each section. The operating conditions of the reactor are:

- temperature (isothermal): 70 °C,
- inlet concentration of SO<sub>2</sub>: 300 ppm (0.075 L/min),
- air inlet velocity: 5 L/min, and
- hydrated lime feed rate: 0.183 g/min.

The experiments were conducted under both dry and humid conditions, with the relative humidity maintained around 30 % – 35 %. Particles of 45 micron are used for the tests. To ensure an accurate temperature control, the entire system was well-insulated with glass wool and aluminum foil, and each section of the reactor was equipped with an individual PID controller and corresponding thermocouples. The inlet concentration of SO<sub>2</sub> was regulated using a flow meter, while the outlet SO<sub>2</sub> was monitored by a High SO<sub>2</sub> analyzer from Thermoscientific instruments. The reactor box was constructed from stainless steel, with a filter cloth placed between the inlet and outlet sections. Humidity was generated using a custom-built humidity chamber, and the resulting relative humidity was controlled using an RH probe, as depicted in Figure A 1.

Figure 2 presents the transparent Plexiglass reactor system (built by CHIMI group) designed specifically to study the flow dynamics of hydrated lime. This system was constructed with the same dimensions as the original stainless-steel reactor given in Figure A 1. In order to observe the flow dynamics of hydrated lime, similar parameters such as air velocity and lime inlet quantity were maintained. Figure A 2a represents the reactor system

prior to the injection of hydrated lime, and Figure A 2b illustrates the system after the test. The flow dynamics were captured as a movie, and the final image indicates the deposition of lime on the filter cloth. Remarkably, the outlet section of the reactor box exhibited an extremely minimal quantity of lime.

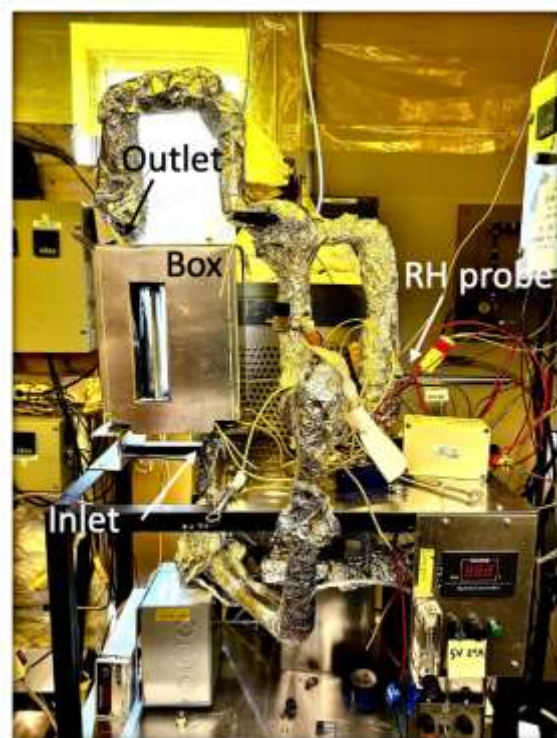


Figure A 1. The reactor system built by CHIMI group

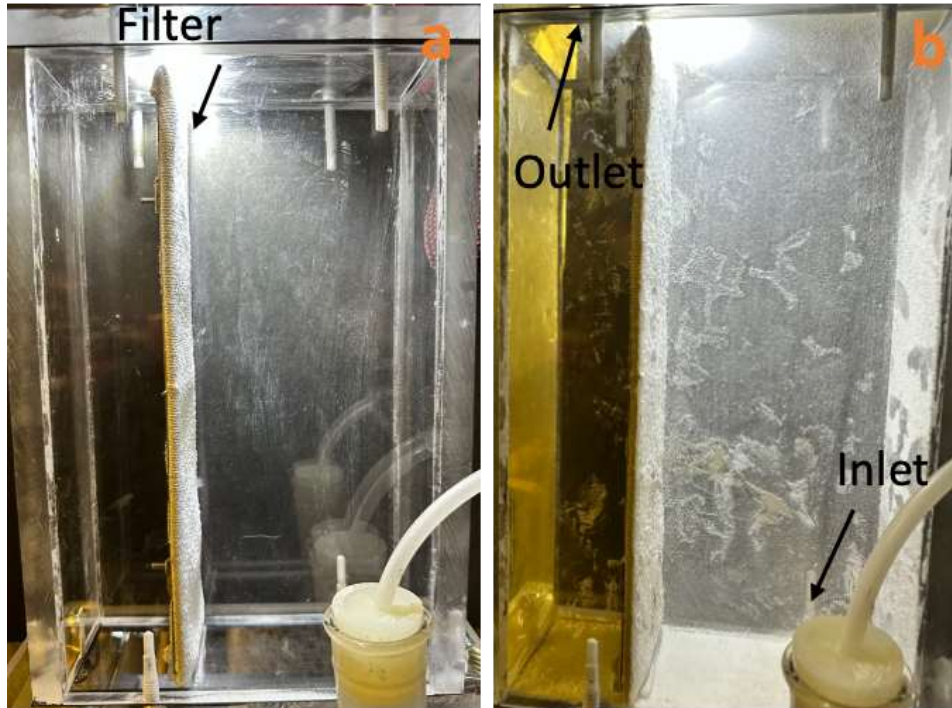


Figure A 2. Images of the transparent reactor system before and after the test

In Figure A 3a and b, the top view of the stainless-steel reactor system and its inlet section are displayed. These images were captured after a reaction period of 5 minutes and 15 minutes, respectively. Figure A 3c shows the final deposited lime collected on the bottom plate of the reactor system.



Figure A 3. Images of the reactor system at (a) 5 min, (b) 15 min, and (c) deposited lime on the bottom plate after reaction

The reaction between hydrated lime and  $\text{SO}_2$  was investigated under both dry and humid conditions. The inlet flow of lime was regulated using a controller, and it was introduced into the system with an airflow rate of 5 L/min, along with an inlet concentration of 300 ppm  $\text{SO}_2$ . Under the dry conditions (in the absence of humidity), the outlet  $\text{SO}_2$  concentration gradually decreased with time. After 8 minutes, the outlet concentration of  $\text{SO}_2$  dropped to less than approximately 5 ppm.

A similar experiment was conducted under humid conditions. Humidity was initially mixed with the  $\text{SO}_2$  and introduced into the inlet section of the reactor together with the lime. The relative humidity, as measured by the RH probe, was maintained within the range of 30 % to 35 %. In the presence of humidity, the outlet  $\text{SO}_2$  concentration decreased more rapidly due to the impact of  $\text{H}_2\text{O}$  vapor. It seems that the water vapor contributed to higher adsorption/absorption of  $\text{SO}_2$  on the lime surface. By the end of 6 minutes, the  $\text{SO}_2$  concentration was less than approximately 5 ppm.

The model was used to simulate the reactor under the same conditions as the experimental ones for semi-dry and dry cases for validation. The experimental results and the model predictions are compared in Figure A 4 for the semi-dry condition at  $RH = 35\%$ . It shows the outlet  $SO_2$  concentration at each minute. The results are in reasonable agreement with each other, and the total error for the semi-dry case is less than  $8.2\%$ .

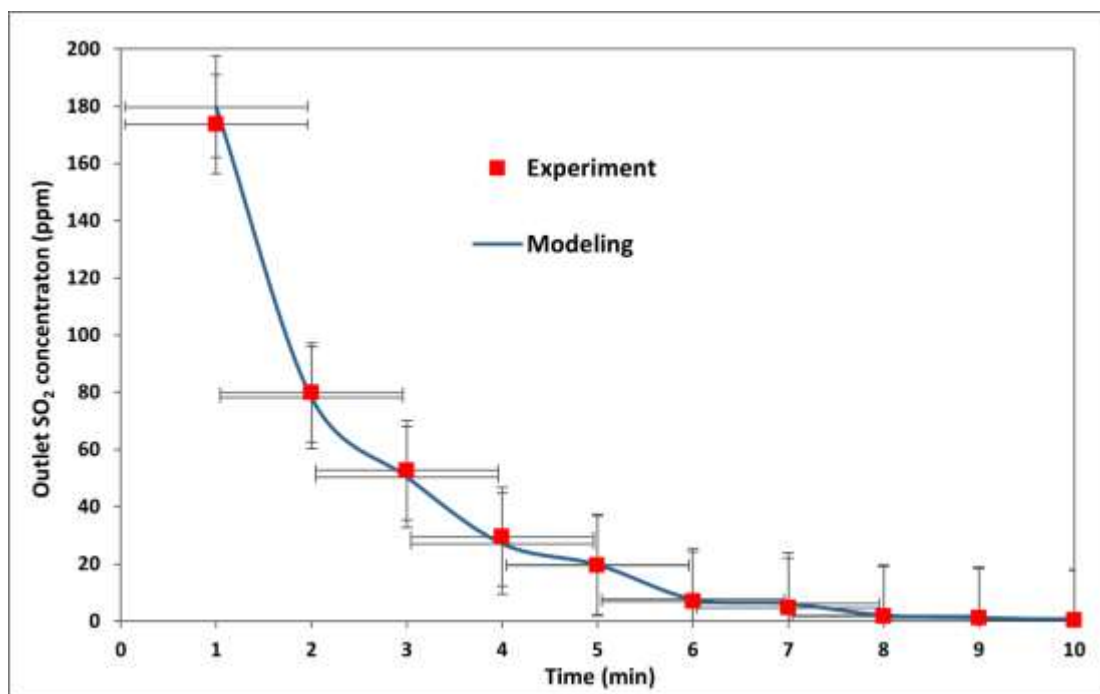


Figure A 4. Comparison of modelling and experimental results for semi-dry conditions ( $RH \sim 35\%$ )

© Arash Fassadi Chimeh, 2023

Figure A 5 presents the same comparison of the outlet  $SO_2$  concentration for the dry conditions. The results are in good agreement with each other, and the total error for the dry case is about  $2.8\%$ . The accuracy is better for the dry case because the measurements are more difficult in the humid medium, resulting in a greater error. The model predicts the reactor behavior well.

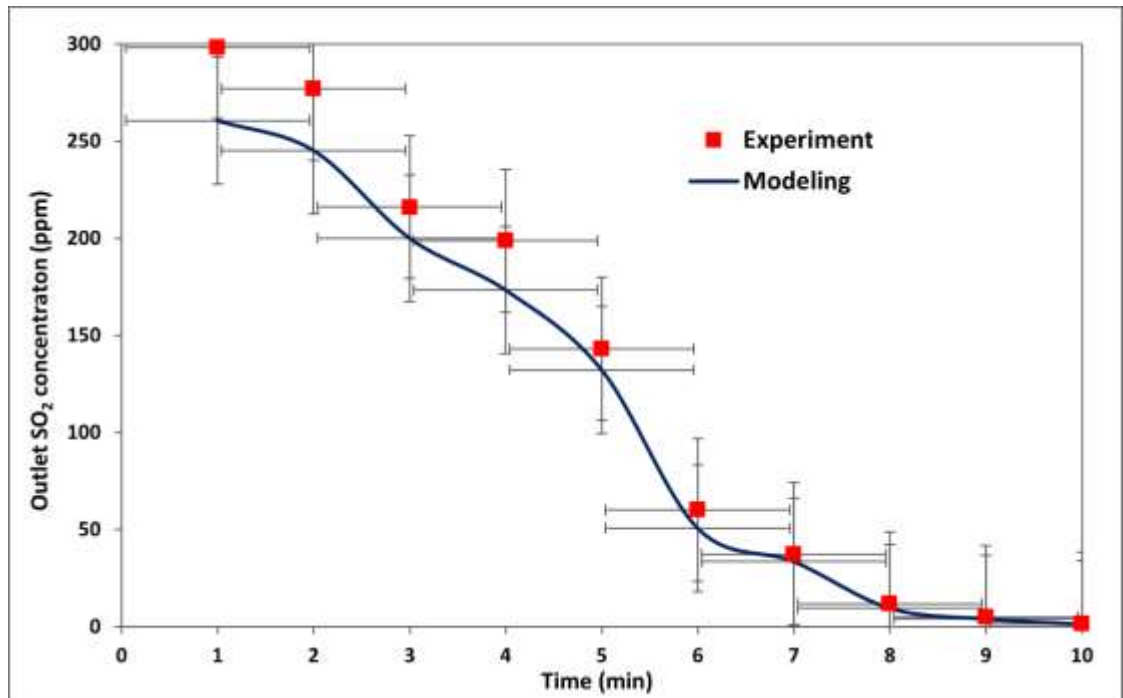


Figure A 5. Comparison of modelling and experimental results for dry conditions

© Arash Fassadi Chimeh, 2023